Consideration and propagation of epistemic uncertainties in New Zealand probabilistic seismic hazard analysis

B.A. Bradley
G.H. McVerry
M.W. Stirling
M. Gerstenberger

GNS Science Consultancy Report 2011/275
October 2011

DISCLAIMER

The data presented in this Report are available to GNS Science for other use from October 2011.

BIBLIOGRAPHIC REFERENCE

Bradley, B.A. (Department of Civil and Natural Resources Engineering, University of Canterbury, PO Box 4800, Christchurch, New Zealand); Stirling, M.W.; McVerry, G.H. and Gerstenberger, M. 2011. Consideration and propagation of epistemic uncertainties in New Zealand probabilistic seismic hazard analysis, *GNS Science Consultancy Report* 2011/275. 67 p.

CONTENTS

FIGURES

TABLES

EXECUTIVE SUMMARY

This report presents the results from the consideration of epistemic uncertainties in New Zealand probabilistic seismic hazard analysis. The methodology accounts for uncertainties in the earthquake rupture forecast due to uncertainties in fault geometry, slip parameters, and magnitude scaling relationships; as well as uncertainty in the predicted distribution of ground motion by utilizing multiple ground motion prediction equations. The hierarchy of ground motion prediction equations was developed based on examination of the bias in various NZ-specific and foreign models using a dataset of observed ground motions in New Zealand. Due to the present lack of fault-specific data quantifying uncertainties for the majority of faults in NZ, representative values based on judgement and a limited number of NZ and foreign fault-specific data available were utilized for such faults. Probabilistic seismic hazard analyses are conducted for two vibration periods of spectral acceleration (PGA and SA(2.0)) for site class B (rock) and D (soft/deep soil) conditions in Wellington and Christchurch. The results illustrate that variation in seismic hazard due to various ground motion prediction model represent the largest source of uncertainty considered. Of the earthquake rupture forecast uncertainties considered, the magnitude-geometry scaling relationships was the most significant, followed by rupture length. Recommendations for prioritization of seismic hazard research are discussed in light of the observed results.

1.0 INTRODUCTION

The location of New Zealand astride the boundary of the Australian and Pacific plates makes it a country of high seismicity. As such, the seismic hazard for various locations in New Zealand is routinely computed on the basis of a probabilistic seismic hazard analysis (PSHA). The two basic ingredients of a PSHA are an earthquake rupture forecast (ERF), which quantifies the location and likelihood of all possible earthquake ruptures which may occur; and a ground motion prediction equation (GMPE) which quantifies the ground motion shaking at a specific location due to the occurrence of an earthquake rupture.

Because of the complexity of earthquake rupture, wave propagation, and local site effects, ERFs and GMPEs are typically probabilistic in the sense that they incorporate uncertainties in the parameters they attempt to quantify. In PSHA, it is common to distinguish between two main types of uncertainties. The first is uncertainties which, for the given models adopted, are deemed to be purely random and unpredictable, and are referred to as aleatory variability. The second source of uncertainty is that which arises due to limited knowledge of the phenomena being predicted, and is referred to as epistemic uncertainty. An example of the aleatory variability is the variability in ground motion amplitudes at a given distance from an earthquake predicted using a ground motion model. An example of epistemic uncertainty is the assessment of which ground motion model is most appropriate to be used for a particular problem under consideration.

The benefit of making the distinction between aleatory variability and epistemic uncertainties is that, in principle, epistemic uncertainties can be reduced with improved knowledge (both empirical and theoretical), whilst aleatory variability cannot. Clearly, such a distinction is idealistic in that some of the observed aleatory variability could be due to systematic effects (hence strictly being a source of epistemic uncertainty), resulting from for example, the simplified nature of a ground motion model. Despite this idealisation, the separation of aleatory variability and epistemic uncertainties has been argued as useful from a conceptual view by many over the past decades.

The basic framework of PSHA was first introduced in the late 1960's (Cornell 1968, Esteva 1968, McGuire 2008). This basic framework enabled seismic hazard curves (ground motion intensity vs. rate or probability of exceedance) to be computed. However, this framework of PSHA was only implemented considering aleatory variability in the occurrence probability of earthquake ruptures, and the aleatory variability in the distribution of ground shaking for a specified rupture. The consideration of epistemic uncertainties in PSHA was first proposed by Kulkarni *et al*. (1984), via the concept of logic trees. Logic trees allow for the consideration of alternative models and the values of their parameters to be used in PSHA, with each alternative possibility given a degree of belief such that the sum of the possibilities adds to 1.0. Although, there is relatively little literature on the logic tree concept (as a result of the field of PSHA being largely practice-driven), Bommer et al. (2008, 2005) provide useful overviews and potential pitfalls.

Since their inception in 1984, logic trees have become commonly employed in PSHA to attempt to account for epistemic uncertainties. However, nationwide seismic hazard analyses for New Zealand (Stirling et al. 2011, Stirling et al. 2002), at present, do not explicitly account for epistemic uncertainties, instead using only preferred values of parameters in the ERF and GMM. The aim of this research is to develop the necessary details required to consider epistemic uncertainties in nationwide PSHA in NZ, and examine the effects of epistemic uncertainties at several locations.

Section 3 examines epistemic uncertainties in ground motion prediction for NZ. This is achieved by comparing the bias of various NZ and foreign ground motion prediction equations with respect to a database of observed NZ ground motions, as well as qualitative considerations based on the underlying dataset used to develop each ground motion model. Based on the observed results, logic trees are developed for each of the three different earthquake tectonic types relevant to NZ.

Section 4 develops a methodology for consideration of epistemic uncertainties in the present method used to compute characteristic earthquake sources for the NZ fault-based seismicity model. Discussion is also given to the determination of the fault parameter uncertainties which are required for the methodology.

Section 5 examines the implications of considering epistemic uncertainties in ground motion prediction and fault-based seismicity on seismic hazard calculations in NZ. Seismic hazard analyses are performed for peak ground acceleration and spectral acceleration at a vibration period of 2.0 seconds for rock and soft/deep soil conditions in Wellington and Christchurch. The observations are discussed, including comparisons of: (i) seismic hazard curves computed considering epistemic uncertainties with those using the conventional (non-epistemic) methodology; and (ii) the magnitude of epistemic uncertainties observed in seismic hazard analyses in the present study with those for the San Francisco Bay Area.

Section 6 discusses the limitations of the present study and suggests topics of future focus based on the outcomes of this study.

2.0 EPISTEMIC UNCERTIANTIES IN GROUND MOTION PREDICTION

2.1 Overview

As previously mentioned, a ground motion model is one of the two ingredients required in PSHA. At present, ground motion models are primarily empirical in nature, due to the current limitations in physics-based ground motion prediction for engineering applications. The availability of empirical ground motion prediction equations (GMPE) in NZ has been historically limited, as compared to equations of a similar era elsewhere, due to a paucity of instrumental ground motion records observed in NZ. For example, the most recent GMPE developed by McVerry et al. (2006) was based on 49 earthquakes and 435 ground motions observed over the period 1966-1995. Because of the limited number of observed ground motions, McVerry et al. based their GMPE to some extent on the functional forms of other foreign GMPEs and also utilized overseas near-source records from large magnitude earthquakes. The McVerry et al. model is the GMPE which has been used in PSHA in NZ for over the last decade (Stirling et al. 2011, Stirling et al. 2002).

Since the development of the McVerry et al. (2006) model, which utilized data from 1966-1995, there has been a significant increase in observed ground motions in NZ as a result of the GeoNet project (2010). This increase in data allows a reassessment of the adequacy of the McVerry et al. model, as well as the applicability of alternative GMPEs developed for overseas environments, which could be utilized in order to account for epistemic uncertainty in ground motion prediction. Here, an overview of the preliminary results of this reassessment is provided. A comprehensive presentation of such preliminary results can be found in Bradley (2010).

2.2 Dataset of NZ ground motions utilized

Based on a ground motion suite developed by Zhao and Gerstenberger (2010), Bradley (2010) applied various quality assurance criteria to obtain a NZ dataset of 213 earthquakes and 2437 ground motions, as illustrated in

Table **1**. In comparison, only 435 ground motions from 49 NZ earthquakes were utilized by McVerry et al. (2006) in deriving their GMPE. Figure 1 provides an example of the ground motions from active shallow crustal earthquakes in the Bradley (2010) dataset compared with the NGA database (Chiou et al. 2008). It can be seen that despite the large number of data, the Bradley (2010) NZ dataset lacks a significant number of strong motion recordings from moderate to large magnitude events at small-to-moderate source-to-site distances. Given that the design PGA values in NZ can be as high as 0.4g (NZS 1170.5 2004), this highlights the robustness (or lack thereof) of empirical ground motion prediction equations which are developed using only NZ data for use in forecasting seismic hazard in New Zealand. An alternative postulate is therefore made that strong ground motion phenomena in other tectonically similar regions of the world should be similar to that in New Zealand (as done by McVerry et al. (2006)). Consequently, empirical GMPEs developed for such regions should also be applicable for estimating strong ground motion intensity measures in NZ.

Table 1 Number of events and recorded ground motions for NZ ground motion datasets.

Dataset	Number of events, N_{eq}	Number of ground motion records, N_{record}
Bradley (2010)	213	2437
McVerry *et al.* (2006)	49	435

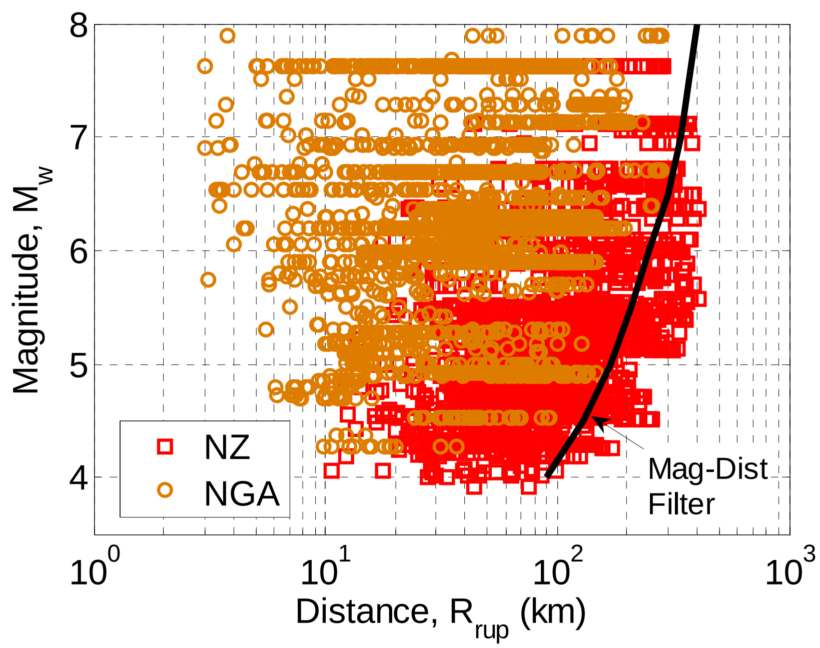

Figure 1 Comparison of the NZ and NGA database, as well as the magnitude-distance filter used to remove ground motions deemed not of engineering significance.

Two different considerations were accounted for in assessing the applicability of GMPEs for NZ. The first is the distribution of inter- and intra-event residuals as a function of various predictor variables. The second is the qualitative scaling of the GMPEs and their underlying empirical database (Bradley 2010). The latter case is important in that the quantitative examination of bias in the inter- and intra-event residuals can only be examined for the empirical data which is available. Thus, with regard to the present NZ database, such an approach cannot ascertain the applicability of foreign GMPEs for large M_w NZ events recorded at small R_{rup} distances, because there are no such observations in the present NZ database.

2.3 Applicability of active shallow crustal GMPEs for New Zealand

There are numerous GMPEs for active shallow crustal earthquakes. The five different GMPEs considered in this study are: McVerry et al. (2006), Zhao et al. (2006), Boore and Atkinson (2008), Chiou and Youngs (2008), and Chiou et al. (2010a). For brevity these equations are herein referred to as McV06, Z06, BA08, CY08, C10, respectively. As previously mentioned, McV06 is the most recent NZ-specific model developed, and hence forms a useful benchmark on the applicability of other GMPEs, and whether there is in fact any benefit to be gained in using foreign GMPEs for ground motion prediction in NZ. The Z06 model is considered, both because it was developed using an extensive database of recordings from Japan, and also because previous research has suggested that the strong motion characteristics in NZ and Japan are similar (Zhao et al. 1997). The BA08 and CY08 models were considered as relatively simple and relatively complex models produced from the Next Generation Attenuation (NGA) project, which utilized arguably the most comprehensive active shallow crustal strong motion database presently available. Finally, a Chiou et al. (2010b)-based (C10) model was also considered, as it has been recently found that the CY08 model was not representative of strong motion observations for small-to-moderate magnitude events in California, (an observation which may also carry-over to NZ strong motion observations).

2.3.1 Scaling of GMPEs with predictor variables

Figure 2a and Figure 2b illustrate the magnitude scaling of the median of the five active shallow crustal GMPEs considered for both PGA and Sa(2.0). Figure 2a illustrates that all of the GMPEs predict similar PGA values for $M_w = 6.5$, but that the scaling to small and large magnitudes is significantly different. It can be seen that the scaling with magnitude of the McV06 model is significantly less ‘concave from below’ than the other models, and in fact for PGA, the scaling is linear (McVerry et al. 2006). As a consequence, the predicted Sa values of the McV06 model at small M_w are significantly larger (more than a factor of two at $M_w = 4.5$) than any of the other GMPEs considered. It should be however noted that the McV06 model is considered only applicable for $M_w > 5.25$ (McVerry et al. 2006). It is also pertinent to note that the small M_w scaling of C10 produces notably smaller PGA amplitudes (and short period amplitudes in general) than the CY08 model. With the exception of the Z06 model, it can be seen that the models exhibit relatively similar scaling at large magnitudes. The difference in the large magnitude scaling of Z06 is significant, with the predicted amplitudes for PGA being a factor of approximately 1.5 larger than the other considered models. Examination of the Z06 model and ground motion database (Zhao et al. 2006), reveals firstly that the largest well recorded crustal Japanese event has a $M_w < 7$ and that overseas ground motion records from events up to $M_w \sim 7.5$ were used to supplement the Z06 Japanese ground motion database. Secondly, the quadratic magnitude scaling in the Z06 model was developed based on the observed residuals of a simpler linear magnitude scaling model, rather than directly employed in the mixed-effects model formulation. As the foreign near-source large magnitude data used by Zhao *et al.* (2006) is notably less comprehensive than that of the NGA database then it is likely that the scaling in the Z06 model in this region is less constrained compared to the BA08, CY08 (and C10) NGA models.

Figure 2c and Figure 2d illustrate the path scaling of the median of the five GMPEs considered for both PGA and Sa(2.0). The near-source scaling of the five models at short periods is similar, with the relatively smaller near-source saturation of the PGA BA08 model, and the McV06 Sa(2.0) model being the only notable observations. At long periods, all models other than McV06 exhibit similar scaling. The difference of the McV06 model is due to smaller geometric spreading coefficients, and larger anelastic attenuation than the other considered models (Bradley 2010).

Figure 2e and Figure 2f illustrate the median response spectra predicted by the five considered GMPEs for magnitudes 5.5 and 7.5 and distances of 10 and 50 km. For $M_w =$ 5.5 it can be seen that the McV06 model generally predicts higher spectral amplitudes (particularly at short periods) as a result of the previously discussed small magnitude scaling. Similarly, for $M_w = 7.5$ the Z06 model predicts higher spectral amplitudes as a result of the Z06 large magnitude scaling.

Figure 2g and Figure 2h illustrate the scaling of the inter- and intra-event standard deviations of the models as a function of vibration period. For those models with magnitude dependent standard deviations (i.e. CY08 and C10 for inter-event, and CY08, C10 and McV06 for intra-event), lines are shown for magnitudes 5 and 7. It can be seen that the BA08, CY08 and C10 (for $M_w = 7$) inter-event standard deviation generally increases with vibration periods above 0.5 seconds, while the Z06 model is relatively constant, and the McV06 model varies significantly. Similar to the inter-event standard deviations it can be seen that the magnitude dependence of the CY08 and C10 intra-event standard deviation decreases with vibration period. In contrast, the intra-event standard deviation of the McV06 model also exhibits magnitude dependence, but notably the magnitude dependent coefficient is not always negative (e.g. Sa(2.0)), as is common in most GMPEs with magnitude dependent standard deviations (e.g. CY08 and C10). This observation, as well as the observed scaling of the McV06 intra-event standard deviation, are a possible consequence of the small number of recordings used in developing the McV06 model.

2.3.2 Observed inter- and intra-event residuals from the NZ database

Now that insight has been obtained as to the general predictor variable scaling features of the considered GMPEs it is possible to thoroughly examine the statistics of the observed inter- and intra-event residuals of the NZ database for each of the considered models. This section presents only sufficient results (for a single vibration period) to convey the general observations of the inter- and intra-event residuals as a function of predictor variables for each of the models. More elaborate discussion and results for five vibration periods are given in Bradley (2010).

In the subsequent examination of the cumulative distribution of the residuals, the Kolmogorov-Smirnov goodness-of-fit test (Ang and Tang 2007) is used to identify statistically significant departures from the residuals having a standard normal distribution. In order to illustrate the key trends in the observed residuals as a function of the predictor variables, the mean residual and its 98% confidence interval are plotted using non-parametric regression (Ruppert et al. 1995, Wasserman 2006), and shown in subsequent figures with solid and dashed lines, respectively. The non-parametric mean can be used to identify statistically significant biases in the prediction models. The high level of confidence used is based on the desire to only identify high significance biases.

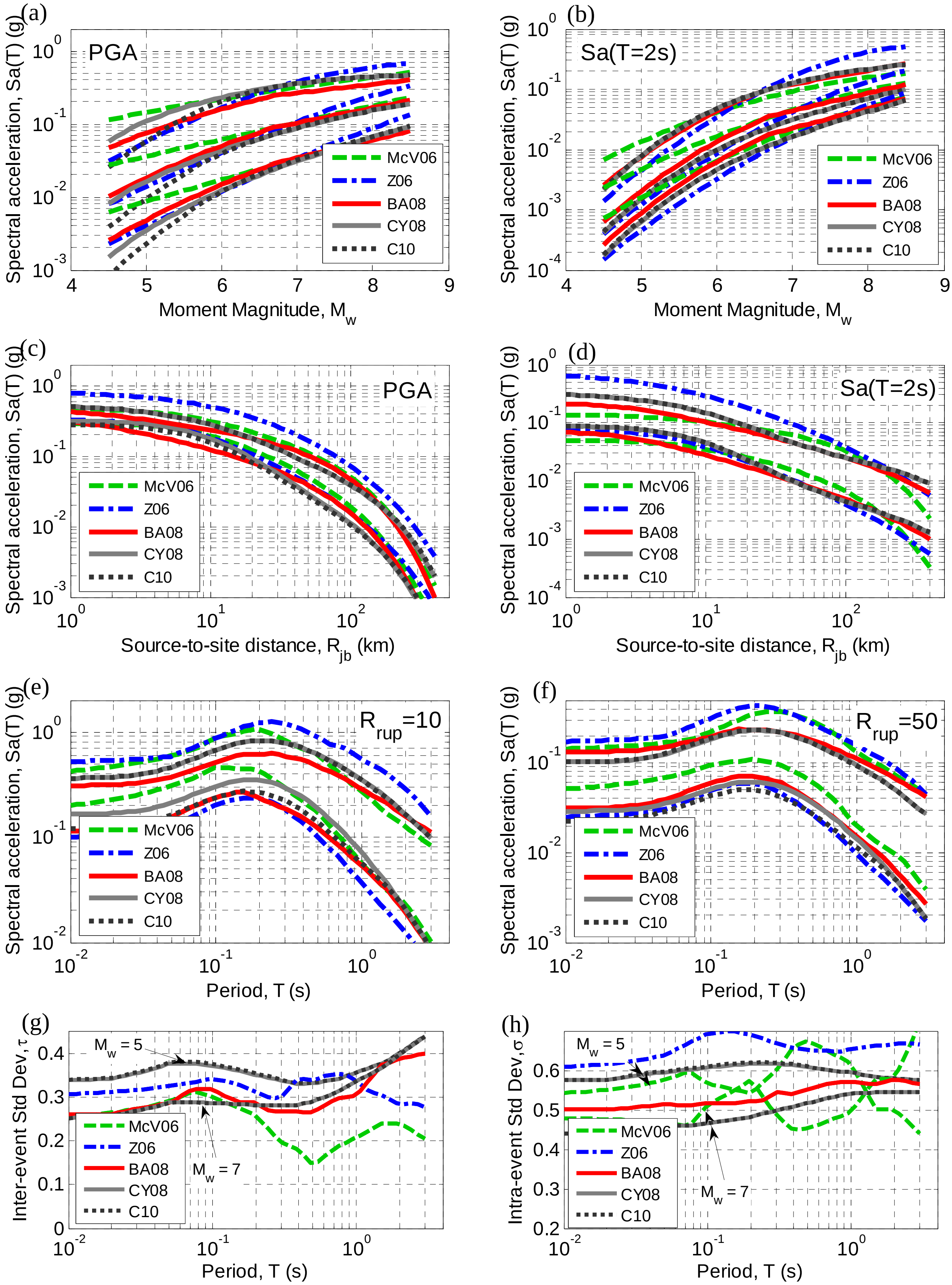

Figure 2 Predictor variable scaling of the considered GMPEs: (a)&(b) magnitude scaling for source-to-site distances of 10, 50 and 120 km; (c)&(d) path scaling for magnitudes 6 and 7.5; (e)&(f) median response spectra for magnitudes 5.5 and 7.5; (g)&(h) inter- and intra-event standard deviation scaling with vibration period. All plots are for a vertical strike slip fault and NZ site class C site.

2.3.2.1 McVerry et al. (2006), McV06

Figure **3** illustrates the observed inter- and intra-event residuals for Sa(0.5) from the NZ database using the McV06 model. It is immediately obvious that the McV06 model significantly over predicts ground motions from $M_w < 6$ events, as seen by the negative trend in the inter-event residuals in

Figure **3**a and its dependence as a function of M_w in

Figure **3**b. Recall that McV06 is deemed appropriate for $M_w > 5.25$. This can be understood based on the magnitude scaling of the McV06 model presented in Figure 2. There is also an observed bias in the intra-event residuals as a function of source-to-site distance (

Figure **3**d).

Figure **3**f illustrates that there is some variation in the mean inter-event residual as a function of focal mechanism, indicating possible bias in the focal mechanism factors. There is no observed bias with respect to source depth as evident in

Figure **3**e.

Figure **3**h illustrates that there is a variation in the mean intra-event residual as a function of site class, with site classes A and E in particular being over- and under-predicted, respectively (relative to the mean residual for site classes B, C, and D). It should be noted that the prediction for site class A is given based on the McV site class A/B factors, which as noted by McVerry et al. (2006), are primarily determined for site class B conditions. Furthermore, as the McV06 model does not have a specific prediction for site class E conditions, those for site class D have been used. Clearly, this assumption, that these site classes on average have the same site effect, is not valid. It can be seen that there is no trend of the intra-event residuals with respect to the normalised path distance through the Taupo Volcanic Zone (TVZ) as the McV06 model considered such phenomena (McVerry et al. 2006).

2.3.2.2 Zhao et al. (2006), Z06

Figure **4** illustrates the observed inter- and intra-event residuals for PGA from the NZ database using the Z06 model. While there is a systematic over-prediction of the ground motions, as evident from the negative mean value of the inter-event residuals in

Figure **4**a and

Figure **4**b, it is notably less than that of the McV06 model previously discussed.

Figure **4**d illustrates that there are marginally apparent biases in the near-source distance scaling and also in the large-distance scaling.

Figure **4**e illustrates that there is bias in the scaling with depth, but this bias was only apparent for PGA and not significant for other vibration periods (Bradley 2010).

Figure **4**f illustrates that there is a significant over-prediction of normal faulting events. This is a result of the fact that the Z06 model considers only ‘reverse’ and ‘other’ focal mechanisms.

Figure **4**g illustrates that there is a significant negative trend in the intra-event residuals as a function of the normalised TVZ distance, indicating the importance of TVZ anelastic attenuation which is not accounted by Z06 (or any of the other foreign models considered here).

Figure **4**h illustrates that the Z06 model provides a relatively good prediction of site class effects with no significant biases for PGA. For short period amplitudes (i.e. Sa(0.2), Sa(0.5), and Sa(1.0)) there was however a statistically significant over-prediction of the amplitudes of site class A motions (Bradley 2010), which can be attributed to the fact that the Z06 Hard rock site class is defined for $V_{s,30}$ > 1100 m/s, while it is $V_{s,30}$ > 1500 m/s for NZ site class A. Finally, it is noted that the over-prediction of site class A amplitudes, neglect of TVZ effects, over-prediction of normal events, and over-prediction at large-distances leads to the resulting observed negative inter-event residuals for several of the large magnitude (M_w > 6) events in the NZ database, which were predominantly normal events near the TVZ and recorded at class A sites (Bradley 2010). Thus, the observed inter-event residuals for these M_w > 6 events are not related to errors in the Z06 magnitude scaling. This same result is also true for the BA08, CY08, and C10 models examined subsequently. Conversely, no significant over-prediction of these large events is observed using the McV06 model because, McV06 accounts for TVZ distance, and also over-predicts site class A motions (based on the site class A/B factors) (

Figure **3**h).

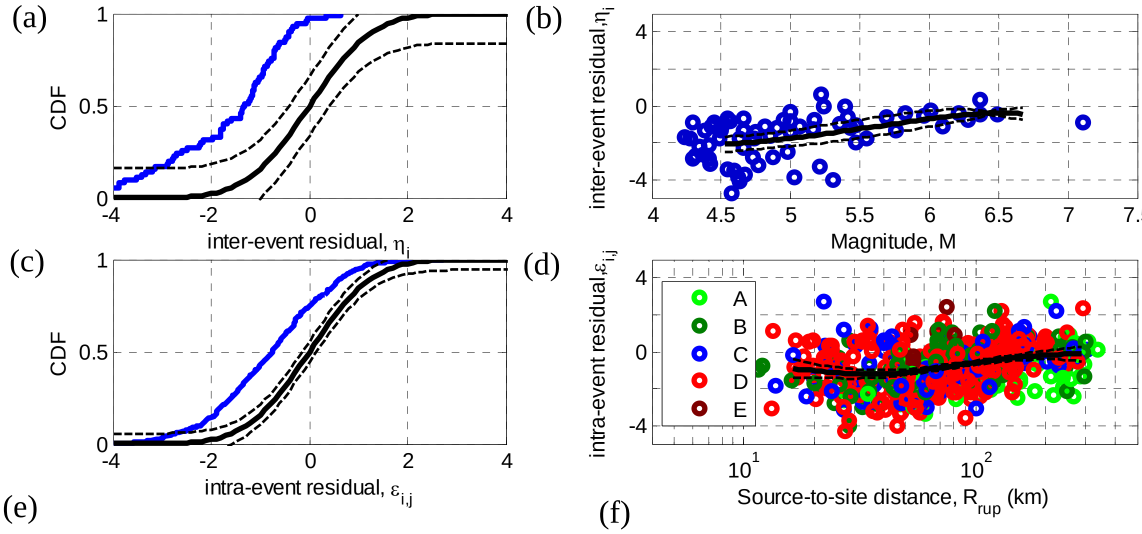

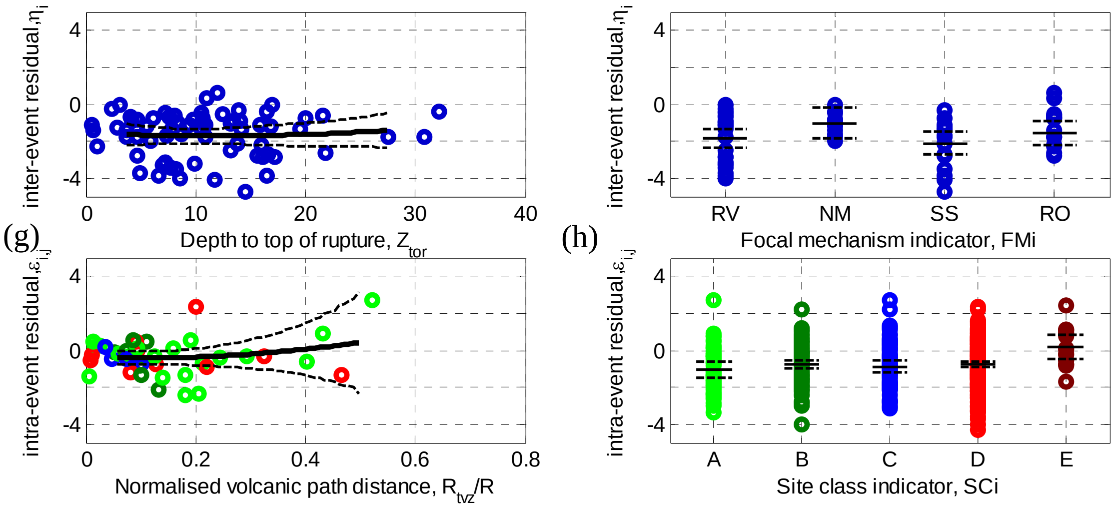

Figure 3 Residuals for Sa(0.5) using the McV06 model: (a) distribution of inter-event residuals; (b) inter-event residuals as a function of magnitude; (c) distribution of intra-event residuals; (d) intra-event residuals as a function of source-to-site distance; (e)&(f) inter-event residuals as a function of depth and focal mechanism; (g)&(h) intra-event residuals as a function of normalised volcanic path distance and site class.

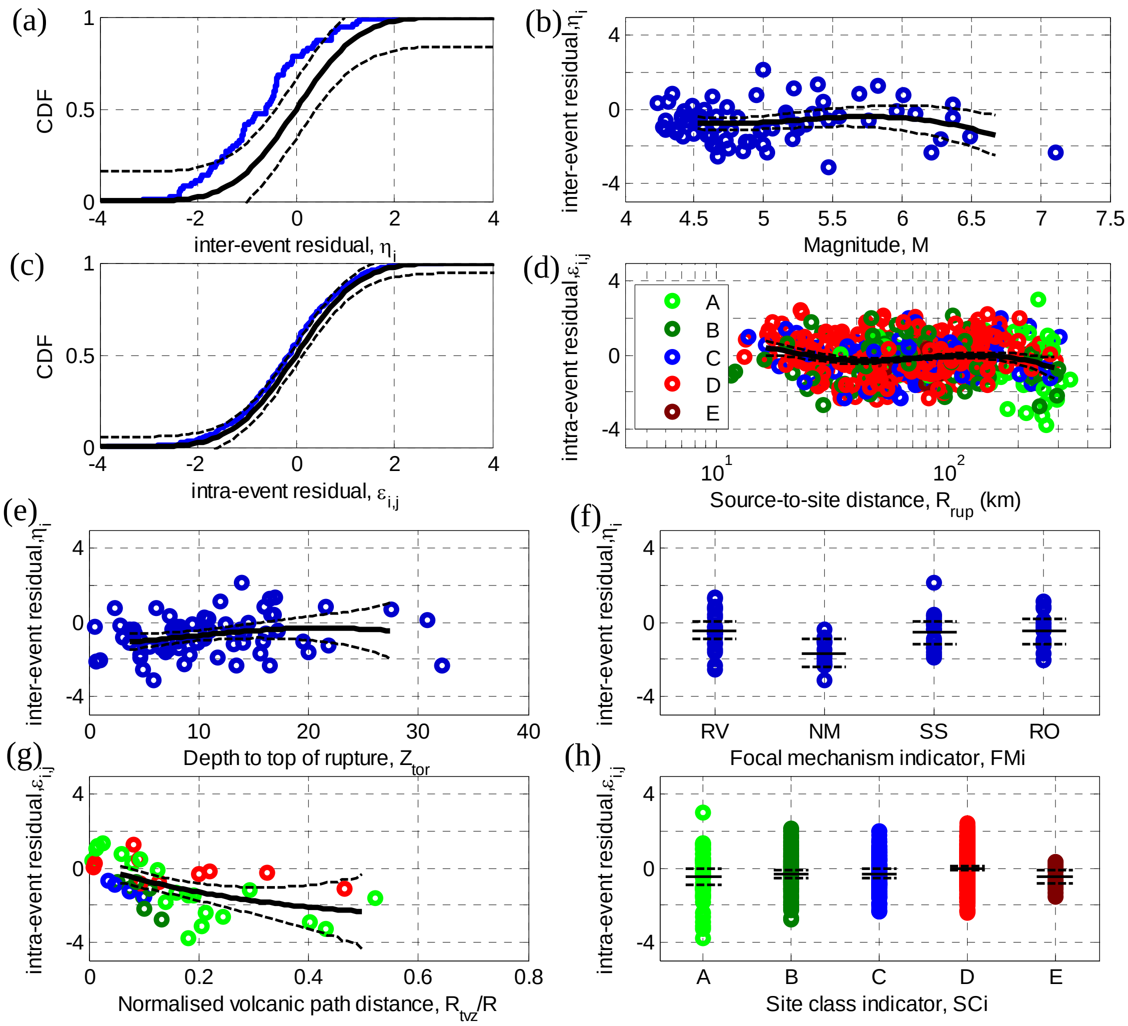

Figure 4 Residuals for PGA using the Z06 model: (a) distribution of inter-event residuals; (b) inter-event residuals as a function of magnitude; (c) distribution of intra-event residuals; (d) intra-event residuals as a function of source-to-site distance; (e)&(f) inter-event residuals as a function of depth and focal mechanism; (g)&(h) intra-event residuals as a function of normalised volcanic path distance and site class.

2.3.2.3 Boore and Atkinson (2008), BA08

Figure 5 illustrates the observed inter- and intra-event residuals for PGA from the NZ database using the BA08 model. Similar to the Z06 model, it can be seen that there is a systematic over-prediction of the ground motions for small magnitudes, and a slight over-prediction for larger magnitudes (M_w>5.5), partially the result of the aforementioned neglect of TVZ effects, and an over-prediction of site class A amplitudes from normal faulting events. Figure 5d illustrates that there is also an apparent bias in the near-source distance scaling ($20 < R_{rup} < 90$km). Figure 5e illustrates that there is a dependence of the inter-event residuals with source depth, because such an effect is not accounted for based on the R_{jb} distance measure. Figure 5f illustrates that there is a significant difference between the mean inter-event residuals as a function of focal mechanism. Normal events, in particular, are consistently over-predicted for short period amplitudes (i.e. $T < 0.5$ seconds) (Bradley 2010). Similar to the Z06 model, Figure 5g illustrates bias of the BA08 model with respect to normalised TVZ distance. Figure 5h illustrates the intra-event residuals as a function of site class. It can be seen that there is a good prediction for site classes B, C, and D, but an over-prediction for site classes A and E. This over-prediction only occurs for short periods (i.e. $T < 0.5$ seconds), with no bias across all site classes for longer vibration periods (Bradley 2010).

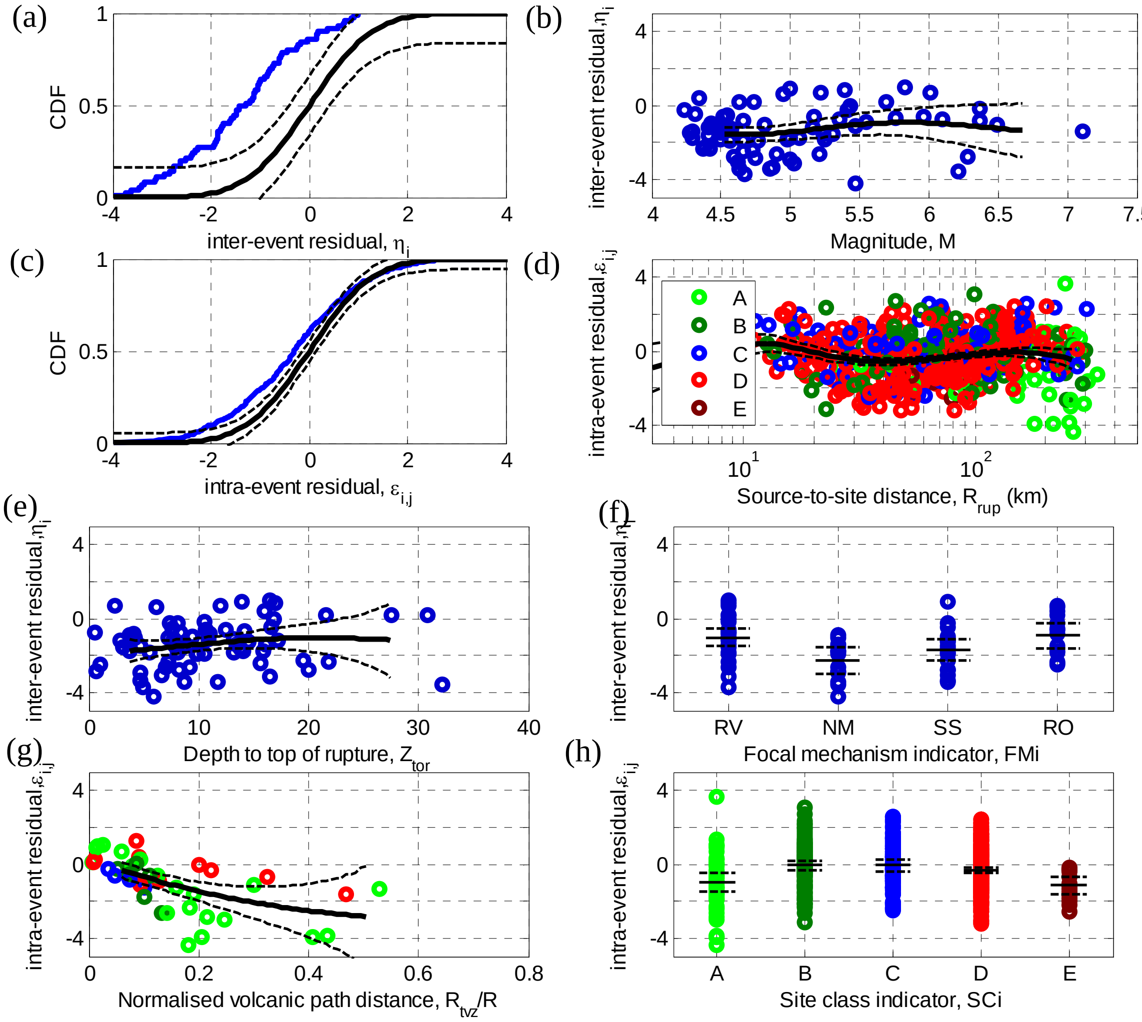

Figure 5 Residuals for PGA using the BA08 model: (a) distribution of inter-event residuals; (b) inter-event residuals as a function of magnitude; (c) distribution of intra-event residuals; (d) intra-event residuals as a function of source-to-site distance; (e)&(f) inter-event residuals as a function of depth and focal mechanism; (g)&(h) intra-event residuals as a function of normalised volcanic path distance and site class.

2.3.2.4 Chiou and Youngs (2008),CY08

This model, developed as part of the NGA project has been updated by Chiou et al. (2010a). It was examined nonetheless by Bradley (2010) but is not discussed herein.

2.3.2.5 Chiou et al. (2010a)-based model, C10

Figure 6 illustrates the observed inter- and intra-event residuals for PGA from the NZ database using the C10 model. It can be seen that based on the distributions of the inter- and intra-event residuals alone (i.e. Figure 6a and Figure 6c) that the C10 model is unbiased (i.e. this is the approach of Stafford *et al*. (2008) and Scherbaum *et al*. (2004)). As can be appreciated from Figure 2a, the C10 model predicts lower ground motions for small magnitude events than the CY08 model. This is clearly apparent in the inter-event residuals as a function of magnitude shown in Figure 6c with negligible bias for M_w<6. Similar to the BA08 and CY08 models there is an observed bias in large distance scaling at short periods, suggesting insufficient anelastic attenuation effects. Unlike the CY08 model, Figure 6e illustrates that there is no significant bias of the intra-event residuals for source depths less than 20km. As the source depth scaling of the CY08 and C10 models is identical this demonstrates the difficulty in examining biases in multidimensional data and models, using uni-dimensional marginal trends. Figure 6f illustrates that the C10 model over-predicts the amplitude of normal faulting events for PGA, and similar to the BA08 and CY08 models, this over-prediction only occurs for short periods (Bradley 2010). Figure 6g illustrates the bias in ground motion amplitudes as a function of normalized TVZ distance, which is not accounted for in the C10 model. Similar to the CY08 model, Figure 6h illustrates that the C10 model (which has the same site response formulation as the CY08 model) provides a good prediction for class B, C, D, E sites. There is also a minor reduction in the bias for site class A sites due to the improved M_w scaling.

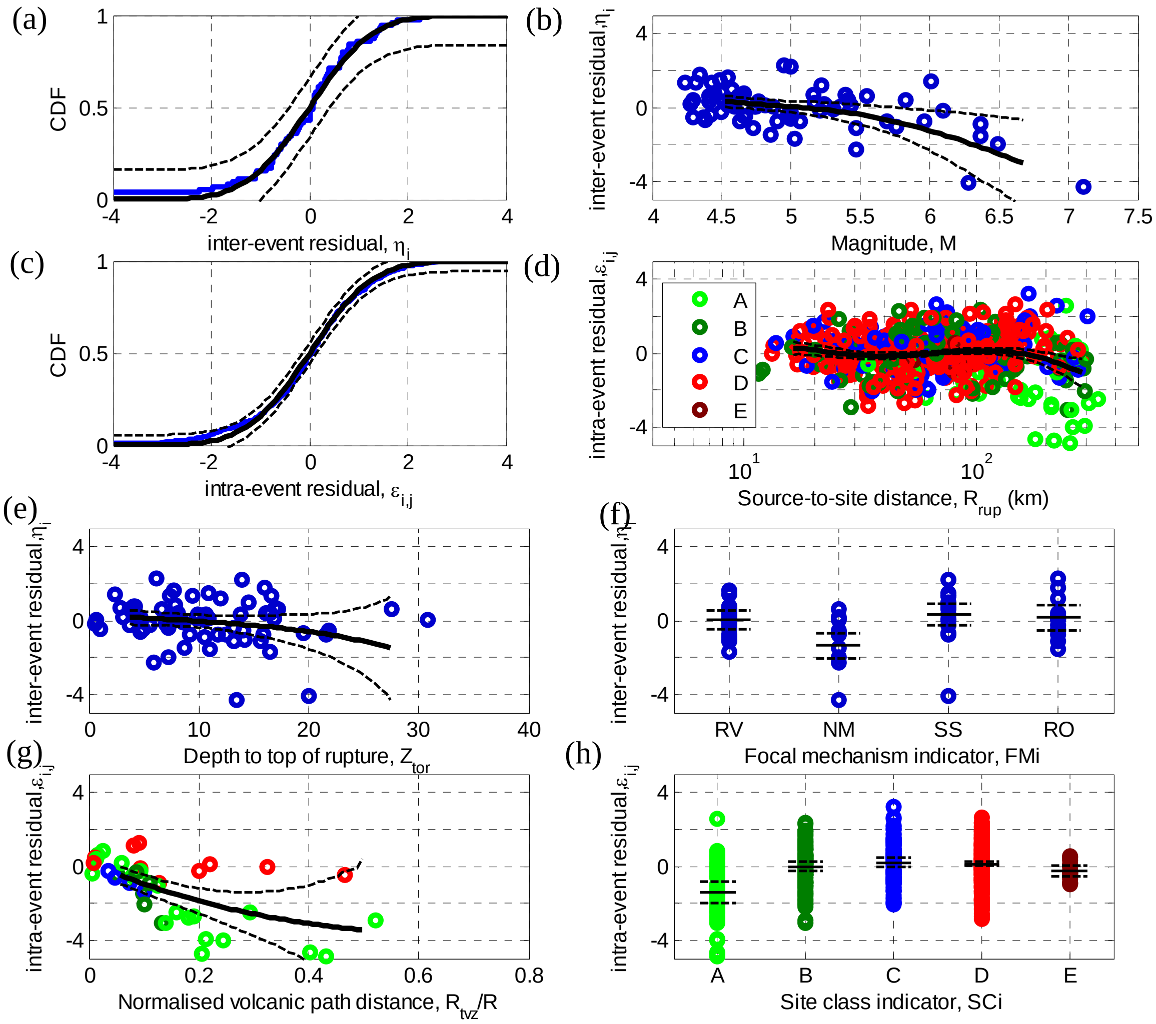

Figure 6 Residuals for PGA using the C10 model: (a) distribution of inter-event residuals; (b) inter-event residuals as a function of magnitude; (c) distribution of intra-event residuals; (d) intra-event residuals as a function of source-to-site distance; (e)&(f) inter-event residuals as a function of depth and focal mechanism; (g)&(h) intra-event residuals as a function of normalised volcanic path distance and site class.

2.4 Applicability of subduction slab GMPEs for New Zealand

The applicability of three different GMPEs for subduction slab events were examined. Firstly, the McVerry *et al.* (2006) (McV06) was considered, as it represents the present model used for NZ-specific seismic hazard studies when subduction slab events are of importance. Secondly, the Japanese-based model of Zhao *et al.* (2006) (Z06) was considered because of its extensive empirical database, and also because of the similarity of ground motions in Japan and New Zealand noted by previous researchers (Zhao et al. 1997). Finally, the Atkinson and Boore (2003) (AB03) GMPE based on world-wide empirical data was also considered.

2.4.1 Scaling of GMPEs with predictor variables

Figure 7a and Figure 7b illustrate the magnitude scaling of the median of the three GMPEs considered for both Sa(0.0) (i.e. PGA) and Sa(2.0). It can be seen that all of the GMPEs predict similar Sa(0.0) and Sa(2.0) amplitudes for $M_w = 7.0$, but that the scaling to small and large magnitudes is significantly different. This is primarily a result of the differences in the empirical databases used in the development of each of these models. It can be seen that the McV06 and Z06 models scale similarly to small magnitudes for Sa(0.0), but the gradient for the McV06 model is smaller than the Z06 model for Sa(2.0). On the other hand, the small magnitude scaling of the AB03 model is significantly more pronounced than the other two models for both Sa(0.0) and Sa(2.0). At large magnitudes (i.e. M_w > 7.5) the three different models display significantly different scaling. The AB03 model exhibits complete magnitude saturation at M_w =8.0, while the reduction in magnitude scaling for the McV06 is less pronounced. The Z06 model has the most significant scaling at large magnitudes, and in fact, for Sa(0.0) the Z06 model magnitude scaling is concave from above (i.e. the quadratic magnitude term is positive (2006)), leading to median predicted PGA values of approximately 2.0g at R_{RUP} = 50km from a M_w = 8.5 event.

The discrepancy between the three models at large magnitudes is concerning, given the importance of such events in seismic hazard studies, and the lack of large magnitude events in the NZ database with which the applicability of such large magnitude scaling for NZ can be scrutinized. The Z06 model utilized an empirical database with three subduction slab events above M_w = 7. However, these three events were not well-recorded (relative to other events in the Z06 database). Furthermore, the records from such events were recorded at large path distances which Zhao (2010) has illustrated that the Z06 model over-predicts. Hence, it is concluded that the large magnitude scaling of the Z06 model (particularly the positive magnitude squared dependence at short periods) is inappropriate. As previously mentioned, the McV06 model used a very small empirical database with only 20 subduction slab events and a maximum magnitude of $M_w = 6.69$. The AB03 model used an empirical database with only four events above $M_w = 7$, with the best recorded event contributing 14 records.

Figure 7c and Figure 7d illustrate the path scaling of the median of the three subduction slab GMPEs considered for both Sa(0.0) and Sa(2.0). In general, the path scaling of GMPEs can be separated into: (i) near-source scaling considering the finite dimension of the fault source; (ii) geometric spreading at moderate to large distances; and (iii) anelastic attenuation at large distances. The different functional forms adopted for each of these three aspects of path scaling for the considered models are discussed below.

Figure 7c and Figure 7d illustrate that the McV06 model exhibits the most pronounced near-source saturation, followed by the AB03 model and then the Z06 model. The lack of near-source saturation for the Z06 model coupled with the aforementioned pronounced large magnitude scaling leads to very large ground motions at near source distances.

The path scaling of the three different models at moderate to large distances (i.e. beyond where finite fault effects are significant), are relatively similar, but have varying values for the geometric spreading coefficient. The McV06 model has a geometric spreading coefficient ranging from approximately -2.5 at short periods to -2.0 at long periods. The Z06 model has an effective geometric spreading coefficient which ranges from -1.5 at short periods to -1.1 at long periods. Finally, the AB03 model has a geometric spreading coefficient which is independent of vibration period, but very weakly dependent on magnitude and has a value of -1.7 for M_w = 7.

At long distances, both the Z06 and the AB03 model include an anelastic attenuation term, but the McV06 model does not (although an anelastic attenuation term for TVZ attenuation is considered). This absence of anelastic attenuation in the McV06 model is clearly evident in the lack of reduction in Sa(0.0) amplitudes at large distances. The magnitude of anelastic attenuation coefficient in the AB03 model, which ranges from 0.002 at short periods to 0.00045 at long periods is notably lower than the Z06 model (similar to the NZ-specific crustal model) values of 0.0056 at short periods to 0.0015 at long periods.

Figure 7e and Figure 7f illustrate the median response spectra predicted by the three considered GMPEs for magnitudes 5.5 and 7.5 and distances of 50 and 150 km. For both magnitudes and path distances considered it can be seen that the shape of the predicted AB03 spectra is significantly ‘flatter’ than that for the McV06 and Z06 models. It can also be seen that the AB03 spectra for $M_w =$ 5.5 are lower than the Z06 and McV06 predictions as a result of the aforementioned magnitude scaling. Similarly, for $M_w =$7.5 the Z06 model predicts higher spectral amplitudes as a result of the Z06 large magnitude scaling. One final observation is the unsmoothed nature of the McV06 predicted spectral amplitudes with period.

Figure 7g and Figure 7h illustrate the dependence of the inter- and intra-event residuals with vibration period.

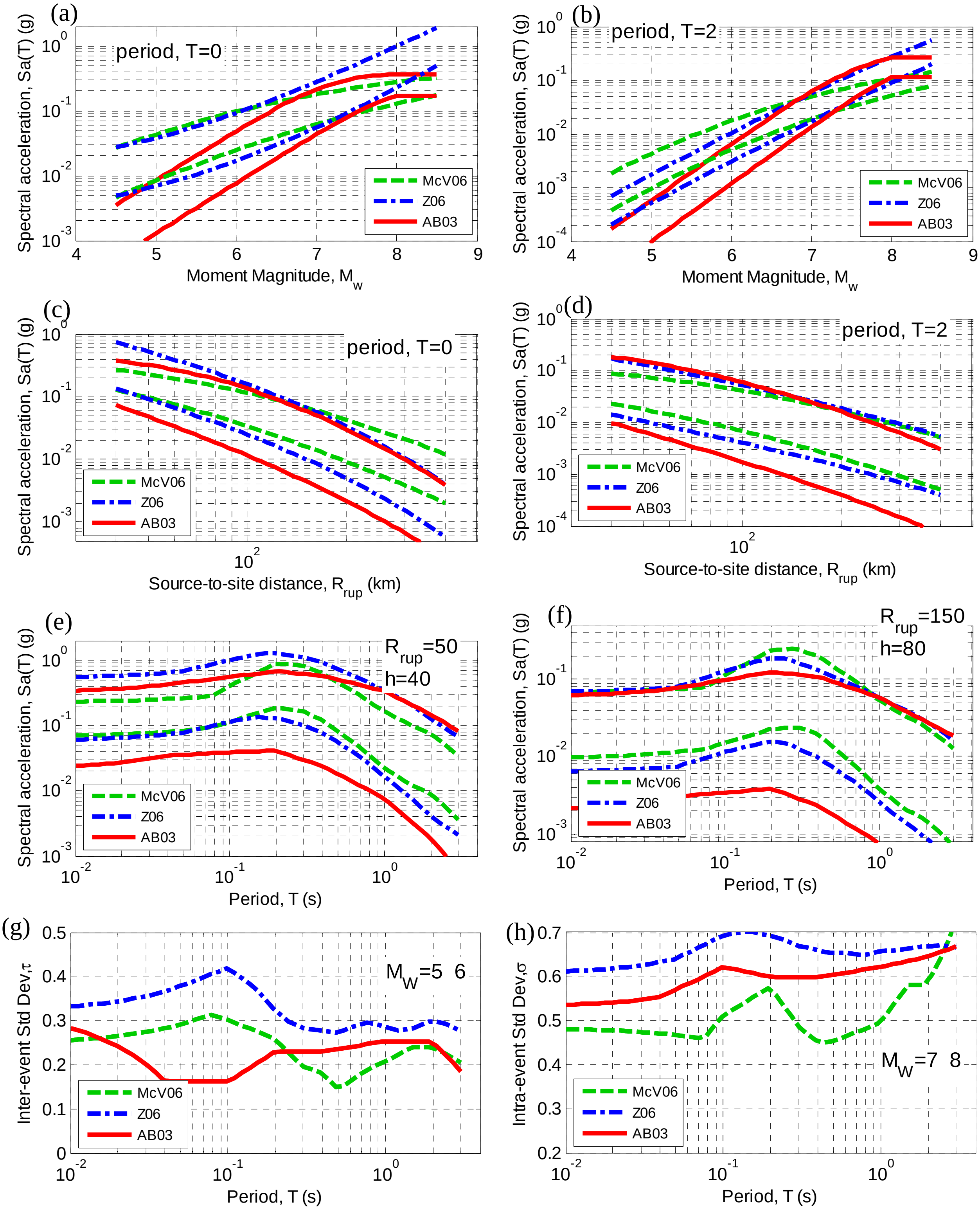

Figure 7 Predictor variable scaling of the considered GMPEs: (a)&(b) magnitude scaling for source-to-site distances of 50 and 120 km; (c)&(d) path scaling for magnitudes 6 and 7.5; (e)&(f) median response spectra for magnitudes 5.5 and 7.5; (g)&(h) inter- and intra-event standard deviation scaling with vibration period. All plots, unless noted, are for a focal depth of 40km and NZ site class C site.

2.4.2 Observed inter- and intra-event residuals from the NZ database

2.4.2.1 McVerry et al. (2006), McV06

Figure 8 illustrates the observed inter- and intra-event residuals for Sa(1.0) from the NZ database using the McV06 model. Similar to the observations for crustal events it is immediately obvious that the McV06 model significantly over-predicts ground motions from $M_w < 6$ events (Figure 8a and Figure 8c). Figure 8e also illustrates that there is some bias of the intra-event residuals as a function of source to site distance (recall in the discussion pertaining to Figure 8 that the geometric spreading coefficient for the McV06 was significantly larger than the Z06 and AB03 models). Figure 8f illustrates that there is a trend in the inter-event residuals as a function of source depth, but this observed trend is likely influenced by the poor magnitude scaling of the McV06 model. Figure 8g illustrates that similar to the observations for crustal events, the McV06 model over- and under-predicts ground motions for site class A and E sites, respectively (using the A/B factors for site class A sites and the D factors for site class E sites). This is because the McV06 model considers the response of sites A and B and sites D and E to be equal (McVerry et al. 2006). Figure 8h provides an insightful result, that despite the McV06 model considering the anelastic attenuation in the TVZ, there is still bias observed in the intra-event residuals as a function of the normalised-TVZ path distance. This observation may be the result of the fact that the McV06 model does not consider anelastic attenuation for the non-TVZ portion of the propagation path.

2.4.2.2 Zhao et al. (2006), Z06

Figure 9 illustrates the observed inter- and intra-event residuals for Sa(1.0) from the NZ database using the Z06 model. Similar to the McV06 model, it can be seen that the Z06 model over-predicts ground motions from events with $M_w < 5$, although the over-prediction is not as pronounced as the McV06 model. Figure 9e also illustrates that there is an under-prediction of ground motions recorded at large source-to-site distances caused by a reduction in the apparent rate of attenuation. Zhao (2010) attributed this reduction in large distance attenuation to constructive interference of waves propagating through the mantle and those propagating a significantly larger distance within the subduction slab itself. It is not immediately clear on inspection of Figure 9a, but Figure 9b illustrates that the standard deviation of the intra-event residuals is less than that for a standard normal distribution. This observation is more pronounced at short vibration periods (see appendix). This is the result of the Z06 model having a relatively large standard deviation in comparison with the McV06 and AB03 models, which based on the NZ database appears to be too large. Figure 9f illustrates that there is negligible dependence of the inter-event residuals as a function of source depth. Figure 9g illustrates that while the mean of the intra-event residuals for site classes C and E are statistically different from zero, that the bias is still relatively minor in relation to the McV06 model site class predictions. Finally, Figure 9h illustrates that there is a dependence of the intra-event residuals as a function of the normalised TVZ distances resulting from the lack of a TVZ-specific term in the Z06 model.

2.4.2.3 Atkinson and Boore (2003), AB03

As is evident from the qualitative predictor variable scaling the AB03 model provided a poor representation of the NZ ground motions (Bradley 2010), and is not discussed further for subduction interface events.

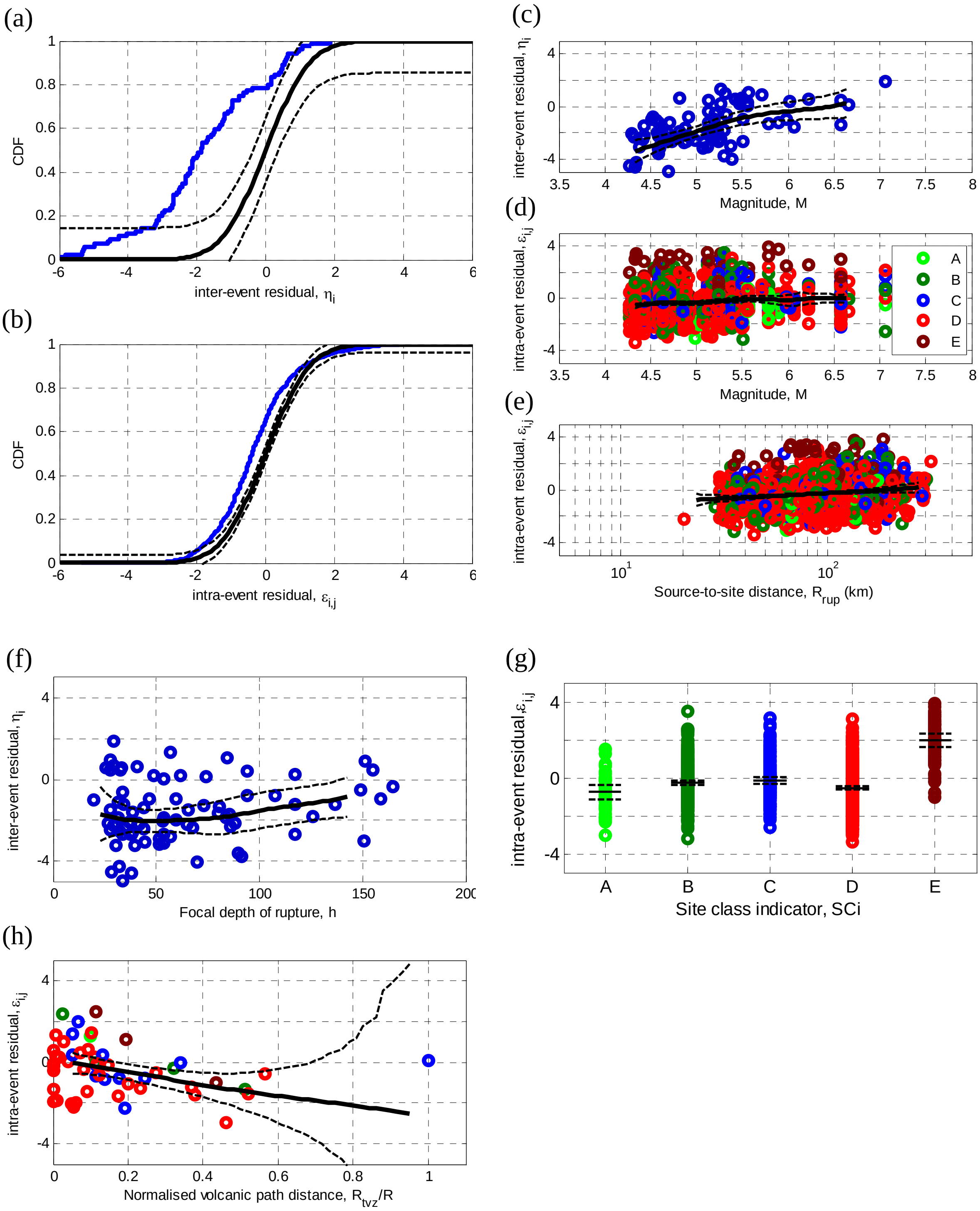

Figure 8 Residuals for Sa(1.0) using the McV06 model: (a)&(b) distribution of inter- and intra-event residuals; (c)&(d) inter- and intra-event residuals as a function of magnitude; (e) intra-event residuals as a function of distance; (f) inter-event residuals as a function of depth; (g)&(h) intra-event residuals as a function of site class and normalised volcanic path distance.

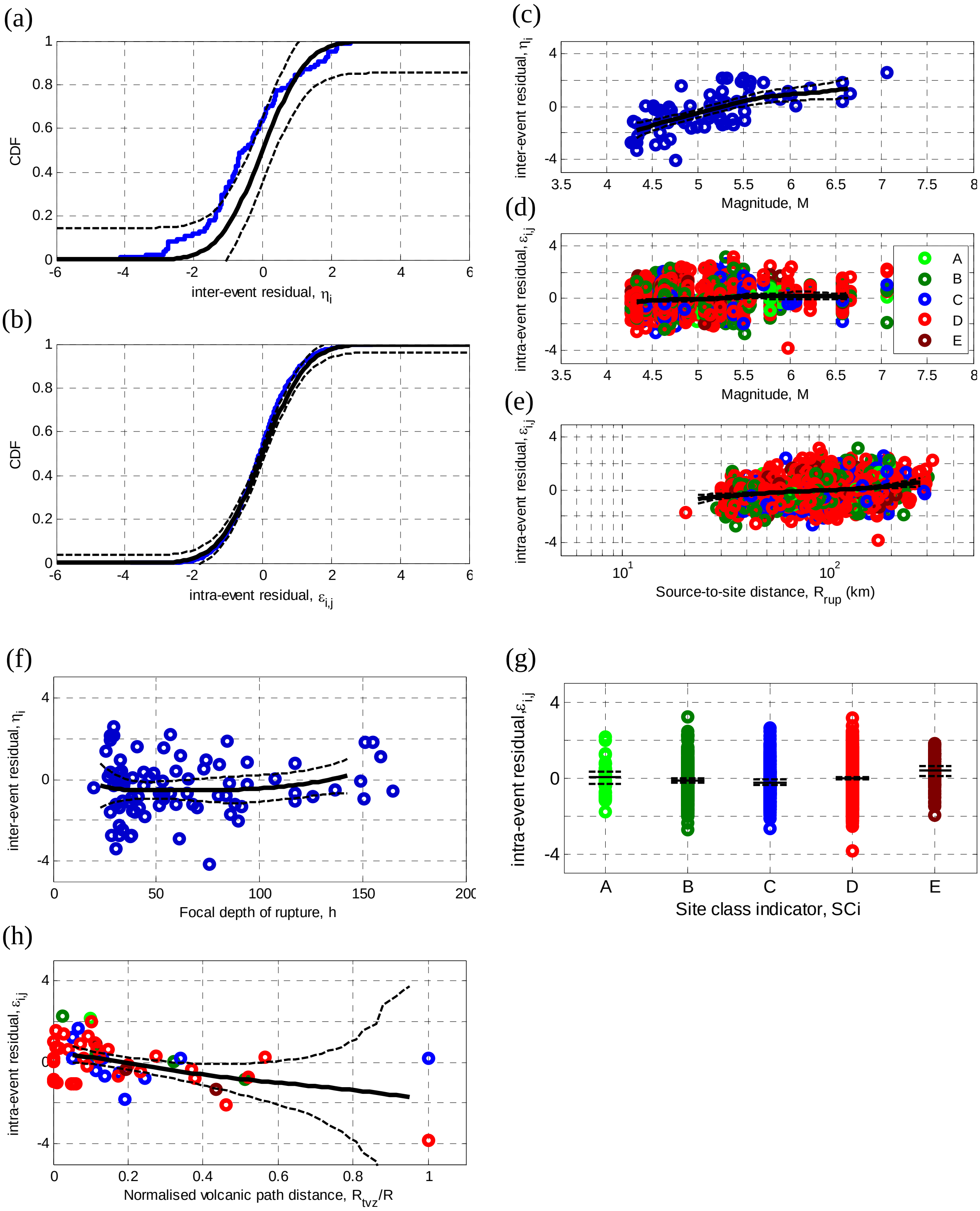

Figure 9 Residuals for Sa(1.0) using the Z06 model: (a)&(b) distribution of inter- and intra-event residuals; (c)&(d) inter- and intra-event residuals as a function of magnitude; (e) intra-event residuals as a function of distance; (f) inter-event residuals as a function of depth; (g)&(h) intra-event residuals as a function of site class and normalised volcanic path distance.

2.5 Applicability of subduction interface GMPEs for New Zealand

The applicability of three different GMPEs for subduction interface events were examined. Firstly, the McVerry *et al.* (2006) (McV06) model was considered, as it represents the present model used for NZ-specific seismic hazard studies when subduction interface events are of importance. Secondly, the Japanese-based model of Zhao *et al.* (2006) (Z06) was considered because of its extensive empirical database, and also because of the similarity of ground motions in Japan and New Zealand noted by previous researchers (Zhao et al. 1997). Finally, the Atkinson and Boore (2003) (AB03) GMPE based on world-wide empirical data was also considered. The Youngs *et al.* (1997) model, which was also utilized in the most recent update of the USGS national seismic hazard maps (Petersen et al. 2008), was not considered because it does not provide a distinction between inter- and intra-event standard deviations making it impossible to partition total residuals into inter- and intra-event components.

2.5.1 Scaling of GMPEs with predictor variables

Figure 10a and **Figure 10**b illustrate the magnitude scaling of the median of the three subduction interface GMPEs considered for both Sa(0.0) (i.e. PGA) and Sa(2.0). Similar to the observations for subduction interface events, it can be seen that at small magnitudes the AB03 model predicts significantly smaller spectral amplitudes than the McV06 and Z06 models. The McV06 model predicts the largest spectral amplitudes for small magnitude events. The Z06 model predicts only slightly smaller Sa(0.0) amplitudes than the McV06 model at small magnitudes, but significantly smaller Sa(2.0) amplitudes. At large magnitudes (i.e. M_w > 7.5) the three models also display significantly different magnitude scaling. The AB03 model exhibits complete magnitude saturation for Sa(0.0), while the reduction in magnitude scaling for the McV06 is less pronounced. Similar to the observations made for active shallow crustal and subduction slab events, the Z06 model exhibits a significantly less pronounced reduction in magnitude scaling at large magnitudes. The discrepancy between the three models at large magnitudes is concerning, given the importance of such events in seismic hazard studies, and the lack of large-magnitude well-recorded subduction interface events in the NZ database with which the applicability of such large magnitude scaling for NZ can be scrutinized. The Z06 model utilized an empirical database with three well-recorded subduction interface events above $M_w = 7$, including the $M_w = 8.29$ 2003 Tokachi-Oki event (319 records), and its $M_w = 7.37$ aftershock (222 recordings). Conversely, the McV06 model was developed from an empirical database containing only 7 subduction interface events, none of which were well recorded. The AB03 contains 11 subduction interface events with $M_w > 7$, with the best recorded having 23 ground motion records.

Figure 10c and **Figure 10**d illustrate the path scaling of the median of the three subduction interface GMPEs considered for both Sa(0.0) and Sa(2.0). In general, the path scaling of GMPEs can be separated into: (i) near-source scaling considering the finite dimension of the fault source; (ii) geometric spreading at moderate to large distances; and (iii) anelastic attenuation at large distances. The different functional forms adopted for each of these three aspects of path scaling for the considered models are discussed below. **Figure 10**c illustrates that the AB03 model exhibits the most pronounced near-source saturation for both Sa(0.0) and Sa(2.0), followed by the McV06 model and then the Z06 model. The less pronounced near-source saturation for the Z06 model coupled with the aforementioned large magnitude scaling leads to large ground motions at near source distances. The path scaling of the three different models at moderate to large distances (i.e. beyond where finite fault effects are significant), are relatively similar, with one notable exception being the very low attenuation of Sa(2.0) amplitudes from an $M_w = 7.5$ event predicted by the AB03 model. At large distances, both the Z06 and AB03 models include an anelastic attenuation term, but the McV06 model does not (although an anelastic attenuation term for TVZ attenuation is considered). This absence of anelastic attenuation in the McV06 model is evident in the lack of reduction in Sa(0.0) amplitudes at large distances. The magnitude of the anelastic attenuation coefficient in the AB03 model, which ranges from 0.002 at short periods and tending to zero for periods greater than 2 seconds, is notably lower than the Z06 model values of 0.0056 at short periods to 0.0015 at long periods.

Figure 10e and **Figure 10**f illustrate the median response spectra predicted by the three considered GMPEs for magnitudes 5.5 and 7.5 and path distances of 25 and 100 km. For the magnitudes and path distances considered it can be seen that the shape of the predicted AB03 spectra is significantly ‘flatter’ than that for the McV06 and Z06 models. It can also be seen that the AB03 spectra for $M_w =$ 5.5 are lower as a result of the aforementioned magnitude scaling. Similarly, for $M_w =$ 7.5 the Z06 model predicts higher spectral amplitudes as a result of the Z06 large magnitude scaling. One final observation is the unsmoothed nature of the McV06 predicted spectral amplitudes with period.

The McV06, Z06 and AB03 models use the same inter- and intra-event standard deviations for both subduction slab and subduction interface models.

2.5.2 Observed inter- and intra-event residuals from the NZ database

2.5.2.1 McVerry et al. (2006), McV06

Figure **11** illustrates the observed inter- and intra-event residuals for Sa(1.0) from the NZ database using the McV06 model. Similar to the observations for active shallow crustal and subduction slab events it is immediately apparent that the McV06 model significantly over-predicts ground motions from $M_w <$ 6 events (

Figure **11**a and

Figure **11**c). This over-prediction is relatively minor at short vibration periods, but increases with increasing vibration period.

Figure **11**e also illustrates that there a dependence of the intra-event residuals as a function of source to site distance for distances less than 100km and vibration periods larger than 0.5 seconds.

Figure **11**f illustrates that there is no apparent trend in the inter-event residuals as a function of source depth.

2.5.2.2 Zhao et al. (2006), Z06

Figure **12** illustrates the observed inter- and intra-event residuals for Sa(1.0) from the slab NZ database using the Z06 model. It can be seen in

Figure **12**c that there is essentially no bias of the inter-event residuals as a function of magnitude for all spectral periods considered.

Figure **12**a and

Figure **12**c illustrate that there is a constant bias in the inter-event residual, but this was only observed for Sa(1.0). One point of note, not apparent in

Figure **12**, is the large over-prediction of the 2009 M_w = 7.63 event (Fry et al. 2010), which had an inter-event residual of approximately -2 for periods of 0.0, 0.2, and 0.5.

Figure **12**e illustrates that there is also no observed bias in the intra-event residuals with source-to-site distance.

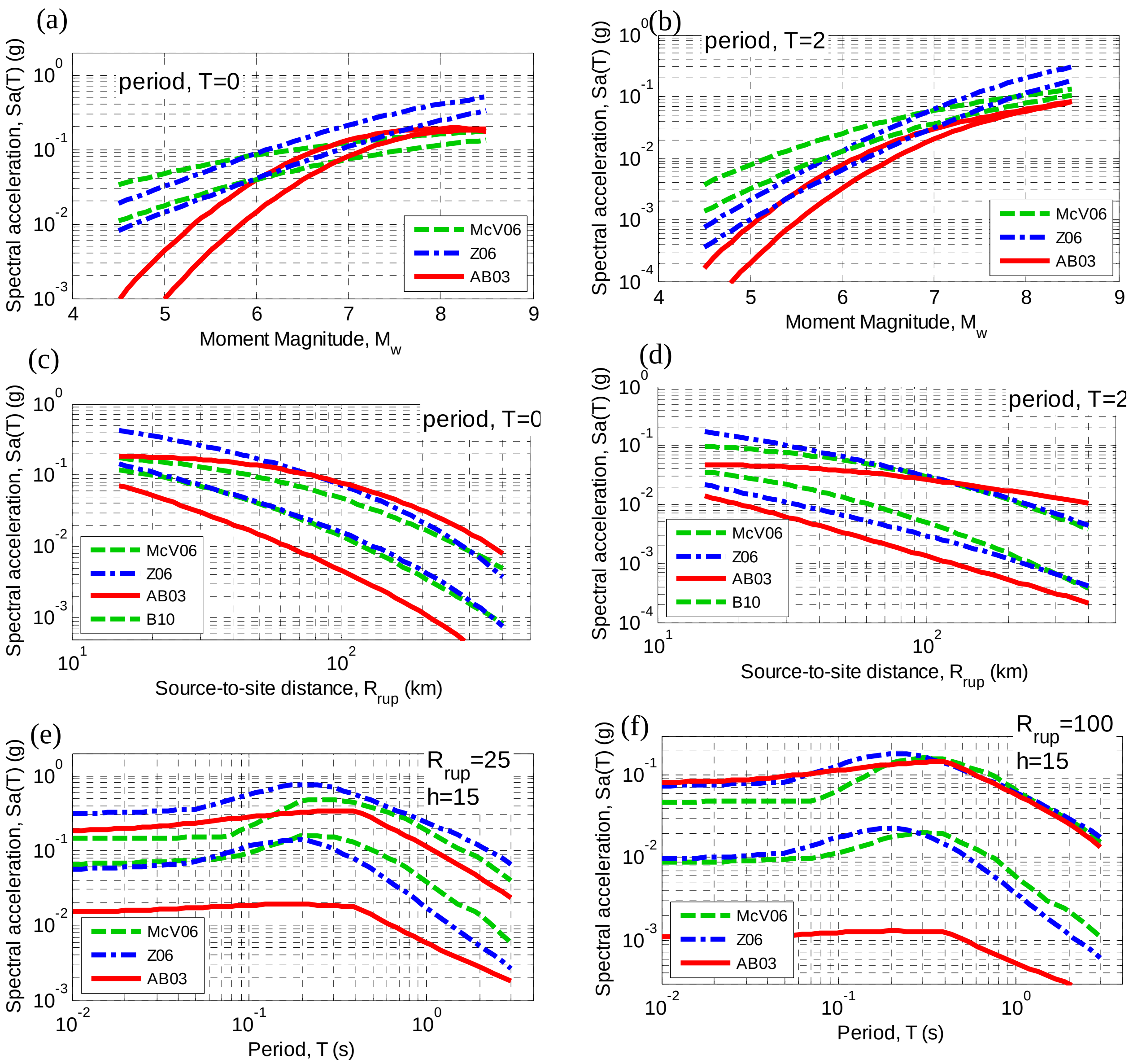

Figure 10 Predictor variable scaling of the considered GMPEs: (a)&(b) magnitude scaling for source-to-site distances of 15 and 25 km; (c)&(d) path scaling for magnitudes 6 and 7.5; (e)&(f) median response spectra for magnitudes 5.5 and 7.5. All plots, unless noted, are for a focal depth of 15 km and NZ site class C site.

Figure **12**b illustrates that the standard deviation of the intra-event residuals is less than that for a standard normal distribution as indicated by the empirical distribution intersecting the KS bounds. This is a possible result of the Z06 model having a relatively large standard deviation in comparison with the McV06 and AB03 models.

Figure **12**f illustrates that there is negligible dependence of the inter-event residuals as a function of source depth.

Figure **12**g illustrates that while there is all small bias in the site class B and D predictions for Sa(1.0) (as indicated mean of the intra-event residuals being statistically different from zero).

At all vibration periods except for Sa(5.0) site class B motions were over-predicted, while site class C and D motions were also biased for Sa(0.5) and Sa(1.0), respectively.

2.5.2.3 Atkinson and Boore (2003), AB03.

As is evident from the qualitative predictor variable scaling the AB03 model provided a poor representation of the NZ ground motions (Bradley 2010), and is not discussed further for subduction interface events.

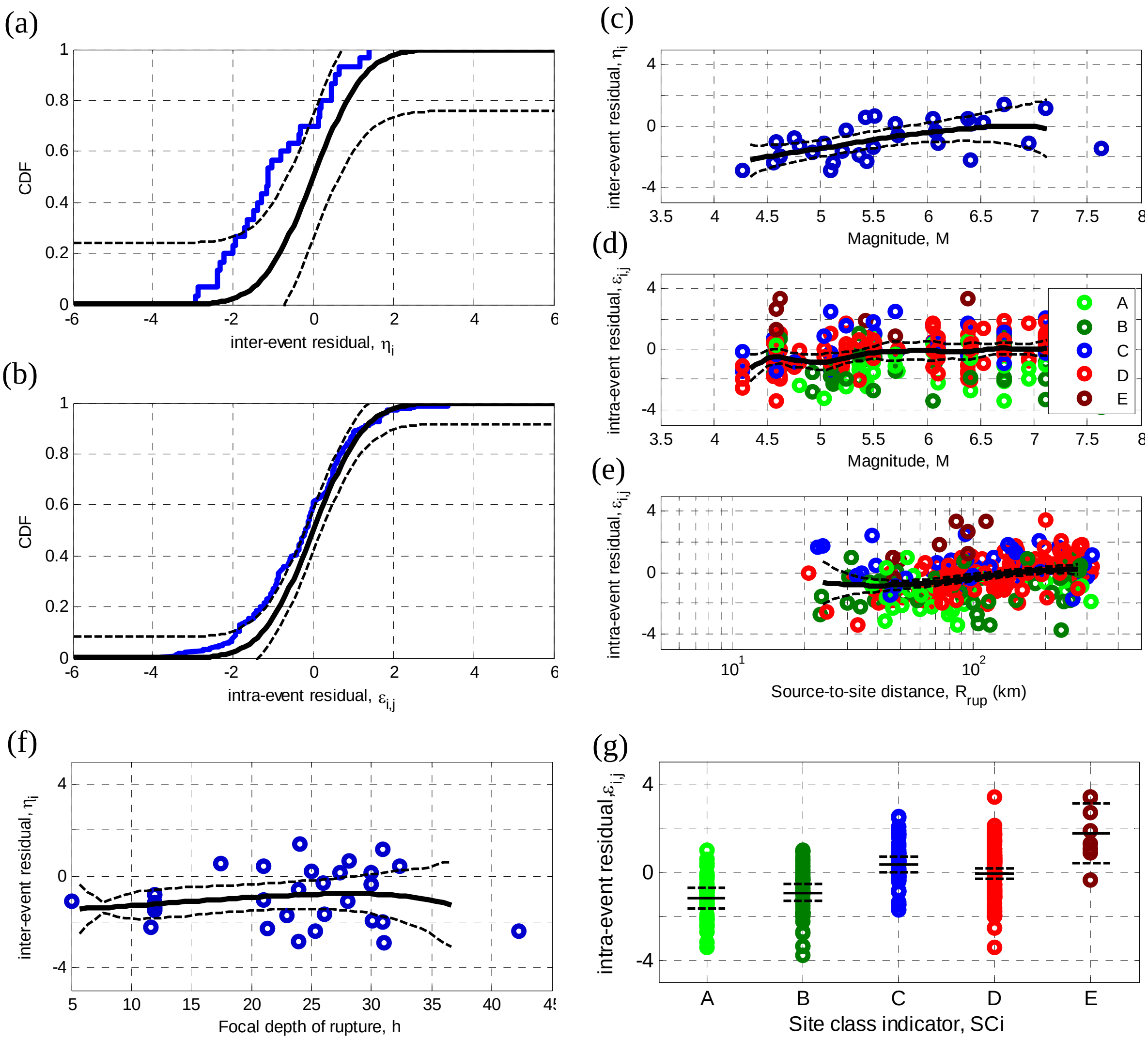

Figure 11 Residuals for Sa(1.0) using the McV06 model: (a)&(b) distribution of inter- and intra-event residuals; (c)&(d) inter- and intra-event residuals as a function of magnitude; (e) intra-event residuals as a function of distance; (f) inter-event residuals as a function of depth; and (g) intra-event residuals as a function of site class.

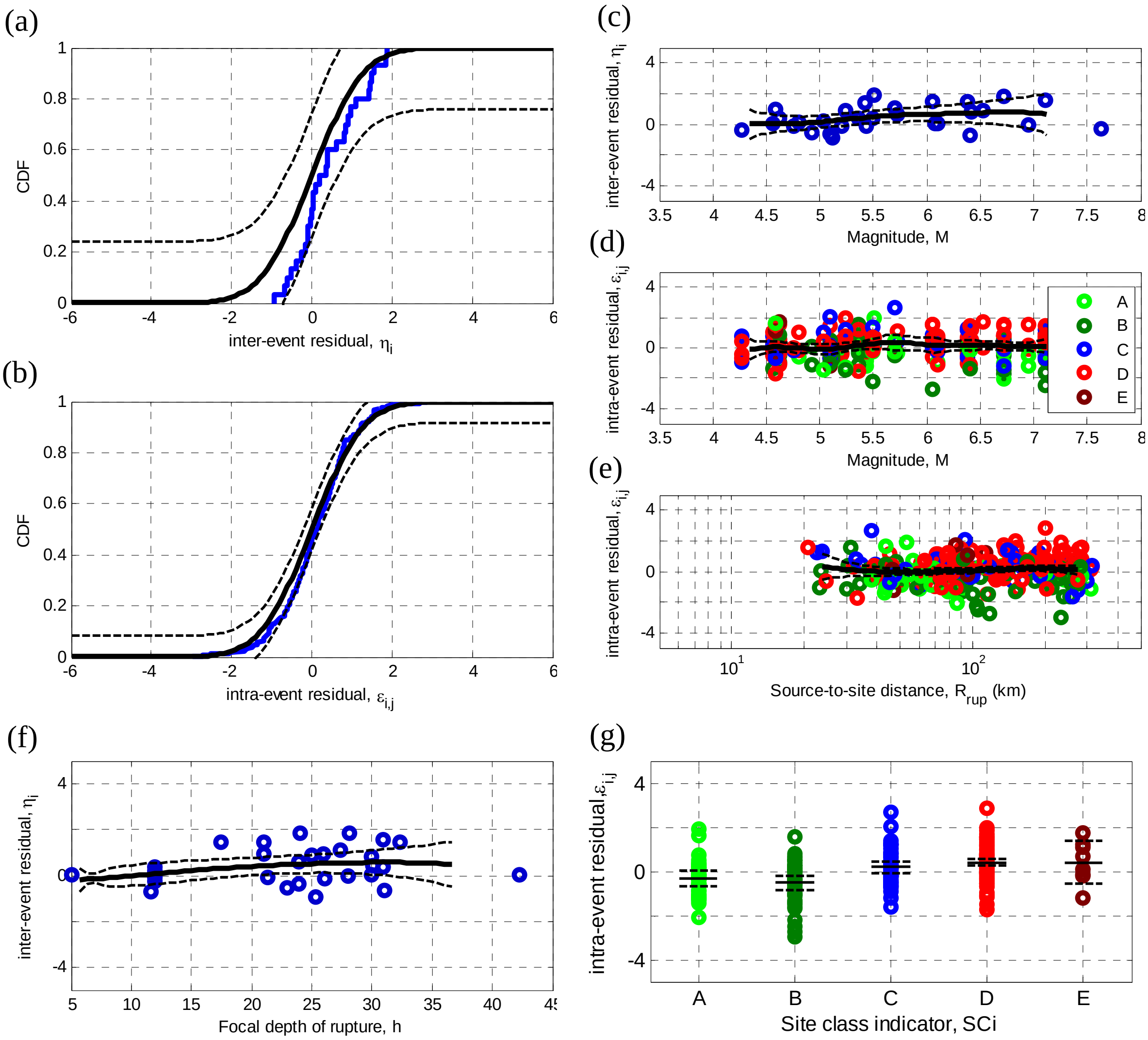

Figure 12 Residuals for Sa(1.0) using the Z06 model: (a)&(b) distribution of inter- and intra-event residuals; (c)&(d) inter- and intra-event residuals as a function of magnitude; (e) intra-event residuals as a function of distance; (f) inter-event residuals as a function of depth; and (g) intra-event residuals as a function of site class.

2.6 Consideration of epistemic uncertainty in NZ ground motion prediction

2.6.1 Active shallow crustal earthquakes

The previous results illustrate that the C10 and BA08 models are considered the most robust for large magnitude active shallow crustal events, due to having the largest number of ground motions from such earthquakes in their derivation. Furthermore the C10 model also did not illustrate any significant bias for small magnitudes. The McV06 model was shown to be biased for small magnitudes and has irregular variation in scaling (distance and standard deviation) likely due to insufficient data for constraint. The Z06 model was likely biased for large magnitude events based on its significantly different value than the remaining models. Based on these main points the following logic tree weights for active shallow crustal events in Table 2 and Figure 13 were assigned.

Table 2 Logic tree weights used for active shallow crustal earthquakes.

McVerry et. al (2006)	0.2
Zhao et al. (2006)	0.2
Boore and Atkinson (2008)	0.28
Chiou et al (2010)	0.32

2.6.2 Subduction slab and subduction interface earthquakes

The previous results illustrated firstly that the AB03 model provided a poor prediction for all magnitudes and distances considered. Secondly, both the McV06 and Z06 model illustrated some bias for small magnitudes (particularly for subduction slab events). Because the Z06 model was based on a more comprehensive dataset it is given a slightly larger logic tree weight than the McV06 model, which are provided in Table 3 and Figure 13.

Table 3 Logic tree weights used for subduction slab and subduction interface earthquakes.

McVerry et. al (2006)	0.4
Zhao et al. (2006)	0.6
Atkinson and Boore (2003)	0.0

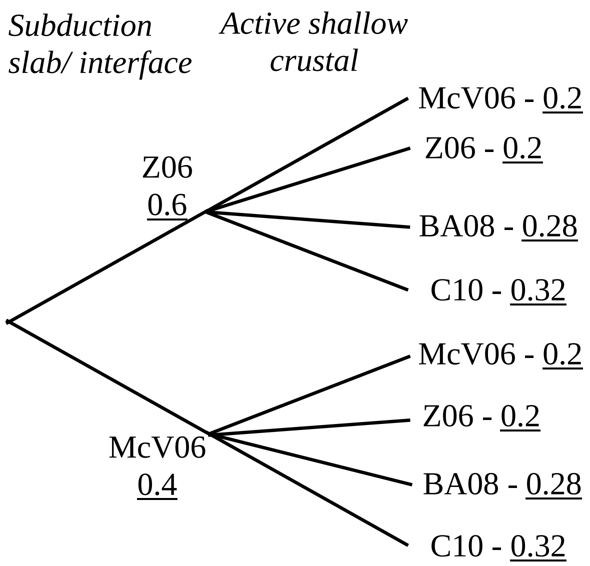

Figure 13 Adopted logic tree for addressing ground motion prediction uncertainty for various tectonic types.

3.0 EPISTEMIC UNCERTIANTIES IN EARTHQUAKE RUPTURE FORECAST (ERF)

3.1 Current Earthquake Rupture Forecast Methodology for NZ

The current methodology adopted for PSHA in NZ, as implemented by Stirling et al. (2002) and Stirling et al. (2011), is based on a combination of fault-based sources and distributed seismicity. The fault source model uses the dimensions and slip rates of mapped fault sources to develop magnitude-frequency estimates for "characteristic" earthquakes, and the spatial distribution of historical seismicity is used to develop magnitude-frequency estimates for the background seismicity model. Because the fault-based seismicity is assumed to be characteristic in nature it is assumed that events less than this characteristic magnitude are modelled by the distributed background sources.

Only epistemic uncertainties in the fault-based component of the ERF are considered in this study, consistent with similar studies conducted elsewhere (WGCEP 2003). That is, no uncertainties in background seismicity are considered. The implications of this are discussed in light of the results obtained at a later section.

3.2 Methodology for consideration of epistemic uncertainties in fault model

3.2.1 Deterministic calculation of source magnitudes and rates of occurrence

The seismic hazard for characteristic ruptures, as modelled in the fault-model of Stirling et al. (2002) and Stirling et al. (2011), is governed by the magnitude, M_w, and recurrence interval, λ, of the characteristic rupture. The calculation of these parameters follows the basics steps below:

The fault is described by several geometrical parameters (length, L, top of rupture extent, D_{top}, bottom of rupture extent, D_{bottom}, dip, δ) and slip parameters (slip rate, $\dot{s}$, coupling coefficient, c). Based on the fault geometry a magnitude scaling relation is used to compute the magnitude of the rupture

$$M_w \sim f(L, W) \tag{1}$$

where the rupture down-dip width is computed from:

$$W = (D_{bottom} - D_{top})/\sin(\delta) \tag{2}$$

Such magnitude scaling relations may be either a function of fault length alone (length scaling), or fault length and width (sometimes via their product, fault area). For New Zealand faults, three different magnitude scaling relations are used dependent on the classification of the fault.

For plate-boundary faults, the relationship of Hanks and Bakun (2002) is utilized:

$$Median: \overline{M_w} = 3.07 + \frac{4}{3} logA$$

$$Sigma: \sigma_{lnMw} = 0.22 \tag{3}$$

For normal faults in volcanic and rift environments, the relation of Villamor et al. (2001) is utilized:

$$Median: \overline{M_w} = 3.39 + \frac{4}{3} logA$$

$$Sigma: \sigma_{lnMw} = 0.195 \tag{4}$$

For all other crustal faults, the relationship of Berryman et al. (2001) is utilized:

$$Median: \overline{M_w} = 4.19 + \frac{2}{3} logW + \frac{4}{3} logL$$

$$Sigma: \sigma_{logMw} = 0.18 \tag{5}$$

For subduction interface events, the relationship of Strasser et al. (2010) is utilized:

$$Median: \overline{M_w} = 4.441 + 0.846 logA$$

$$Sigma: \sigma_{logMw} = 0.286 \tag{6}$$

Subduction slab events were modelled as point sources in the background seismicity model. In Equations (3)-(6) all logarithms are base 10. It is noted that only the median magnitude obtained from the above magnitude-scaling relationships are used in computing the characteristic magnitudes in Stirling et al. (2002) and Stirling et al. (2011). The exception is for subduction interface events, where the magnitudes were based on the definition of moment magnitude (Equation (8)) with assumed values for average displacement (Stirling et al. 2011).

For the given source magnitude, the moment magnitude, M_o, can be computed from:

$$logM_o = 16.05 + 1.5M_w \tag{7}$$

The total moment rate for the fault can be computed as follows:

$$\dot{M}_o = \mu A \dot{s} c \tag{8}$$

where μ is the shear rigidity of the fault interface; $\dot{s}$ is the average slip rate over the area of the fault surface, and c is the coupling coefficient. Based on the assumption that all of the moment rate accumulating on the fault surface is released in characteristic events, the mean occurrence rate can be computed from:

$$\lambda = \frac{\dot{M}_o}{M_o} \tag{9}$$

Table 4 provides a summary of the key parameters and relationships which are required in the determination of the fault-based parameters (i.e. magnitude and recurrence interval). Each of these parameters/relationships contain epistemic uncertainty.

Table 4 Key parameters and relationships in the determination of fault-based parameters

Length of fault plane, *L*
Top of rupture extent, D_{top}
Bottom of rupture extent, D_{bottom}
Fault dip, δ.
Fault slip rate, $\dot{s}$
Coupling coefficient, *c*.
Magnitude scaling relationship, $M_w \sim f(L, W)$

3.2.2 Consideration of epistemic uncertainties in the fault-model

Based on the procedure outlined in the previous section epistemic uncertainties can be considered in the Monte Carlo simulation procedure given in Table 5.

Table 5 Monte Carlo procedure for fault-based epistemic uncertainty consideration

for i=1:nsimulation

- For each fault *j*:
- Generate a random set of geometrical fault parameters ($L, D_{top}, D_{bottom}, \delta$) and deformation parameters ($\dot{s}$, c)
- Using the appropriate magnitude scaling relation determine the mean, and standard deviation of the characteristic magnitude (i.e. Equations (3)-(5)).
- From the mean and standard deviation of the characteristic magnitude, generate a randomly realized magnitude, $M_W^{j,i}$ (for fault j and realization i).
- For the generated magnitude $M_W^{j,i}$ get the associated seismic moment (Equation (7) and (8)), and then determine the mean annual rate of occurrence, $\lambda^{j,i}$ (Equation (9)).

end of loop

3.2.3 Specific values of fault based uncertainties used in the present study.

Table 4 listed the seven parameters/relationships for the fault component of the ERF which contain epistemic uncertainty. Given that epistemic uncertainties are a result of a lack of knowledge (both theoretical and empirical), then obviously those faults which have had less attention devoted to them will be modelled with parameters/relationships which have a greater epistemic uncertainty. Therefore, ideally one would have estimates for the magnitude of the parameter/relationships uncertainties that are fault-specific. Unfortunately, for the faults in the NZ seismic hazard model this is not the case, with the majority of such data not presently catalogued. As a result, the approach taken here is to make use of available fault-specific data, and judgement in the absence of such data, to assign uncertainties to each of the parameters. A key consideration in the subsequent analyses conducted is a sensitivity study to assess the importance of each parameter uncertainty in the overall picture of seismic hazard, therefore indicating which parameters deserve more rigorous estimation in future.

In determining the magnitude of uncertainties to assign to faults without specific parameter uncertainty estimates, use was made of both NZ-specific and also foreign data. The primary foreign data used were those of the Working Group on California Earthquake Probabilities (WGCEP), who developed an ERF for the San Francisco Bay Area with a detailed assessment of epistemic uncertainties (WGCEP 2003). Table 6 presents data directly from the WGCEP study for the various faults they were concerned with. On the basis of this table the following summary information can be obtained: (i) coefficients of variation (COV) for fault length range from 0.06-0.28 with a mean of 0.15; (ii) width COVs range from 0.08-0.12 with a mean of 0.10; (iii) slip rate COVs range from 0.06-0.34 with a mean of 0.18.

In addition to the parameter uncertainty magnitudes in the WGCEP study, various estimates are also available for well-studied and/or recently studied NZ faults. Examples of such estimates include slip rate COVs of: 0.14 - Wellington fault (Van Dissen and et al 2010); 0.10 - Ostler and Irishman creek faults (Amos et al. 2007); 0.16 - Ohariu fault (Heron et al. 1998); 0.1 – Hope fault (Langridge and Berryman 2005); 0.15 – Porters Pass fault (Howard et al. 2005); 0.16 – Blue Mountain fault (Pace et al. 2005); 0.15 – Ohariu fault (Litchfield et al. 2006); 0.25 – Taupo rift faults (Villamor and Berryman 2006); 0.13 – Wairau fault (Zachariasen et al. 2006); 0.08 – Alpine fault (Zachariasen et al. 2006); 0.08 - Wairarapa fault (Van Dissen and Berryman 1996); and 0.1 – Hikurangi subduction zone sources (Wallace et al. 2010); among others. On the basis of these and the WGCEP values a COV of 0.20 was assigned to slip rate uncertainties for general faults. Estimates for fault length, depth, dip uncertainties for NZ faults are few and far between and therefore use was largely made of the WGCEP study in assigning values for these uncertainties. The general parameter uncertainties are given in Table 7. For use in the later Monte Carlo simulations, these parameter distributions were truncated at two standard deviations from the mean.

Note that (truncated) Normal distributions were used for representing uncertainties in parameter values (the exception being fault depth which was assigned a uniform distribution). Since there is a paucity of data to even estimate fault-specific uncertainties (i.e. COV), then it is not possible to scrutinize appropriate distributions for each parameter considered. Given that the magnitude of uncertainty is likely more important than the distribution considered, the normal distribution was adopted as it requires only two parameters to be uniquely defined.

Table 6 Parameter uncertainties adopted by the Working Group on California Earthquake Probabilities (WGCEP 2003).

		Length, km			Width, km		R (seis. scaling factor)		Slip rate, mm/yr	
Fault	Seg.	Preferred	Min	Max	Preferred	90% bounds	Values	Weights*	Preferred	95% bounds
San Andreas	SAS	62	47	77	15	13-17	0.8/0.9/1.0	(a)	17	13-21
	SAP	85	60	110	13	11-15	0.9/1.0	(b)	17	13-21
	SAN	191	171	211	11	9-13	0.9/1.0	(b)	24	21-27
	SAO	135	115	155	11	9-13	0.9/1.0	(b)	24	21-27
Hayward/RC	HS	53	34	71	12	10-14	0.4/0.6/0.8	(a)	9	7-11
	HN	35	20	50	12	10-14	0.4/0.6/0.8	(a)	9	7-11
	RC	63	53	73	12	10-14	0.9/1.0	(b)	9	7-11
Calaveras	CS	19	9	29	11	9-13	0.0/0.2/0.4	(a)	15	12-18
	CC	59	49	69	11	9-13	0.1/0.3/0.5	(c)	15	12-18
	CN	45	35	55	13	11-15	0.7/0.8/0.9	(a)	6	4-8
Concord/GV	CON	20	12	28	16	14-18	0.2/0.5/0.8	(d)	4	2-6
	GVS	22	16	28	14	12-16	0.2/0.5/0.8	(d)	5	2-8
	GVN	14	6	22	14	12-16	0.2/0.5/0.8	(d)	5	2-8
San Gregorio	SGS	66	46	86	12	10-14	0.8/0.9/1.0	(a)	3	1-5
	SGN	110	85	134	13	11-15	0.8/0.9/1.0	(a)	7	4-10
Greenville	GS	24	15	31	15	12-18	0.8/0.9/1.0	(a)	2	1-3
	GN	27	17	37	15	12-18	0.8/0.9/1.0	(a)	2	1-3
Mt Diablo	MTD	25	15	35	14	12.2-16.2	1.0	1.0	2	1-3

* Weights: (a) Mean and 90% bounds: 0.185/0.63/0.185. (b) Only lower 90% bound set: 0.185/0.815.
(c) Weights determined by WG02: 0.4/0.5/0.1 (see text). (d) Equal weighting of 1/3 on each branch.

Table 7 General uncertainties assigned to fault parameters where site-specific data is not available

Parameter	Uncertainty
Length of fault plane, L	$\delta^{*} = 0.15\ (Trunc.Norm.)$
Top of rupture extent, D_{top}	$\sigma^{**} = \frac{1}{\sqrt{12}} km\ (Uniform)$
Bottom of rupture extent, D_{bottom}	$\sigma = 1km\ (Trunc.Norm.)$
Fault dip, δ.	$\sigma = 5°\ (Trunc.Norm.)$
Fault slip rate, $\dot{s}$	$\delta = 0.20\ (Trunc.Norm.)$
Coupling coefficient, c.	$\delta = 0.15\ (Trunc.Norm.)$ [interface sources only]
Magnitude scaling relationship, $M_W \sim f(L,W)$	Fault type specific [i.e. Equations (3)-(6)]

* δ=coefficient of variation, equal to the standard deviation divided by the mean.
**For a uniform distribution a standard deviation of $1/\sqrt{12}$ refers to maximum and minimum values that are 0.5 units above and below the mean value.

3.2.4 Theoretical uncertainty propagation

While the uncertainties in the fault-based component of the ERF can be considered simply by Monte Carlo simulation as described above, significant insight can be gained by understanding the theoretical uncertainty propagation.

In logarithmic form (all base 10 logs used), the mean annual rate of occurrence (i.e. Equation (9)) can be expressed as:

$$log\lambda = log\dot{M}_o - logM_o \tag{10}$$

where from Equations (7) and (8)

$$log\dot{M}_o = log\mu + logA + log\dot{s} + logc$$

$$logM_o = 16.05 + 1.5M_w \tag{11}$$

hence

$$log\lambda = (log\mu + logA + log\dot{s} + logc) - (16.05 + 1.5M_w) \tag{12}$$

Therefore the uncertainty in the rate of rupture occurrence can be given by (as $\mu = constant$):

$$\sigma^2_{log\lambda} = \left(\sigma^2_{logA} + \sigma^2_{log\dot{s}} + \sigma^2_{logc}\right) + \left(1.5^2\sigma^2_{M_w}\right) \tag{13}$$

now as $A = LW$ then (assuming L and W are uncorrelated):

$$logA = logL + logW$$

$$\sigma^2_{logA} = \sigma^2_{logL} + \sigma^2_{logW} \tag{14}$$

and as scaling relations are of the form (in the case of area-based scaling):

$$M_w = a + blogA + \epsilon_{M_w|A} \tag{15}$$

where the value of $b \approx 1$ and $\sigma^2_{M_w|A} = Var\left[\epsilon_{M_w|A}\right]$. Therefore the two relations for the uncertainty in characteristic magnitude and recurrence rate are obtained:

$$\sigma^2_{logM_w} = b^2\sigma^2_{logA} + \sigma^2_{M_w|A}$$

$$\sigma^2_{log\lambda} = \left(\sigma^2_{logA} + \sigma^2_{log\dot{s}} + \sigma^2_{logc}\right) + 1.5^2\sigma^2_{logM_w} \tag{16}$$

These two equations above give the uncertainties in the estimated magnitude and rate of occurrence, which are the two primary quantities which influence the seismic hazard posed by a characteristic earthquake source.

If one then examines the typical magnitudes of the above uncertainties:

$$\sigma_{logL} \sim 0.15$$

$$\sigma_{logW} \sim 0.1$$

$$\sigma_{logs} \sim 0.2$$

$$\sigma_{logc} \sim 0.15 \text{ (interface sources only)}$$

$$\sigma_{M_W|A} \sim 0.2$$

so

$$\sigma_{logA} \sim 0.18$$

Hence

$$\sigma^2_{logM_W} \sim 1^2 * (0.18^2) + 0.2^2 \sim 0.27^2$$

and

$$\sigma^2_{log\lambda} \sim (0.18^2 + 0.2^2 + [0, 0.15]^2) + 1.5^2(0.27^2)$$

$\sim 0.49^2$ (not interface)

$\sim 0.51^2$ (interface)

Hence it can be seen that the uncertainties considered are significant. However, it should be noted that the above analysis is for the uncertainty of a single fault. When a total exceedance rate is to be calculated, as in a magnitude-frequency plot, or seismic hazard calculation, then multiple seismic sources are combined. In this case, the uncertainty in the (logarithm of the) exceedance rate will decrease as the number of sources which contribute to the exceedance increases (since epistemic uncertainties in the sources are independent). Therefore the uncertainty in the magnitude-frequency rate for a large region will be relatively small for small magnitudes (where many source contribute), but larger for larger magnitudes (where only a few major faults contribute). On the other hand, at a single location, where few faults significantly contribute to the seismic hazard, then it is likely that all uncertainties will be important, and hence are all considered subsequently.

4.0 APPLICATION OF METHODOLOGY TO NZ SEISMIC HAZARD ANALYSIS

4.1 Implementation in OpenSHA

The methodology for consideration of epistemic uncertainties in GMPE and ERF discussed in the previous sections was implemented in the open-source seismic hazard analysis software OpenSHA (Field et al. 2003). A key element of the OpenSHA framework is its object-oriented nature, enabling a ‘plug-and-play’ environment in which any specific type of GMPE or ERF can be handled. Such an environment is beneficial in this implementation due to the nature in which epistemic uncertainties can be considered, as well as the ease at which the methodology can be modified in future.

Another feature of the object-oriented nature of OpenSHA that offers considerable benefit, is the partial removal of the problems of GMPE parameter consistency across models, which several studies have noted to be a significant cause of uncertainty in hazard calculations (e.g. Bommer and Scherbaum (2008) and references therein). By treating earthquake ruptures as objects, GMPEs that use different definitions of magnitude, source-to-site distance, and fault mechanism classification can be easily handled. The only consistency consideration which remains are those parameters which relate to the classification of local site effects. This is discussed further in the following section.

4.2 Case study sites considered

In order to examine the importance of various epistemic uncertainties in seismic hazard analysis we consider two different sites, two different soil classes, and two different intensity measures. Wellington (Lon 174.7772, Lat -41.2889) and Christchurch (Lon 172.6200, Lat -43.5300) are selected, both because they are NZ’s largest two cities, and conveniently because at the 475yr return period, Wellington’s hazard tends to be dominated by fault sources, in contrast with Christchurch’s hazard in which the background sources provide a significant contribution. Hazard analyses are performed at these two generic city locations for both site class B (weathered rock) and site class D (deep soil) site conditions (see NZS1170.5 (2004) for site classification). These two different site classes are considered to examine what additional epistemic uncertainty arises due to the different classification of site effects (with, for example, McV06 and Z06 using discrete site classes, while C10 and BA08 use continuous Vs30, and C10 also uses a basin depth parameter, $Z_{1.0}$). Finally, hazard analyses are performed for both PGA and SA(2.0), in order to understand the magnitude of epistemic uncertainties at short and long vibration periods.

In line with the results of Bradley (2010), who examined the adequacy of the various GMPEs for application to NZ, the following parameters were used for site class B and D sites.

Table 8 Site class compatibility of the various GMPEs

NZS1170.5 Site Class	McVerry et al site class	Zhao et al site class	Vs30 (m/s)	$Z_{1.0}$ (m)
B	B	Soft rock	760	50
D	D	Medium soil	250	500

4.3 Uncertainty in Nationwide magnitude-frequency distribution

4.3.1 Fault model

Figure 14 illustrates the nationwide magnitude-frequency distributions from fault-source seismicity due to the consideration of various parameter uncertainties. Each of the plots in Figure 14 illustrate the nominal distribution (obtained without the consideration of epistemic uncertainties), the individual distributions from 50 Monte Carlo simulations (grey lines), as well as the mean, 16th and 84th percentiles of the simulated distributions. Firstly, it can be seen that generally the mean distribution and the nominal distribution are relatively similar. The main exception of the above comment is for large magnitudes, where the parameter uncertainties mean a smoother variation in frequency compared with the ‘step’ changes that result in the case of no uncertainties. Also it is worth recalling that magnitudes for subduction interface events were estimated using Strasser et al. (2010), compared with the assumed average displacements used by Stirling et al. (2011). Comparison of the size of the uncertainty in the magnitude-frequency distribution due to each parameter uncertainties illustrates that magnitude-scaling uncertainties are the most significant, followed by length uncertainties.

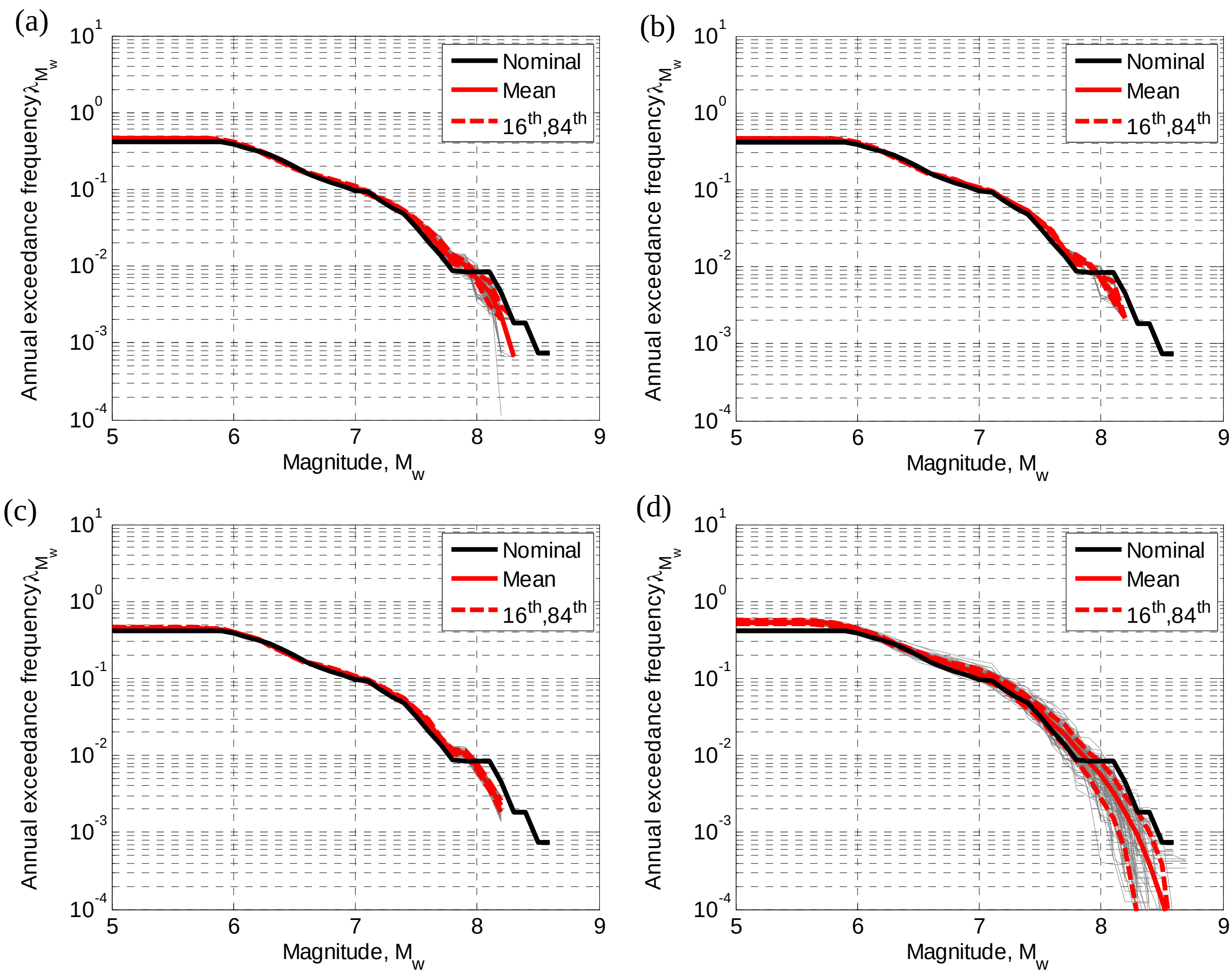

Figure 14 Epistemic uncertainties in the nationwide Magnitude-frequency relationship due to fault-source seismicity alone due to: (a) fault length uncertainty only; (b) depth of rupture uncertainty only; (c) slip rate uncertainty only; and (d) magnitude-scaling relationship uncertainty only.

Figure 15 compares explicitly the magnitude of the uncertainties in the magnitude-frequency distribution by plotting the lognormal standard deviation of the exceedance frequency as a function of magnitude for various parameter uncertainties. As mentioned with respect to **Figure 14**, it can be seen that magnitude scaling uncertainty leads to the largest uncertainty, followed by fault length uncertainty. **Figure 15**b presents the uncertainty in the magnitude-frequency distribution when multiple uncertainties are considered. Specifically, all the parameter uncertainties related to fault geometry (i.e. fault length, rupture top, rupture depth, fault dip), fault deformation (i.e. slip rate and coupling coefficient (for interface sources)) were considered simultaneously. **Figure 15**b illustrates that despite grouping the uncertainties, magnitude scaling uncertainty remains the dominant uncertainty.

Note that Mw scaling uncertainty was treated on a fault-by-fault basis through the use of the Mw-scaling relationships (Equations (3)-(5)). Hence this suggests that the approximate uncertainty values that are prescribed to the other fault parameters (in the cases where fault-specific parameter uncertainties were unavailable) do not have a significant effect on the magnitude of the total uncertainty (that is, assuming that the fault-specific parameter uncertainties are approximately equal to the general values prescribed). Finally, it is worth noting that the results in **Figure 15** compare well with the theoretical uncertainty propagation presented in the previous section.

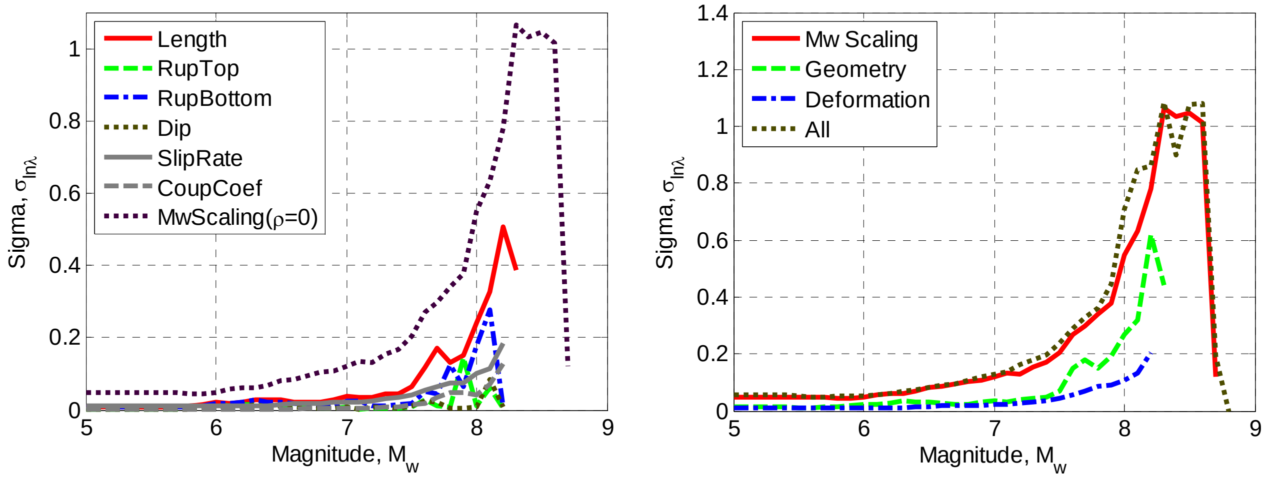

Figure 15 Lognormal standard deviation in the exceedance rate of various magnitudes due to various fault parameter uncertainties: (a) individual parameter uncertainties; and (b) parameter uncertainties by group.

Figure 16 presents the uncertainty in the magnitude-frequency distribution due to the consideration of all fault parameter uncertainties. Similar to the previous figures it can be seen that the nominal and mean curves are similar with exceptions at larger magnitudes, where the mean frequency if higher for M_w=7.5-7.8 and lower above that, and also for very small magnitudes. Further insight into the size of the epistemic uncertainties can be gained by examining the magnitude-frequency relationship in the form of a magnitude – probability of exceedance plot using the Poisson assumption, which leads to $P = 1 - \exp(-\lambda * t)$, where λ is exceedance frequency and t is exposure time. An exposure time of 50 years is selected as this is a typical design life used in building codes. Figure 17 illustrates the 50 year probability of exceedance of various magnitude earthquakes resulting from fault-based seismicity. Firstly, it can be seen that there is essentially a 100% probability of an earthquake of magnitude 7 or greater on a mapped fault in NZ in the next 50 years. A magnitude 7.5 event has a nominal probability of exceedance of 79%, a mean probability of 84% with a 68% confidence interval (i.e. that between the 16th and 84th percentiles) of 73-88% (i.e. the 68% CI has a width of 15%). For a magnitude 8 earthquake the nominal probability of exceedance is 35%, while the mean probability is 25% with a 68% CI of 12-31% (i.e. the width of the 68% CI is 19%).

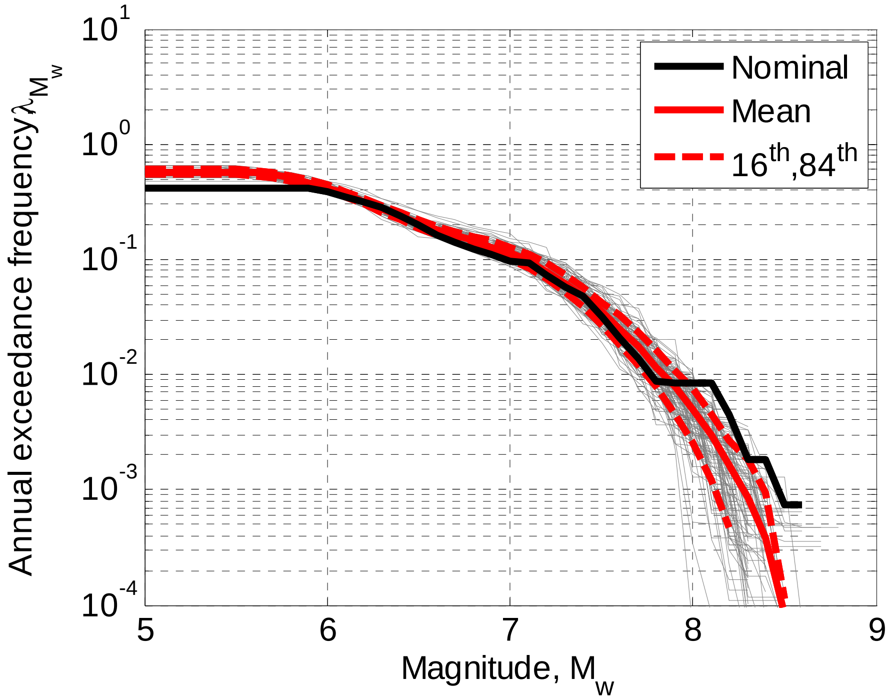

Figure 16 Uncertainty in the nationwide magnitude-frequency distribution due to fault-based seismicity due to all fault parameter uncertainties.

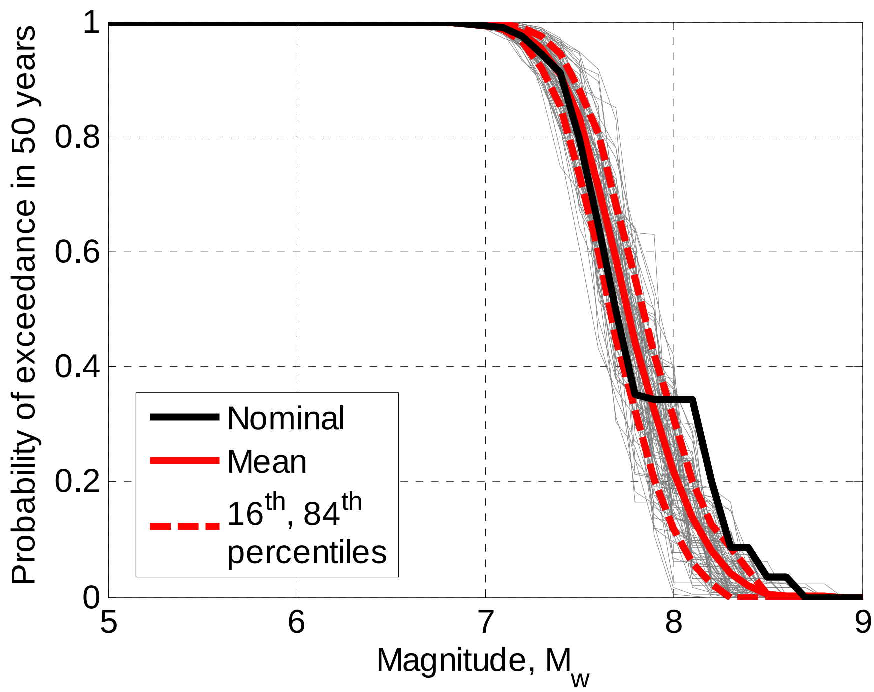

Figure 17 Probability of exceedance of various magnitude earthquakes, with uncertainty due to fault parameter uncertainties.

As was previously noted in the theoretical uncertainty propagation section, because fault parameter uncertainties are not correlated between different faults, a magnitude frequency distribution for all faults has a smaller uncertainty than that for a single fault. Hence in the consideration of seismic hazard at a single site, which will be dominated by only a handful of faults, it is likely that the uncertainty will be higher. This statement is shown to be the case in the following section.

4.4 Uncertainty in seismic hazard for Wellington

This section examines the epistemic uncertainty in seismic hazard analysis for a generic site in downtown Wellington (Lat: -41.2889, Lon: 174.7772) for an exposure time of 50 years. In order to get a general understanding of the magnitude of the epistemic uncertainties due to various sources four hazard curves are computed at this site: (a) PGA hazard treating the site as class B (rock) conditions; (b) PGA hazard treating the site as class D (soft/deep soil) conditions; (c) SA(2.0) hazard site class B; and (d) SA(2.0) hazard site class D. These four conditions allow for the differences in uncertainty due to the different GMPEs, and seismic sources in the ERF (because of the different manner in which IM's scale with site class and seismic sources etc.). For each of these four different scenarios, hazard curves were computed and are presented illustrating: (a) epistemic uncertainty in the ERF parameters and each of the different active shallow crustal and subduction zone GMPE combinations shown in **Figure 13**; and (b) the mean, median, 5^{th} and 95^{th} percentiles of the seismic hazard. In order to understand the magnitude of the epistemic uncertainties, plots are also shown which illustrate the lognormal standard deviation (i.e. dispersion) of the exceedance probability for a given IM level, plotted against the mean exceedance probability for that IM level (Bradley 2009). The use of the lognormal standard deviation is based on the fact that the epistemic uncertainty tends to be well approximated by the lognormal distribution (Bradley 2009), as demonstrated in

Figure 18. In all of the figures that follow, 50 simulations for each different GMPE combination were used to sample the ERF epistemic uncertainties (i.e. **Table 5**). The mean, 5^{th} and 95^{th} percentiles account for the non-uniform weights given to each of the GMPEs.

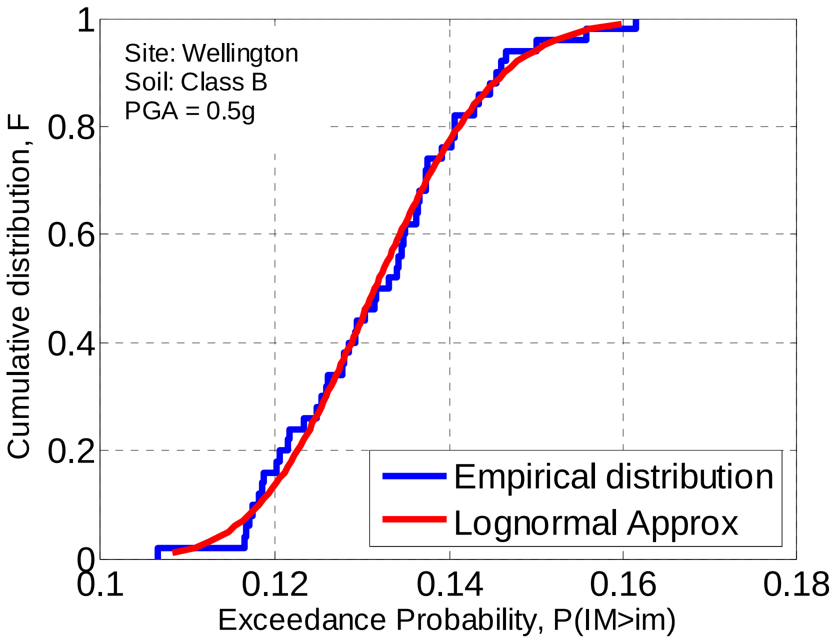

Figure 18 Adequacy of the lognormal distribution for representing the uncertainty in the exceedance probability for a given IM value due to fault-source uncertainty.

Figure 19 illustrates the seismic hazard curves for PGA in Wellington site class B. In Figure 19a, individual simulations are shown in grey, with the mean hazard curve accounting for ERF uncertainty, but for a single GMPE, shown in coloured lines. Figure 19b illustrates the 400 different simulated hazard curves (i.e. 50 simulations x 8 GMPE combinations), and the summarised mean, median, 5th and 9th percentiles (the likelihood associated with each simulation is 1/50 multiplied by the logic tree weight for the specific GMPE combination given in Figure 13). Figure 20a and Figure 20b illustrate the magnitude of the epistemic uncertainty due to “ERF only”, and “ERF and GMPE” uncertainties, respectively. Firstly, examination of Figure 20 illustrates that the epistemic uncertainty generally increases as the exceedance probability reduces. Secondly, as can be seen from Figure 20b and also in Figure 19a, the GMPE uncertainty tends to be larger than that due to ERF uncertainty. The effect of which seismic sources contribute most significantly to the seismic hazard can be seen by examining the differences in the seismic hazard curves due to different GMPE combinations in Figure 19a. It can be seen that both active shallow crustal and subduction zones sources contribute significantly to the hazard (e.g. the difference between Z06/McV06 and Z06/Z06 illustrates the importance of subduction zone sources and McV06/Z06 and BA08/Z06 illustrate the importance of active shallow crustal sources). This observation is consistent with the fact that Wellington is known to be located close to several active shallow crustal faults (most notably the Wellington fault), and also the Hikurangi subduction zone passes approximately 20km underneath Wellington. In such high seismic locations it is generally found that seismic hazard is dominated by fault-based seismicity (that is, at ground motion levels with the potential to cause damage to structures), rather than background sources, and therefore the neglect of background seismicity epistemic uncertainties is inconsequential for Wellington. Finally, it can be seen that the magnitude of epistemic uncertainties are clearly significant in determining the ground motion hazard level for a given exceedance probability or vice versa. For example, while the mean hazards for the 10% and 2% exceedance probabilities in 50 years are 0.48g and 0.93g, respectively, the 90%

confidence intervals are [0.41g,0.57g] and [0.76,1.19g]. That is, the 90% confidence interval for the 10% in 50 year exceedance probability is almost 0.2g, and slightly over 0.4g for the 2% in 50 year exceedance probability.

Figure 21-Figure 26 present the remaining three combinations of seismic hazard curves and epistemic uncertainty magnitudes for the PGA and SA(2.0) hazard in Wellington for site class B and D. Similar to the previously discussed results for PGA and site class B, it can be seen that the uncertainty in the hazard is dominated by GMPE uncertainty and that both crustal and subduction zone sources are significant.

In order to understand the salient differences in epistemic uncertainties for the four different cases of PGA and SA(2.0) for site classes B and D, Figure 27 presents, side-by-side, the seismic hazard curves illustrating the mean, median, 5^{th} and 95^{th} percentiles for the these cases, and Table 9 tabulates the mean, 5^{th} and 95^{th} percentiles of the hazard for the 10% and 2% exceedance probabilities in 50 years. Interesting observations based on Figure 27 and Table 9 include the fact that the uncertainty in the hazard generally increases as the exceedance probability reduces, and in particular that the uncertainty is not systematically larger for site class D cases than for site class B cases. This may be assumed to be the case *a priori*, because of the likely different manner in which GMPEs account for local site response, something which should be insignificant for rock (class B) sites, where there is essentially no local site effect.

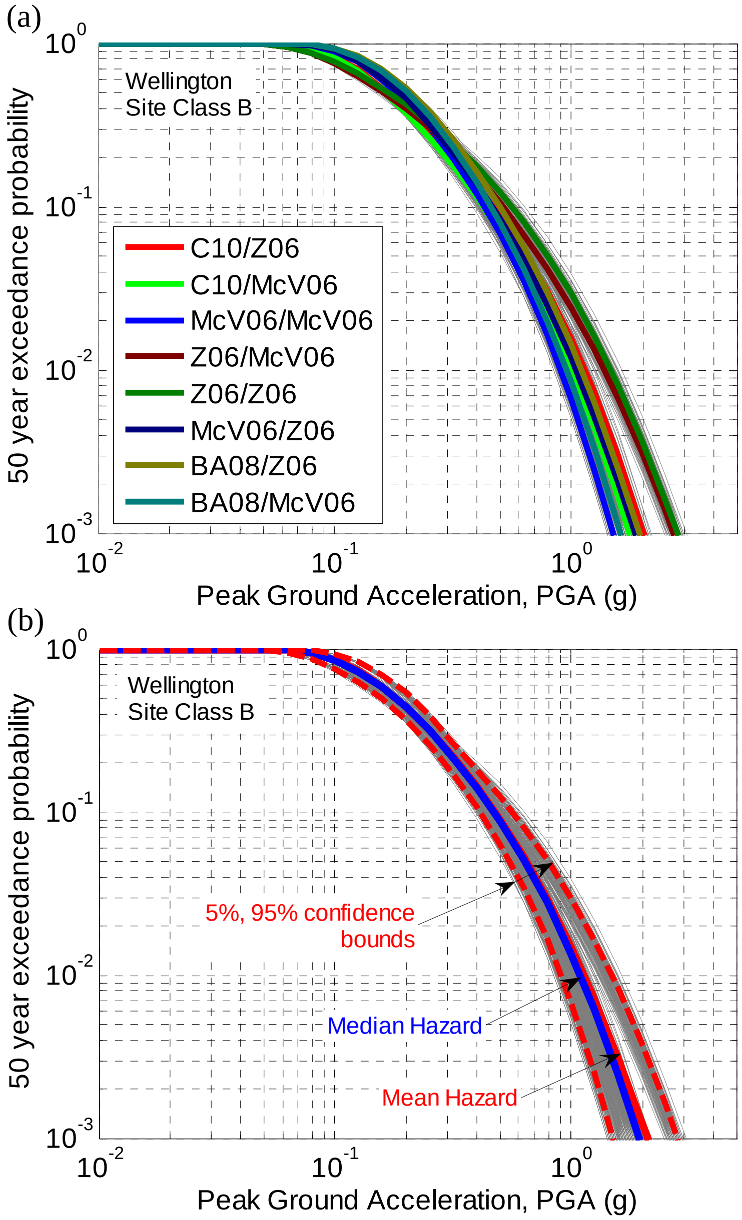

Figure 19 Seismic hazard curves for PGA in Wellington site class B: (a) effect of different GMPEs and fault-source uncertainty; and (b) mean, median and percentile hazard values.

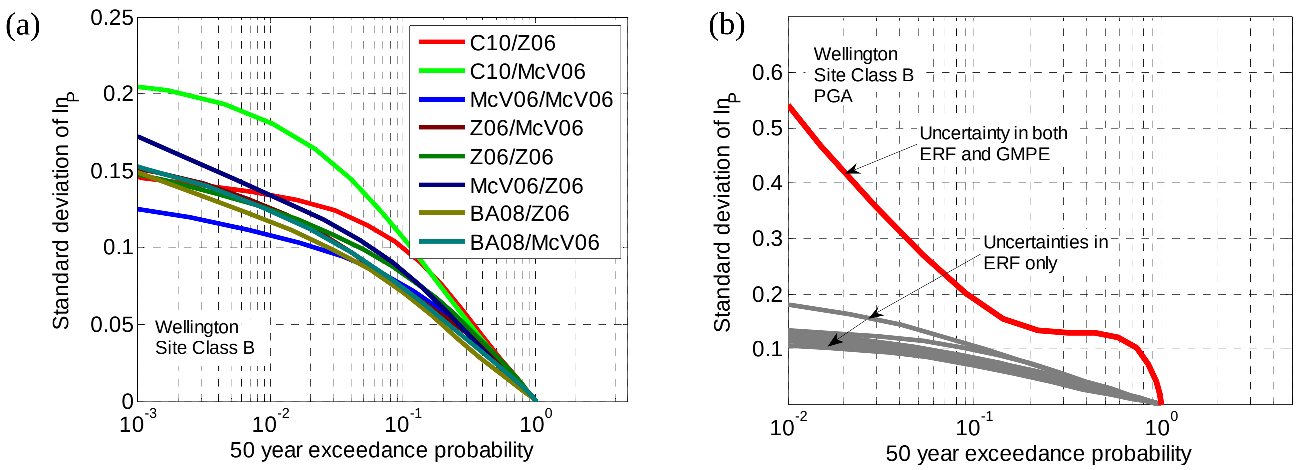

Figure 20 Uncertainty in seismic hazard PGA in Wellington site class B as a function of exceedance probability: (a) ERF only; and (b) ERF and GMPE uncertainties.

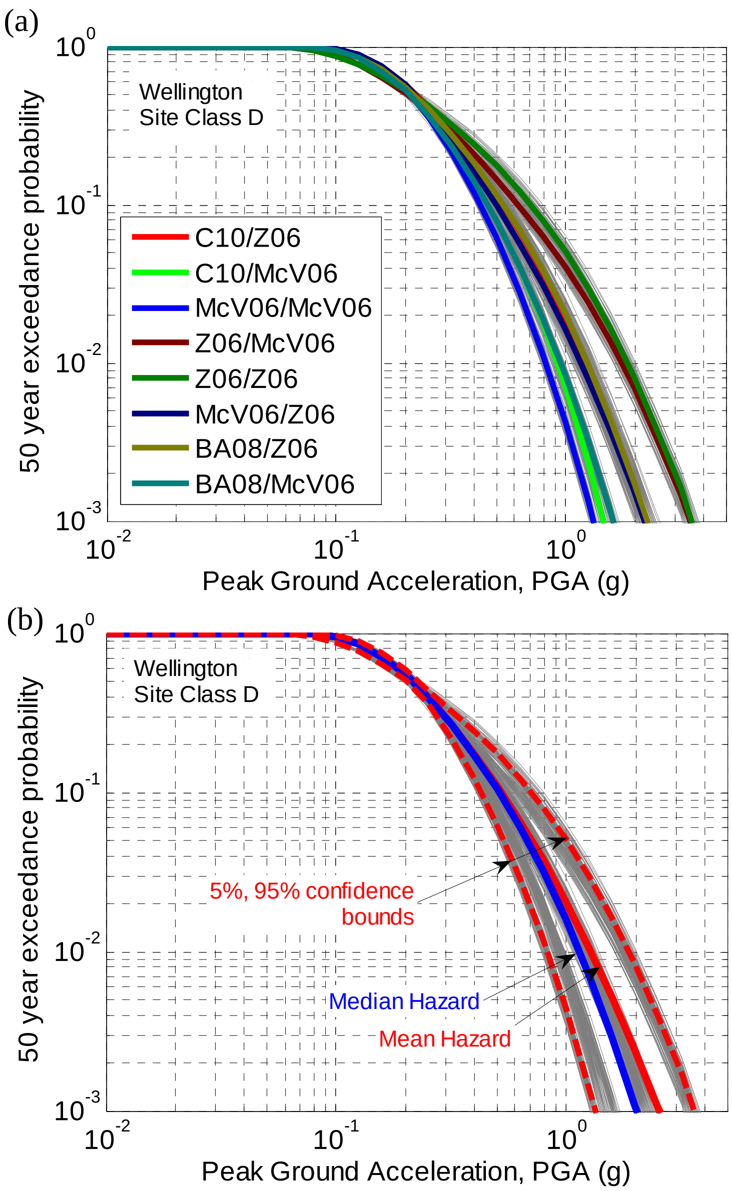

Figure 21 Seismic hazard curves for PGA in Wellington site class D: (a) effect of different GMPEs and fault-source uncertainty; and (b) mean, median and percentile hazard values.

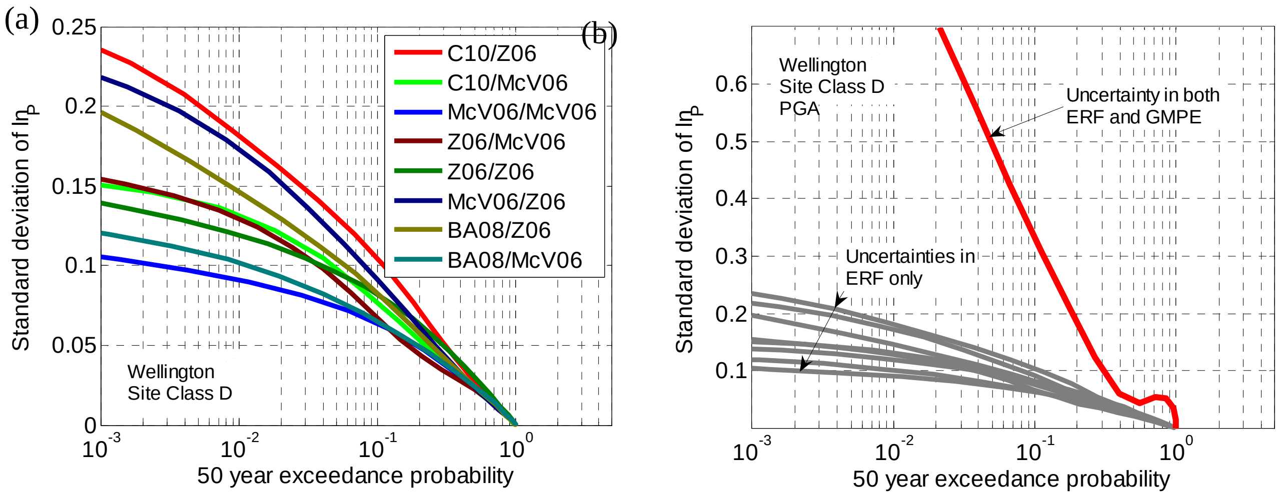

Figure 22 Uncertainty in seismic hazard PGA in Wellington site class D as a function of exceedance probability: (a) ERF only; and (b) ERF and GMPE uncertainties.

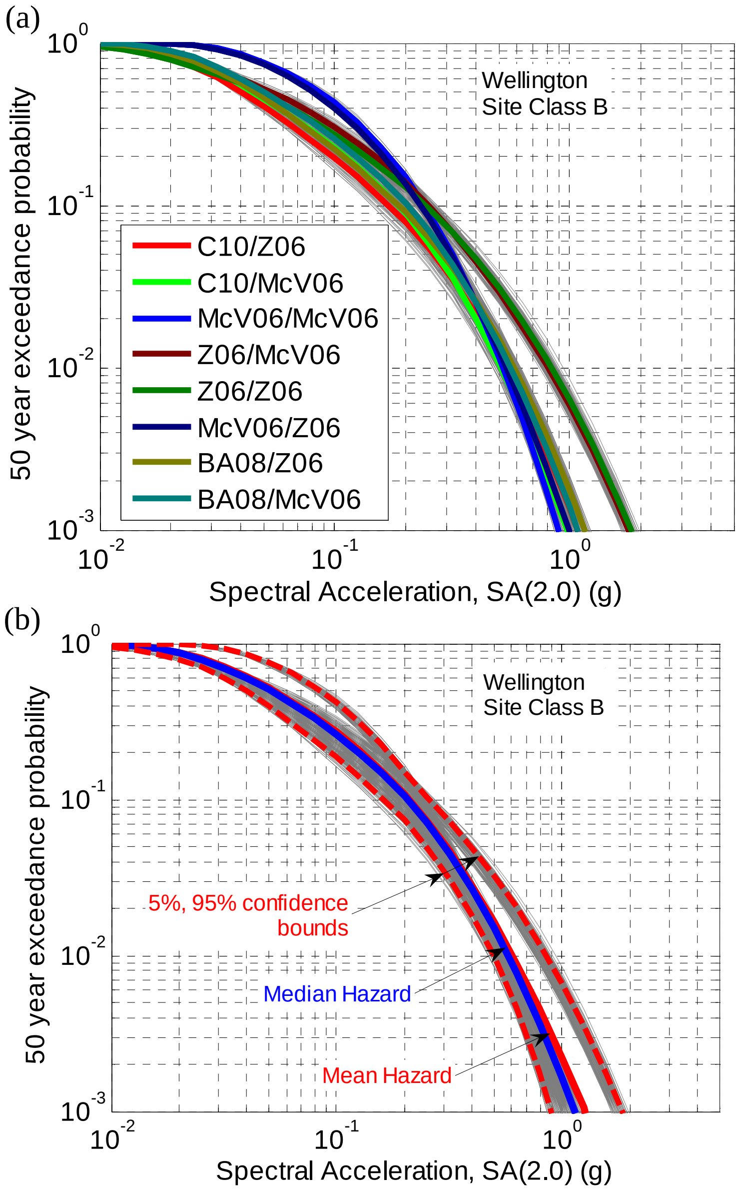

Figure 23 Seismic hazard curves for SA(2.0) in Wellington site class B: (a) effect of different GMPEs and fault-source uncertainty; and (b) mean, median and percentile hazard values.

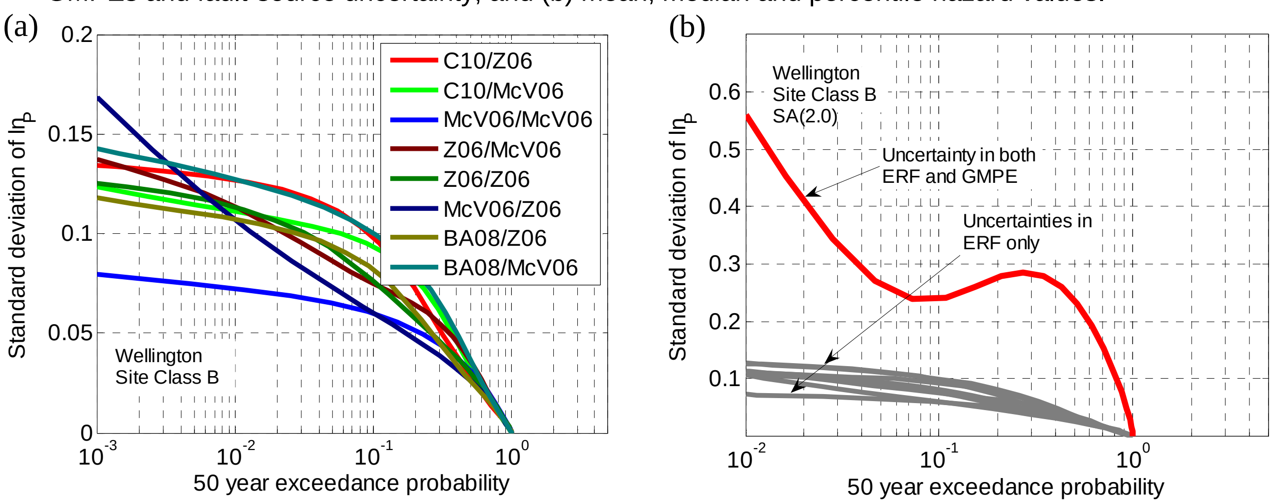

Figure 24 Uncertainty in seismic hazard SA(2.0) in Wellington site class B as a function of exceedance probability: (a) ERF only; and (b) ERF and GMPE uncertainties.

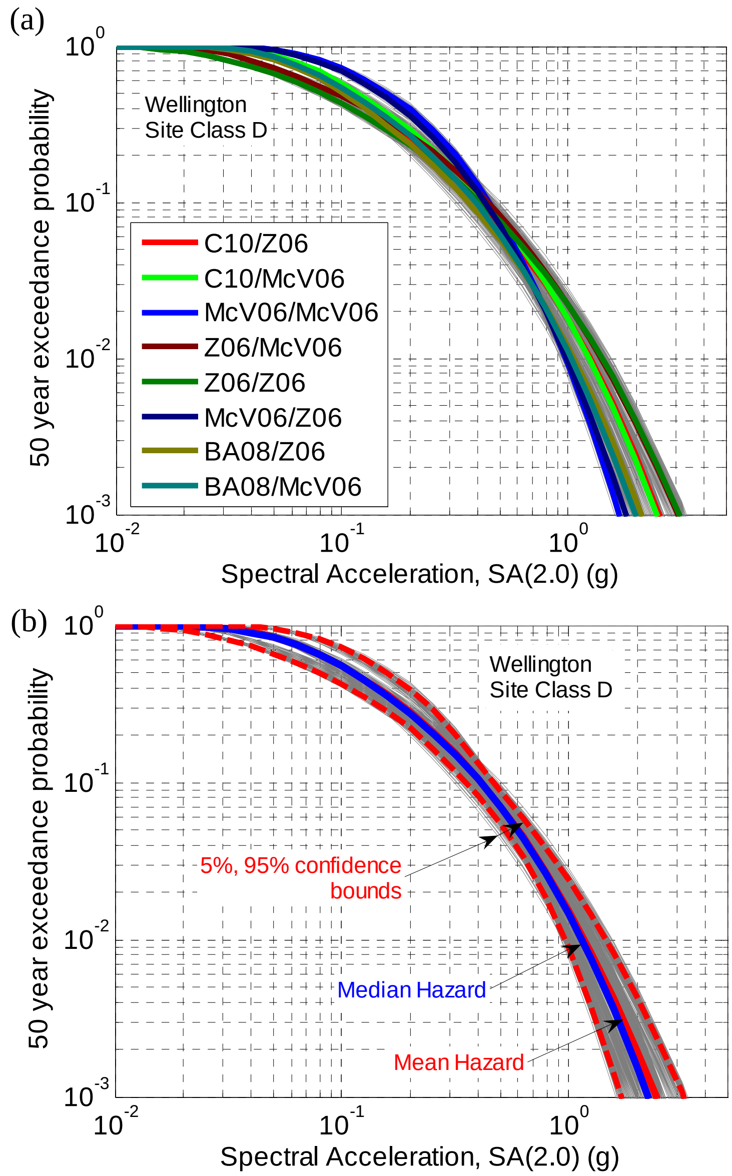

Figure 25 Seismic hazard curves for SA(2.0) in Wellington site class D: (a) effect of different GMPEs and fault-source uncertainty; and (b) mean, median and percentile hazard values.

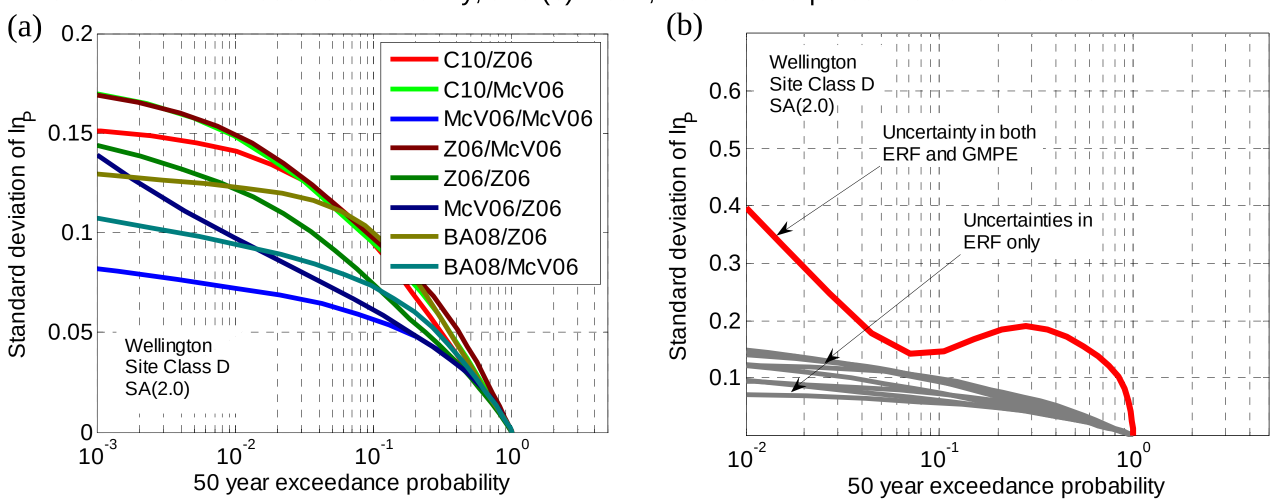

Figure 26 Uncertainty in seismic hazard SA(2.0) in Wellington site class D as a function of exceedance probability: (a) ERF only; and (b) ERF and GMPE uncertainties.

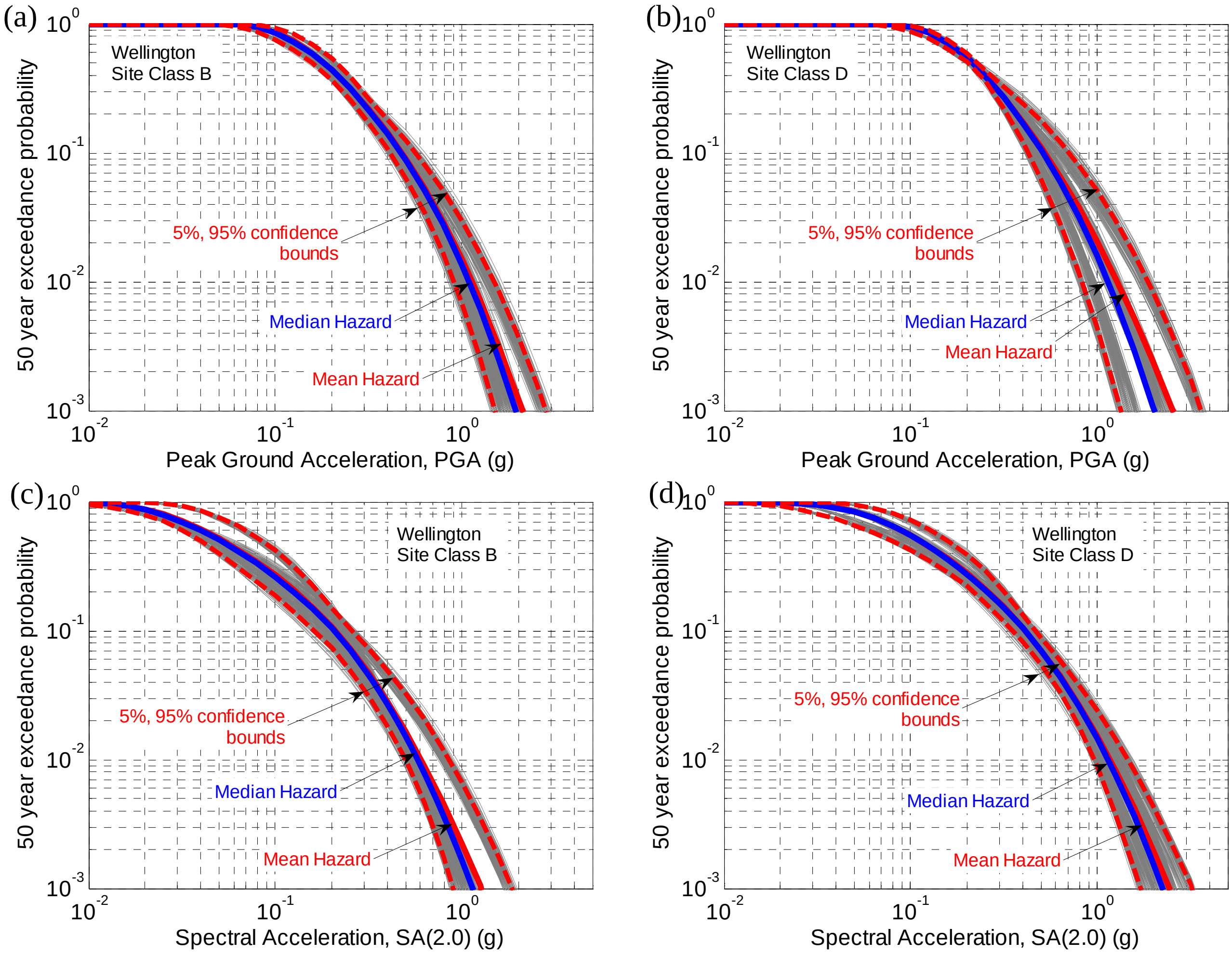

Figure 27 Comparison of the seismic hazard curves for Wellington: (a) PGA and site class B; (b) PGA and site class D; (c) SA(2.0) and site class B; and (d) SA(2.0) and site class D.

Table 9 Summary of mean, 5th and 9th percentile hazard values for 10% and 2% exceedance probabilities in 50 years in Wellington.

		PE = 10% in 50 years		PE = 2% in 50 years	
IM	Site Class	Mean	[5%,95%]	Mean	[5%,95%]
PGA	Rock, B	0.48	[0.41,0.57]	0.93	[0.76,1.19]
	Soft/deep soil, D	0.53	[0.44,0.72]	1.01	[0.72,1.50]
SA(2.0)	Rock, B	0.21	[0.16,0.26]	0.47	[0.39,0.63]
	Soft/deep soil, D	0.41	[0.35,0.47]	0.92	[0.78,1.11]

4.5 Uncertainty in seismic hazard for Christchurch

This section examines the epistemic uncertainty in seismic hazard analysis for a generic site in central Christchurch (Lat: -43.5300, Lon: 172.6203). Similar to the analyses presented for Wellington in the previous section, four different cases are considered here for PGA and Sa(2.0) on site class B and D conditions.

Figure 28-Figure 35 illustrate the four combinations of seismic hazard curves and epistemic uncertainty magnitudes for the PGA and SA(2.0) hazard in Christchurch for site class B and D. It is noted that as Christchurch is subject to negligible seismic hazard caused by subduction zone sources (which was explicitly checked to be the case). Hence, only the results for the four different crustal GMPEs are shown in these figures. An obvious observation to note in these figures is the reduction in the seismic hazard uncertainty due to ERF uncertainty relative to that observed for Wellington (i.e. Figure 28c vs. Figure 20c). This observation can be explained based on two causes. Firstly, unlike Wellington, which is a high seismic region dominated by only a hand full of fault-based seismic sources, Christchurch is a region of relatively lower seismicity, and its seismic hazard is contributed to significantly by both fault-based and background seismicity (discussed further in the following section). As no epistemic uncertainties were considered in the background seismicity model then there is consequently less uncertainty in the total seismic hazard due to both fault and background seismicity. The second reason for the reduction in ERF uncertainty for Christchurch is a result of the fact that there are numerous fault-based sources which significantly contribute to the seismic hazard. As was previously noted with respect to the uncertainty in the nationwide magnitude frequency distribution, because fault source uncertainty is not correlated between different faults, a larger number of fault sources which provide a substantial contribution to the seismic hazard will consequently lead to a reduction in the magnitude of the epistemic uncertainty in the seismic hazard. The effect of removing the background sources for Christchurch seismic hazard is explored in the following section.

Figure 36 presents, side-by-side, the seismic hazard curves illustrating the mean, median, 5th and 95th percentiles for the these aforementioned cases examined, and

Table **10** provides the mean, 5th and 95th percentiles of the hazard for the 10% and 2% exceedance probabilities in 50 years. With the above comments in mind, it can be seen that the epistemic uncertainty in the seismic hazard is completely dominated by the GMPE uncertainty. Furthermore, the size of this uncertainty is large as demonstrated by

Table **10**. For example, for site class D (the predominant site class in Christchurch basin region), the mean Sa(2.0) hazard for the 10% and 2% exceedance probabilities are 0.16g and 0.28g respectively. However, the 90% confidence interval ranges on these mean values are [0.11g,0.21g] and [0.21g,0.35g], respectively. That is, the range of the 90% confidence interval is 0.1g and 0.14g for these two exceedance probabilities, respectively.

Other observations from Figure 36 include the fact that, similar to the results for Wellington, the magnitude of the uncertainty is not systematically higher for site class D sites (with PGA on site class D in fact having the lowest, and SA(2.0) site class B having the highest uncertainty of the four cases considered).

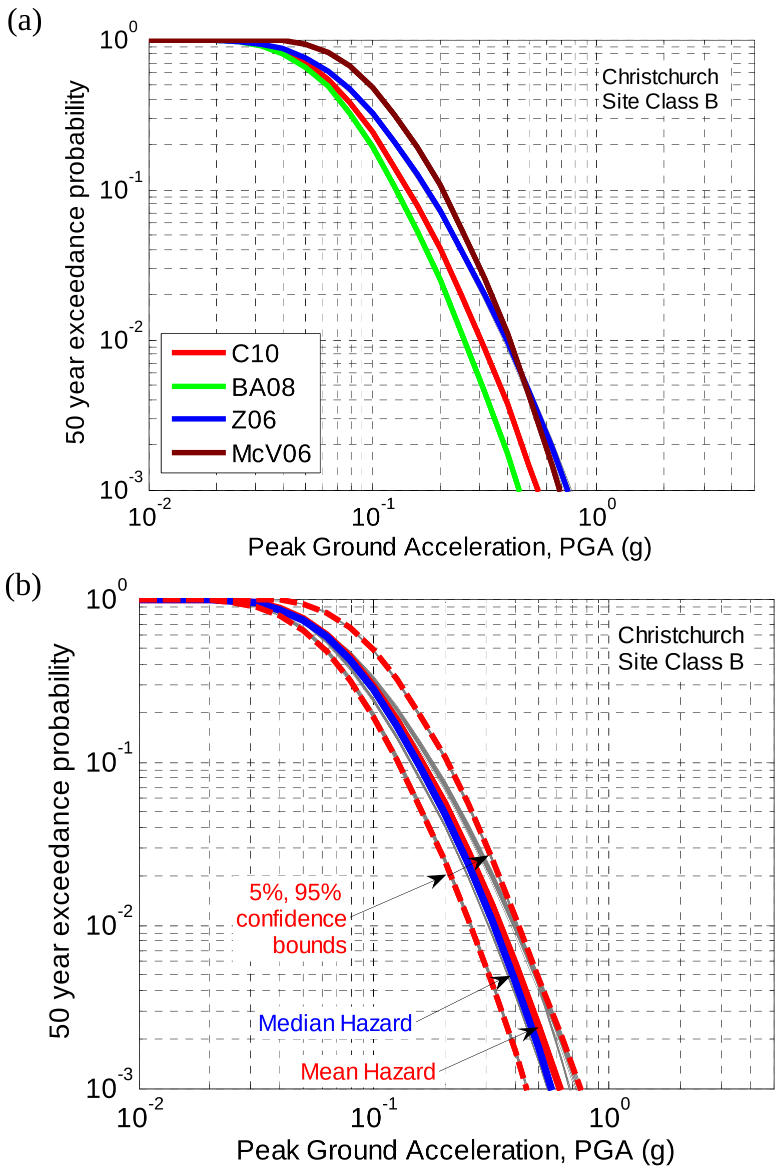

Figure 28 Seismic hazard curves for PGA in Christchurch site class B: (a) effect of different GMPEs and fault-source uncertainty; and (b) mean, median and percentile hazard values.

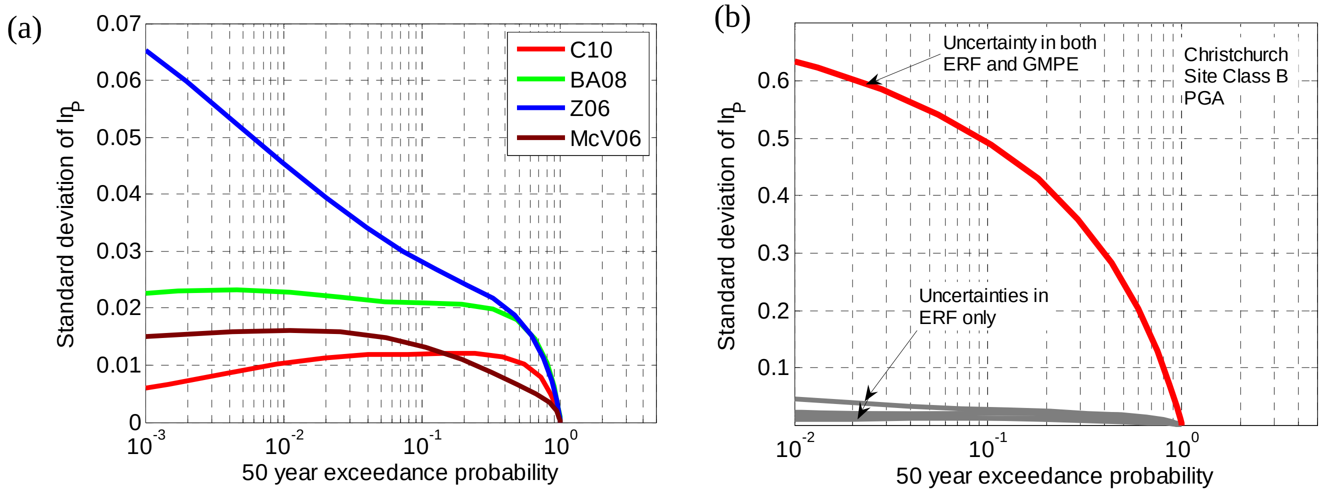

Figure 29 Uncertainty in seismic hazard PGA in Christchurch site class B as a function of exceedance probability: (a) ERF only; and (b) ERF and GMPE uncertainties.

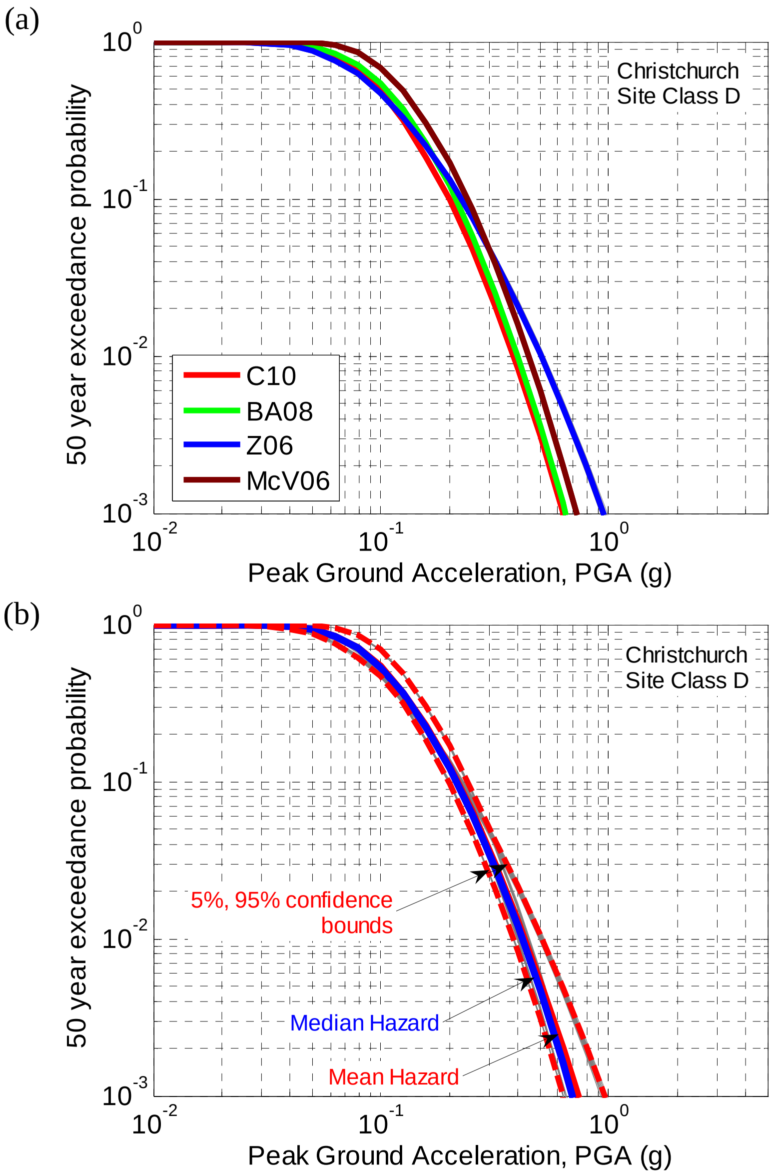

Figure 30 Seismic hazard curves for PGA in Christchurch site class D: (a) effect of different GMPEs and fault-source uncertainty; and (b) mean, median and percentile hazard values.

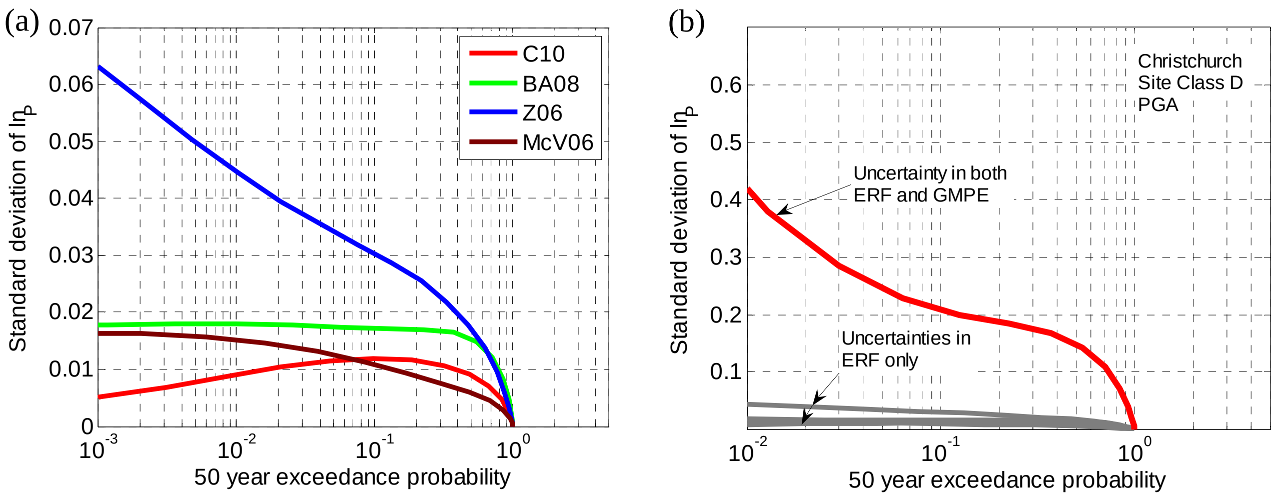

Figure 31 Uncertainty in seismic hazard PGA in Christchurch site class D as a function of exceedance probability: (a) ERF only; and (b) ERF and GMPE uncertainties.

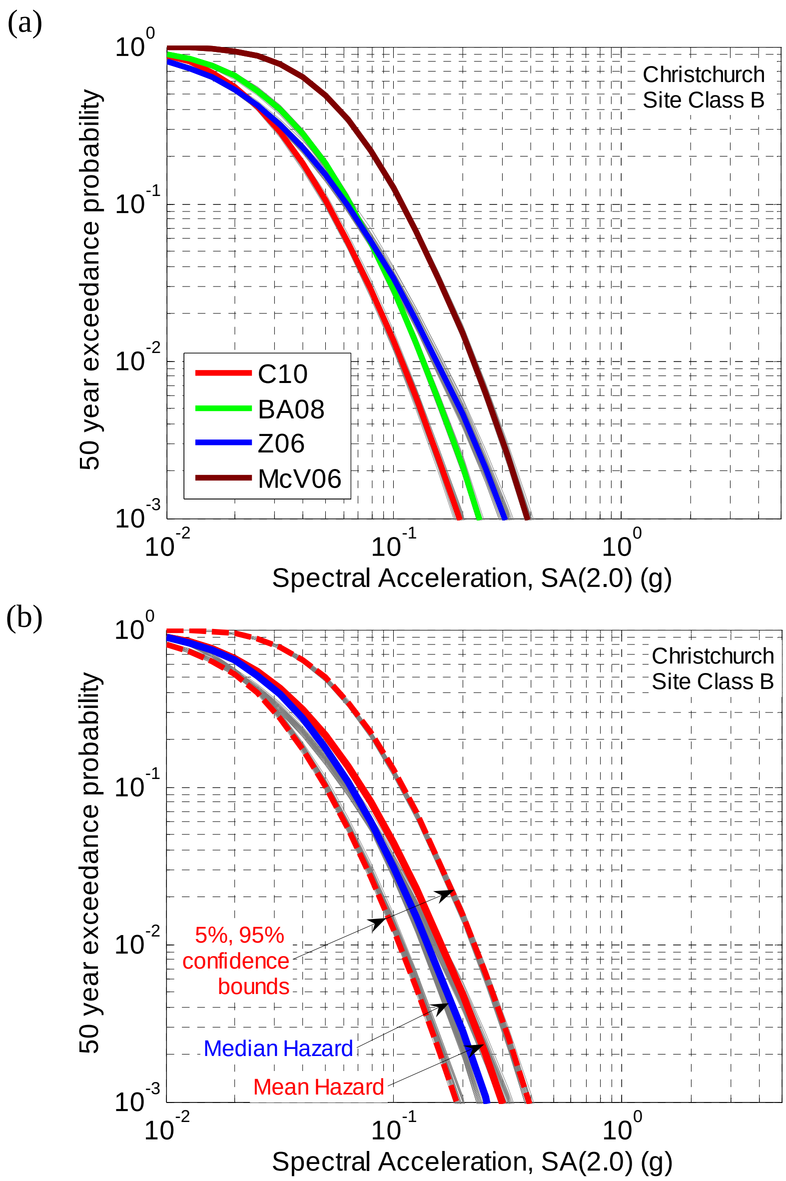

Figure 32 Seismic hazard curves for SA(2.0) in Christchurch site class B: (a) effect of different GMPEs and fault-source uncertainty; and (b) mean, median and percentile hazard values.

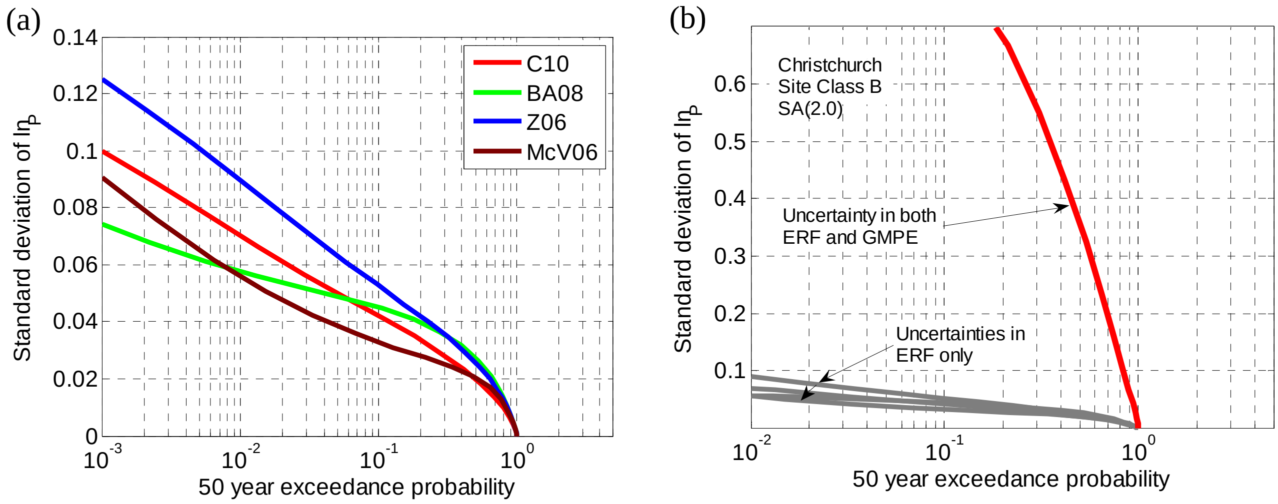

Figure 33 Uncertainty in seismic hazard SA(2.0) in Christchurch site class B as a function of exceedance probability: (a) ERF only; and (b) ERF and GMPE uncertainties.

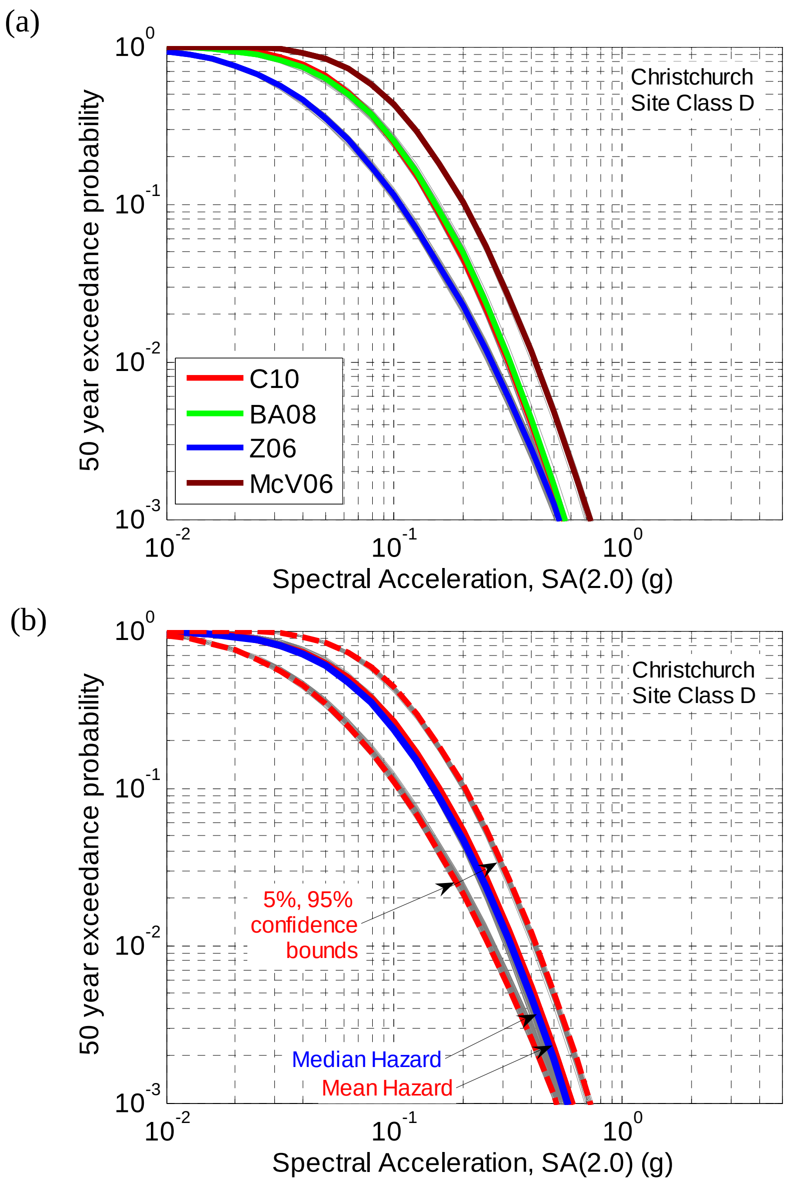

Figure 34 Seismic hazard curves for SA(2.0) in Christchurch site class D: (a) effect of different GMPEs and fault-source uncertainty; and (b) mean, median and percentile hazard values.

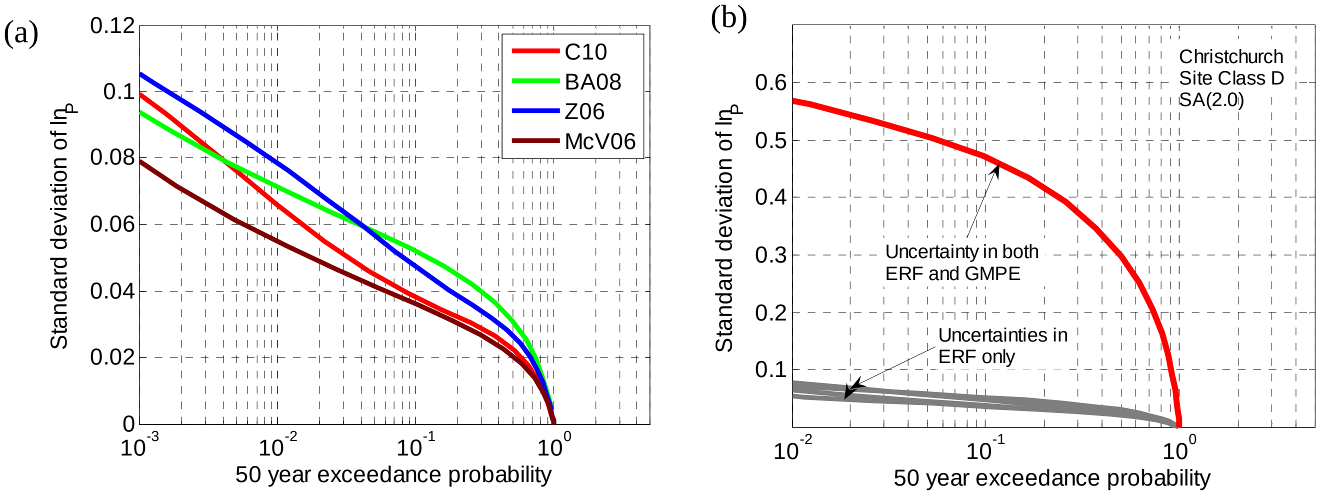

Figure 35 Uncertainty in seismic hazard SA(2.0) in Christchurch site class D as a function of exceedance probability: (a) ERF only; and (b) ERF and GMPE uncertainties.

(b)

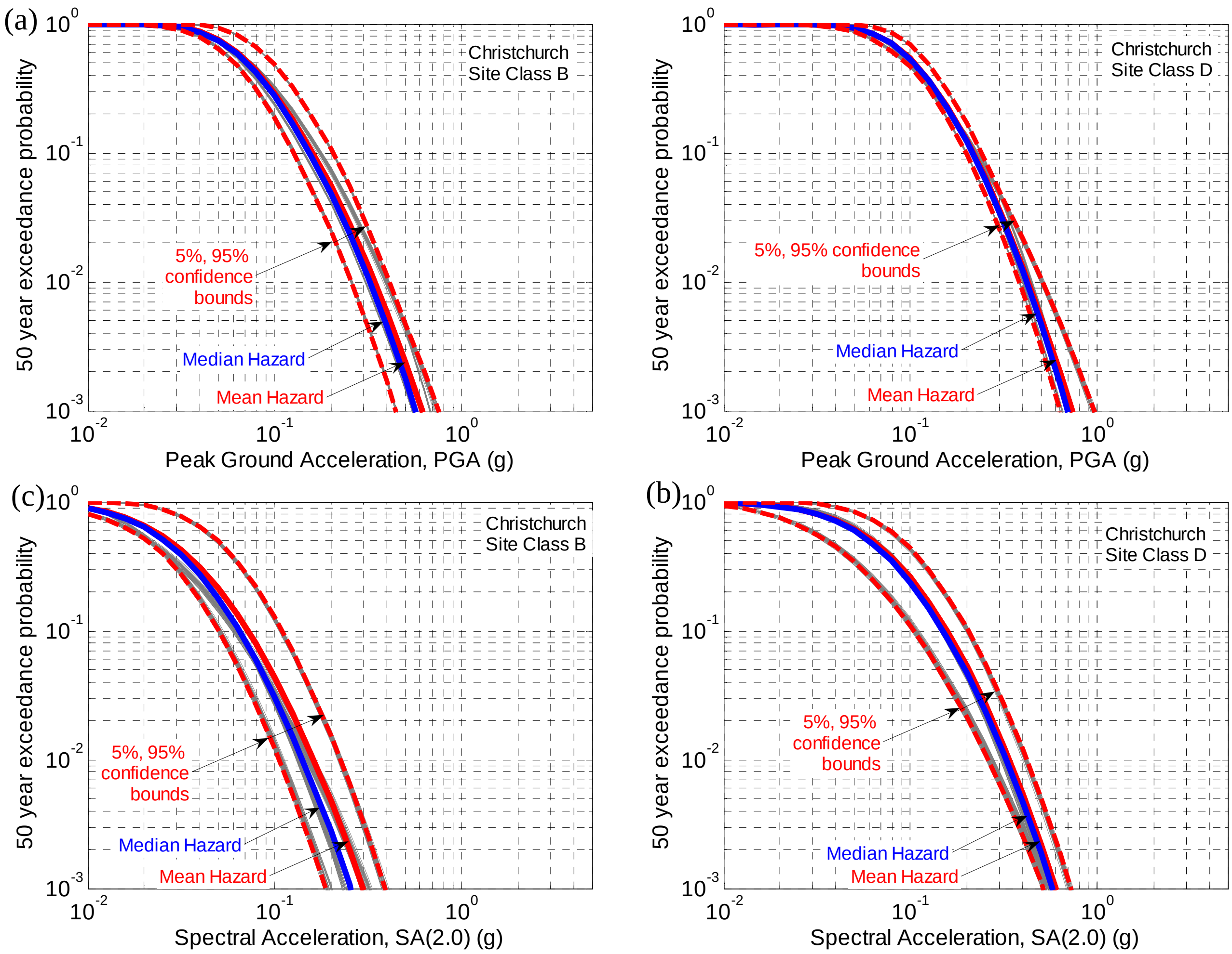

Figure 36 Comparison of the seismic hazard curves for Christchurch: (a) PGA and site class B; (b) PGA and site class D; (c) SA(2.0) and site class B; and (d) SA(2.0) and site class D.

Table 10 Summary of mean, 5th and 9th percentile hazard values for 10% and 2% exceedance probabilities in 50 years in Christchurch.

		PE = 10% in 50 years		PE = 2% in 50 years	
IM	Site Class	Mean	[5%,95%]	Mean	[5%,95%]
PGA	Rock, B	0.16	[0.12,0.21]	0.29	[0.22,0.35]
	Soft/deep soil, D	0.22	[0.20,0.24]	0.36	[0.32,0.41]
SA(2.0)	Rock, B	0.07	[0.05,0.11]	0.13	[0.09,0.19]
	Soft/deep soil, D	0.16	[0.11,0.21]	0.28	[0.21,0.35]

4.6 Christchurch hazard with the removal of background seismicity

As was previously mentioned, the seismic hazard in Christchurch differs from that in Wellington, in that both fault and background seismicity sources contribute significantly to the seismic hazard, and that the fault contribution is comprised of numerous faults, as depicted in

Figure **37**. In order to convey the impact of background seismicity on the seismic hazard results for Christchurch, including epistemic uncertainty magnitude, an analysis was performed considering only fault-based seismicity sources for PGA and site class D.

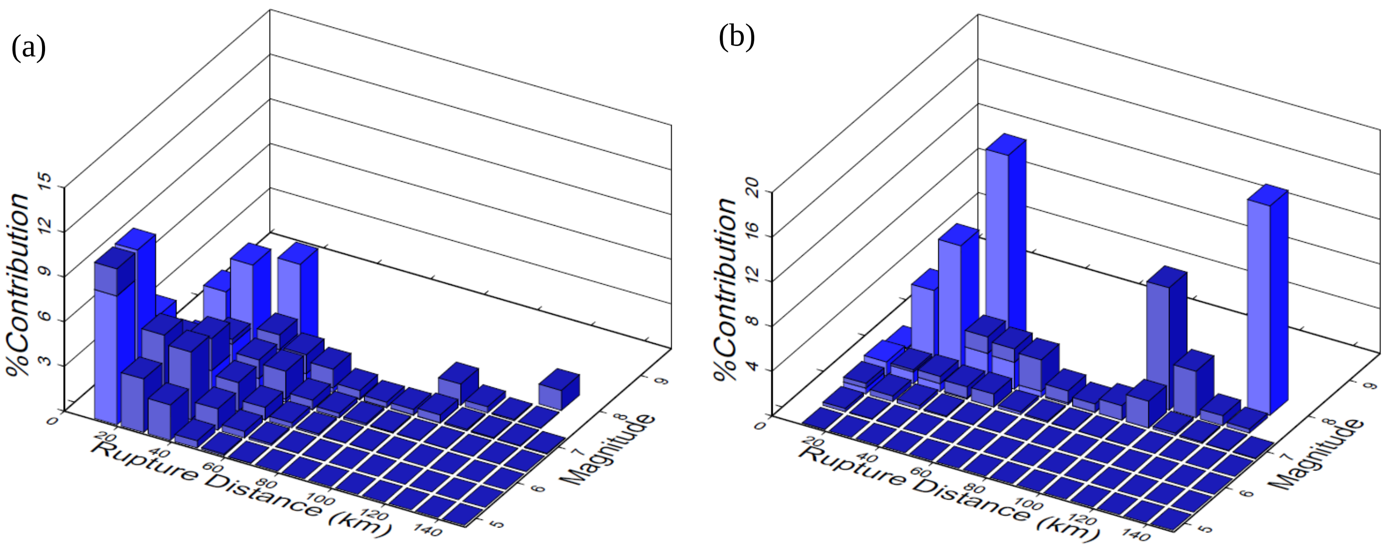

Figure 37 Seismic hazard deaggregation for Christchurch (site class D) for 2% in 50 year exceedance probability: (a) PGA; and (b) SA(2.0) considering both fault and background seismicity sources.

Figure 38 compares the seismic hazard computed with and without the consideration of background seismicity sources. Similar to previous figures, in Figure 38 individual simulations are shown in grey, with the mean hazard curve accounting for ERF uncertainty, but for a single GMPE, shown in coloured lines. Firstly, it can be seen that the background sources are significant, with the 10% in 50 year exceedance probability being approximately 0.2-0.25g when background sources are considered (i.e. Figure 38a) and 0.12-0.2g when background sources are neglected (i.e. Figure 38b). Secondly, it can be seen in Figure 38 that even in the ‘fault only’ case, the ERF component of the total epistemic uncertainty is insignificant compared with the GMPE uncertainty (i.e. the variation in the seismic hazard considering ERF uncertainty, but only a single GMPE is relatively small). Finally, and most importantly, it can be seen that the McV06 model provides the largest seismic hazard for exceedance probabilities greater than 10% in 50 years when background sources are considered, but the second smallest seismic hazard when background sources are neglected. This occurs because the McV06 model was shown to significantly over-predict the ground motions produced by small magnitude ($M_w < 6$) events, particularly as the source-to-site distance increases (i.e. Figure 2a and Figure 2b).

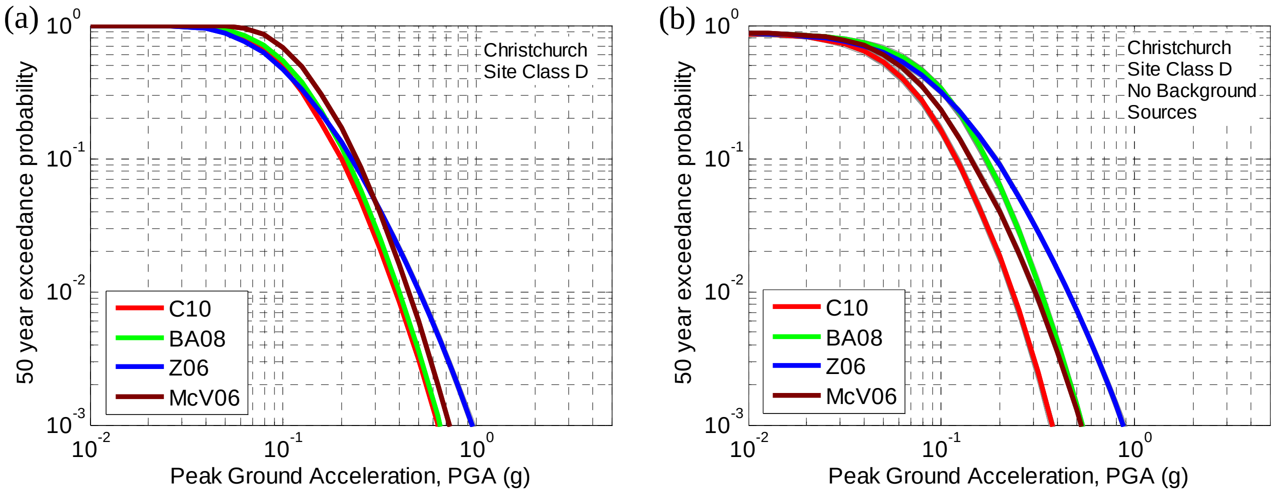

Figure 38 Comparison of seismic hazard curves (including epistemic uncertainties) computed considering: (a) both fault and background seismicity; and (b) only fault-based seismicity.

4.7 Comparison of uncertainties in seismic hazard for Wellington and Christchurch

Table 11 provides a broad comparison of the magnitude of epistemic uncertainties for the eight different seismic hazard analysis cases considered. The magnitude is quantified as the ratio of the difference between the 95% and 5% values divided by the mean hazard value. As previously discussed in specific cases, this table illustrates that: (i) the magnitude of the uncertainties are significant, and that the uncertainties are a similar order of magnitude for both Wellington and Christchurch; (ii) the uncertainty is not systematically higher for site class D sites compared with site class B sites; (iii) broadly speaking, the largest uncertainty was for SA(2.0) in Christchurch.

Table 11 Ratio of the difference between the 95% and 5% percentiles divided by the mean hazard in Wellington and Christchurch indicating the significance of epistemic uncertainties.

		Ratio = [95%-5%]/Mean			
		Wellington		Christchurch	
IM	Site Class	10% PE	2% PE	10% PE	2% PE
PGA	Rock, B	0.33	0.46	0.49	0.46
	Soft/deep soil, D	0.53	0.77	0.20	0.25
SA(2.0)	Rock, B	0.44	0.53	0.85	0.75
	Soft/deep soil, D	0.28	0.36	0.63	0.53

4.8 Comparison of preferred hazard with hazard with explicit epistemic uncertainties

The consideration of epistemic uncertainties allows one to understand the impact of certain assumptions on the outcomes of a seismic hazard analysis. The previous sections of this report have demonstrated that in the current methodological framework, GMPE epistemic uncertainty is the largest source of uncertainty on PSHA results. Therefore, it is insightful to scrutinize how the present NZ seismic hazard analyses using the McV06 model compare with the results presented here (considering multiple GMPEs). Figure 39 compares the previously presented seismic hazard analyses with epistemic uncertainties, with the single hazard curve that is obtained using the conventional NZ PSHA methodology (that is, neglecting epistemic uncertainties in ERF parameters, and using the McV06 GMPE). This is referred to as the "NSHM Hazard" in Figure 39. It can be seen that for the PGA hazard in Wellington (for both site class B and D), that the NSHM hazard is approximately equal to the 5% fractile of the hazard analysis considering epistemic uncertainties for the 10% and 2% in 50 year exceedance probabilities. For the SA(2.0) hazard in Wellington (for both site class B and D) the preferred hazard is approximately the 95% fractile for the 10% in 50 year exceedance probability, but the 5% fractile for the 2% in 50 year exceedance probability. For Christchurch, with the exception of PGA on site class D, it can be seen that the preferred hazard is approximately equal to the 95% fractile of the hazard considering epistemic uncertainties. As previously discussed, GMPE uncertainty produces the largest variation in the considered seismic hazard analyses, and hence the observations of the NSHM hazard as compared with the mean, 5th and 95th percentiles from the seismic hazard considering epistemic uncertainties largely result from the use of only the McV06 GMPE in the NSHM hazard calculations.

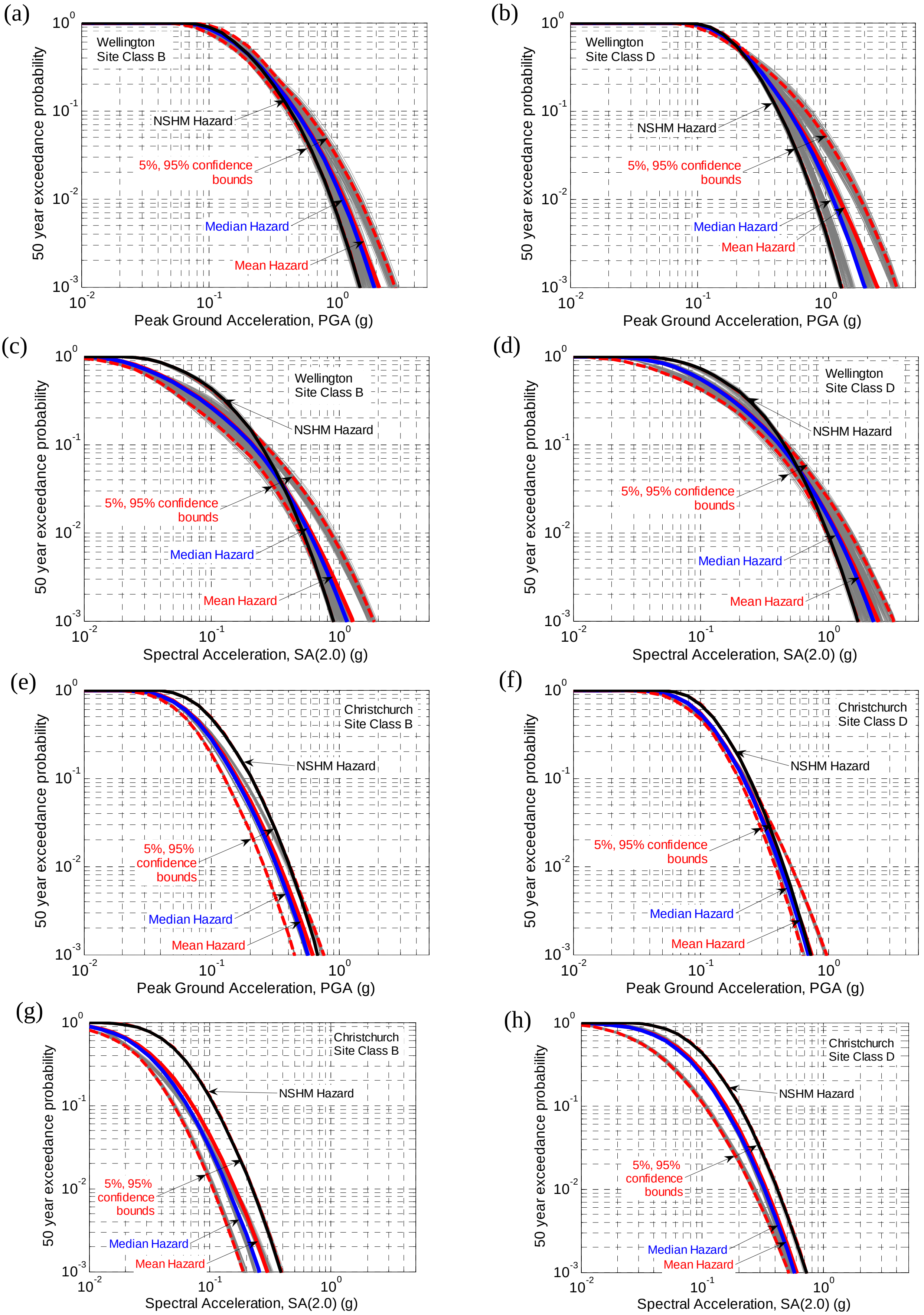

Figure 39 Comparison of the preferred hazard (i.e. the McV06 GMPE and ERF without epistemic uncertainties) with the epistemic uncertainty explicit hazard computed in this study.

4.9 Comparison of epistemic uncertainty magnitude for NZ with that of the San Francisco Bay Area, USA

One of the fundamental difficulties with assessing epistemic uncertainties in seismic hazard analyses is that while the ultimate aim is to represent the uncertainty in the seismic hazard estimate, most often the consideration of epistemic uncertainties simply reflects the range of scientific models available (Abrahamson 2006). A consequence of this is that using available models for a site with little or no data will indicate smaller epistemic uncertainty compared with a well-studied site with many available models, when clearly the poorly studied site will have a larger epistemic uncertainty. Along this line of thought, Bradley (2009) examined the magnitude of epistemic uncertainty in PSHA conducted for the San Francisco Bay Area (SFBA), using the ERF developed by the Working Group on California Earthquake Probabilities (WGCEP 2003) which extensively considered epistemic uncertainties, and for which a range of four different, western USA-specific GMPEs, are available. Hence, it is insightful to compare the magnitude of epistemic uncertainty from Bradley (2009) with those obtained in this study.

Figure 40a and Figure 40b illustrate the magnitude of the epistemic uncertainties obtained in this study in comparison with the bounds that were obtained by Bradley (2009) in the SFBA due to ERF uncertainty only and ERF and GMPE uncertainty, respectively. As previously discussed, it can be seen that ERF uncertainty for the four cases considered in Christchurch is less than that in Wellington, and both are less than those obtained for the SFBA. With respect to the total seismic hazard uncertainty (i.e. due to both ERF and GMPE uncertainty) it can be seen that the results obtained in this study are similar to those for the SFBA using the Next Generation Attenuation (NGA) Relations (namely Chiou and Youngs (2008), Boore and Atkinson (2008), and Campbell and Bozorgnia (2008)), but less than that obtained for the SFBA using the 'older' 1997-version GMPEs (namely Boore et al. (1997), Abrahamson and Silva (1997), Campbell and Bozorgnia (1997), and Sadigh et al. (1997)).

In order to reconcile the differences between the magnitude of the ERF uncertainties observed in this study and those obtained from SFBA it is necessary to consider firstly the ERF-uncertainties that WGCEP03 accounted for, which were (Bradley 2009, WGCEP 2003): (i) time dependence of characteristic ruptures; (ii) uncertainty in Mw-geometry scaling relationships; (iii) fault segmentation endpoints; (iv) seismogenic thickness; (v) slip rate; (vi) frequency of multi-segment ruptures; (vii) anelastic slip; and (ix) magnitude frequency distribution (i.e. either characteristic or Gutenberg-Richter). Thus, with respect to the present study, it can be stated that uncertainties (ii), (iii), (iv), (v), and (vii) noted above were considered, however uncertainties (i) Time dependence; (vi) multi-segment ruptures; and (ix) Characteristic vs. Gutenberg Richter uncertainties were not considered. The NZ ERF methodology (Stirling et al. 2011) is a time-independent ERF (with the exception of the Wellington, Wairarapa and Ohariu faults which are given time independent rates that are equivalent to their conditional probabilities over 50 years), with implementation of the Characteristic rupture hypothesis (i.e. without considering multi-segment ruptures, or Characteristic vs. Gutenberg-Richter magnitude-frequency distributions). One exception of the above statement is the treatment of subduction zone sources, in which two scenarios are considered based on the unknown seismogenic potential of some areas of this interface source (Stirling et al. 2011). Field (2007) noted that of all of the uncertainties considered in the WGCEP03 forecast it was the assumption of which time-dependent model to use which lead to the largest uncertainty. Hence, given the omission of time-dependent models in the

NZ ERF, as well as the other omitted uncertainties noted above, it is logical to see the reason for the under-estimation of ERF uncertainty observed in the present student relative to the WGCEP03 ERF.

Figure 40b illustrated that despite the lower epistemic uncertainty in the NZ ERF compared with that of the WGCEP03 ERF, that the total epistemic uncertainty (due to both ERF and GMPE uncertainty) was similar to that obtained for the SFBA using the NGA GMPEs. Hence it can be roughly stated that the GMPE uncertainty for NZ PSHA presented in this study is larger than that which exists for the SFBA using the NGA GMPEs, but likely still less than that using the 'old 1997' version GMPEs. Again, this result agrees with intuition given that the NGA GMPEs were developed specifically for the western US, while for NZ only the McV06 GMPE (based on pre-1995 data) is NZ-specific and the remaining model are foreign.

(a)

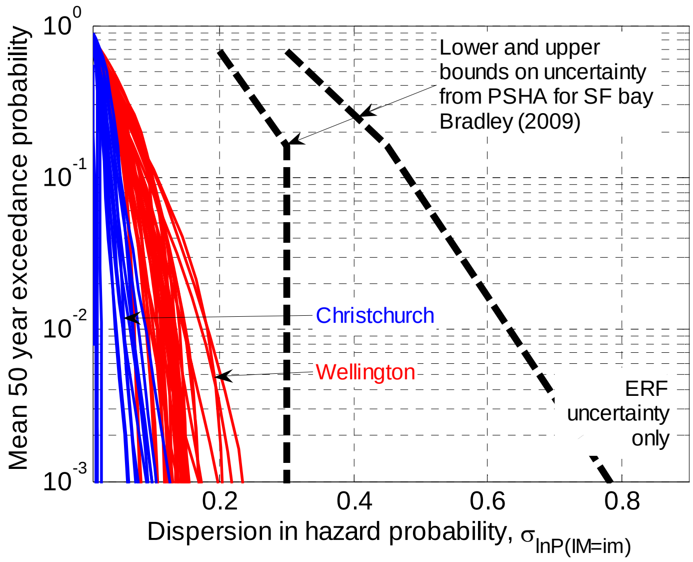

(b)

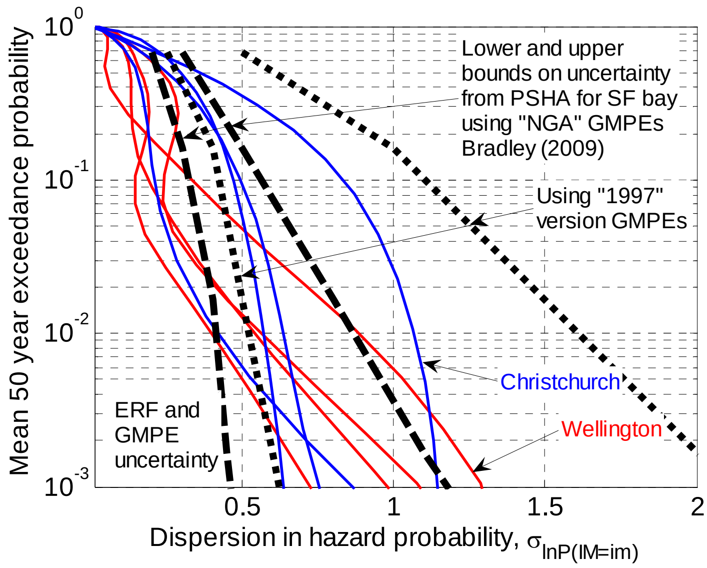

Figure 40 Comparison of the magnitude of epistemic uncertainty in seismic hazard (dispersion) as a function of exceedance probability for Wellington and Christchurch compared with that of the San Francisco Bay Area from the PSHA conducted by Bradley (2009): (a) uncertainties due to ERF uncertainties only; and (b) uncertainty due to both ERF and GMPE uncertainty.

5.0 LIMITATIONS OF PRESENT STUDY AND RECOMMENDATIONS FOR FUTURE WORK

5.1 Ground motion prediction equations

The consideration of various GMPEs for each of the three tectonic types of earthquakes that NZ is exposed to via logic trees is consistent with the state-of-practice in PSHA. However, there are some potential problems with the fundamentals of the logic tree framework as applied to PSHA, namely the assumptions that the various GMPEs considered are mutually exclusive and collectively exhaustive (Abrahamson and Bommer 2005, Bommer et al. 2005, McGuire et al. 2005, Musson 2005). As a result, these two conditions are more likely to be fulfilled if each individual model is assigned its own epistemic uncertainty, due to, among others, finite data, and functional form. Therefore the consideration of model-specific epistemic uncertainty should be considered in future empirical GMPEs.

Because of the timing at which the ground motion assessment was conducted as part of this study (April – July 2010) it was not possible to incorporate the recent earthquakes and aftershocks in the Christchurch region. These events, as well as a more comprehensive cataloguing of their resulting ground motions and metadata are presently being compiled and will be used in other projects by the authors to further improving the understanding of ground motions in NZ. A key consideration will be the development of (multiple) NZ-specific ground motion prediction equations. This is particularly imperative in light of the outcomes of this study which illustrate that a great reduction in NZ PSHA uncertainty can be achieved by developing more robust NZ-specific GMPEs.

Historically GMPEs have been entirely based on empirical considerations. However, in the past decade it is has become widely accepted that the most damaging ground motions (i.e. those produced by large magnitude near source events) are poorly represented in empirical ground motion databases, something which is unlikely to change drastically in the near future. As a result, future empirical GMPEs will benefit greatly from the consideration of results from physics-based rupture, wave propagation, and site-response simulations. At the same time, functional forms of empirical models should not become overly complex with too many parameters which cannot be easily obtained for individual PSHA applications.

5.2 Earthquake rupture forecast

In this study epistemic uncertainties were considered in the fault-based component of the earthquake rupture forecast. However, as mentioned in comparison with the WGCEP03 ERF for the SFBA, not all epistemic uncertainties in the fault-based ERF were considered. Furthermore, for the majority of faults, the magnitudes of the epistemic uncertainties considered were assigned based on judgement as fault-specific estimates were not available. Finally, epistemic uncertainties were not considered in the parameters (including their spatially correlation) which define the Gutenberg-Richter distribution for the background seismicity sources.

Therefore firstly, maintenance of the fault-database which is used to develop the fault-based component of the NZ ERF should devote further attention to the cataloguing of epistemic uncertainties. Such epistemic uncertainties should be catalogued for raw (i.e. measured) data directly (i.e. slip rates, fault geometry, timing of past events etc.), and not for interpreted data (e.g. fault length, which depends on inferred segment endpoints; or the distribution of time dependence which depends of event timings). Secondly, this study focused on the uncertainties of the parameters of the fault-based component of the ERF, but not on the ERF methodology itself. Field (2007) noted that the level of complexity in treating time dependence in the WGCEP03 model was inconsistent with other fundamental assumptions such as fault segmentation. A data-driven methodology, with fewer ideologically-driven assumptions is required for future fault-based seismicity models. One approach which shows promise along these lines is that recently proposed by Field and Page (2011). While this methodology is presently still under development (particularly in its application to vast fault systems), it should be thoroughly considered (along with other viable models) for the subsequent NZ ERF development in the next decade.

The implications for seismic hazard of parameter uncertainty and model uncertainty for background seismicity were not considered in this study. Such development should be conducted in parallel with fault-based methodologies. In particular, the consideration of time-dependence in background seismicity; assignment of historical seismicity to fault or background sources; and treatment of background sources as finite faults rather than point sources, are all key issues.

6.0 CONCLUSIONS

This study presented the results of considering epistemic uncertainties in probabilistic seismic hazard analyses for locations in New Zealand. The methodology accounted for the uncertainties in the characteristic rupture magnitude and recurrence rate of the fault-based component of the seismicity, but uncertainties in background seismicity were not considered. Uncertainties were also accounted for in ground motion prediction via the use of multiple ground motion prediction equations in a logic tree.

The hierarchy of ground motion prediction equations was developed based on examination of the bias in various NZ and foreign models using a dataset of observed ground motions in New Zealand.

Due to the present lack of fault-specific data quantifying uncertainties for the majority of faults in NZ, representative values based on judgement and a limited number of NZ and foreign fault-specific data available were utilized where required.

Probabilistic seismic hazard analyses were conducted for two vibration periods of spectral acceleration for site class B (rock) and D (soft/deep soil) conditions in Wellington and Christchurch. The obtained results illustrated that uncertainties in ground motion prediction result in the largest variation in PSHA results. Of the earthquake rupture forecast uncertainties considered, that due to the magnitude-geometry scaling relationships was the most significant, followed by rupture length.

7.0 ACKNOWLEDGEMENTS

Financial support for this study provided by the New Zealand Earthquake Commission (EQC) is greatly appreciated.

8.0 REFERENCES

Abrahamson, N. A., 2006. Seismic hazard assessment: problems with current practice and future developments, in 1st European Conference on Earthquake Engineering and Seismology: Geneva, Switzerland p. 17.

Abrahamson, N. A., Bommer, J. J., 2005. Probability and uncertainty in seismic hazard analysis, Earthquake Spectra, **21**, 603-607.

Abrahamson, N. A., Silva, W. J., 1997. Empirical Response Spectral Attenuation Relations for Shallow Crustal Earthquakes, Seismological Research Letters, **68**, 94-127.

Amos, C. B., Burbank, D. W., Nobes, D. C., Read, S. A. L., 2007. Geomorphic constraints on listric thrust faulting: Implications for active deformation in the Mackenzie Basin, South Island, New Zealand, J. Geophys. Res., **112**, B03S11.

Ang, A. H. S., Tang, W. H., 2007. Probability concepts in engineering: Emphasis on applications in civil and environmental engineering. John Wiley & Sons.

Atkinson, G. M., Boore, D. M., 2003. Empirical ground-motion relations for subduction-zone earthquakes and their application to cascadia and other regions, Bulletin of the Seismological Society of America, **93**, 1703–1729.

Berryman, K. R., Webb, T. H., Hill, N., Rhoades, D., Stirling, M. W., 2001. Seismic loads on dams - Waitaki system. Development of fault scaling relationships and their application to fault source characterisation, GNS Client Report 2001/129, pp.

Bommer, J. J., Scherbaum, F., 2008. The use and misuse of logic trees in probabilistic seismic hazard analysis, Earthquake Spectra, **24**, 997-1009.

Bommer, J. J., Scherbaum, F., Bungum, H., Cotton, F., Sabetta, F., Abrahamson, N., 2005. On the use of logic trees for ground-motion prediction equations in seismic hazard assessment, Bulletin of the Seismological Society of America, **95**, 377–389.

Boore, D. M., Atkinson, G. M., 2008. Ground-motion prediction equations for the average horizontal component of PGA, PGV, and 5%-damped PSA at spectral periods between 0.01s and 10.0s, Earthquake Spectra, **24**, 99-138.

Boore, D. M., Joyner, W. B., Fumal, T. E., 1997. Equations for estimating horizontal response spectra and peak acceleration from western North American earthquakes: A summary of recent work, Seismological Research Letters, **68**, 128-153.

Bradley, B. A., 2009. Seismic hazard epistemic uncertainty in the San Francisco bay area and its role in performance-based assessment, Earthquake Spectra, **25**, 733-753.

Bradley, B. A., 2010. NZ-specific pseudo-spectral acceleration ground motion prediction equations based on foreign models, Department of Civil and Natural Resources Engineering, University of Canterbury, Department of Civil and Natural Resources Engineering, University of Canterbury, Christchurch, New Zealand. 324pp.

Campbell, K. W., 1997. Empirical Near-Source Attenuation Relationships for Horizontal and Vertical Components of Peak Ground Acceleration, Peak Ground Velocity, and Pseudo-Absolute Acceleration Response Spectra, Seismological Research Letters, **68**, 154-179.

Campbell, K. W., Bozorgnia, Y., 2008. NGA Ground Motion Model for the Geometric Mean Horizontal Component of PGA, PGV, PGD and 5% Damped Linear Elastic Response Spectra for Periods Ranging from 0.01 to 10 s Earthquake Spectra, **24**, 139-171.

Chiou, B., Darragh, R., Gregor, N., Silva, W. J., 2008. NGA project strong-motion database, Earthquake Spectra, **24**, 23-44.

Chiou, B., Youngs, R., Abrahamson, N., Addo, K., 2010a. Ground-Motion Attenuation Model for Small-To-Moderate Shallow Crustal Earthquakes in California and Its Implications on Regionalization of Ground-Motion Prediction Models, Earthquake Spectra, **26**, 907-926.

Chiou, B., Youngs, R. R., Abrahamson, N. A., Addo, K., 2010b. Ground-motion attenuation model for small-to-moderate shallow crustal earthquakes in california and Its implications on regionalization of ground-motion prediction models, Earthquake Spectra, **(to appear)**.

Chiou, B. S. J., Youngs, R. R., 2008. An NGA Model for the average horizontal component of peak ground motion and response spectra, Earthquake Spectra, **24**, 173-215.

Cornell, C. A., 1968. Engineering seismic risk analysis, Bulletin of the Seismological Society of America, **58**, 1583–1606.

Esteva, L., 1968. Bases para la formulaci´on de decisiones de diseˇno s´ısmico. Universidad Nacional Aut´onoma de M´exico: Mexico City.

Field, E. H., 2007. A summary of previous working groups on California earthquake probabilities, Bulletin of the Seismological Society of America, **97**, 1033-1053.

Field, E. H., Jordan, T. H., Cornell, C. A., 2003. OpenSHA: A developing community-modelling environment for seismic hazard analysis, Seismological Research Letters, **74**, 406-419.

Field, E. H., Page, M. T., 2011. Estimating Earthquake-Rupture Rates on a Fault or Fault System, Bulletin of the Seismological Society of America, **101**, 79-92.

Fry, B., Bannister, S., Beavan, J., Bland, L., Bradley, B. A., Cox, S., Cousins, J., Gale, N., Hancox, G., Holden, C., Jongens, R., Power, W., Prasetya, G., Reyners, M., Ristau, J., Robinson, R., Samsonov, S., Wilson, K., 2010. The Mw 7.6 Dusky Sound earthquake of 2009: Preliminary report, Bulletin of the New Zealand Society for Earthquake Engineering, **43**, 24-40.

GeoNet, 2010. GeoNet, http://www.geonet.org.nz/ (last accessed: February 2010).

Hanks, T. C., Bakun, W. H., 2002. A bilinear source-scaling model for M-log A observations of continental earthquakes, Bulletin of the Seismological Society of America, **92**, 1841-1846.

Heron, D., van Dissen, R., Sawa, M., 1998. Late Quaternary movement on the Ohariu Fault, Tongue Point to MacKays Crossing, North Island, New Zealand, New Zealand Journal of Geology and Geophysics, **41**, 419 - 439.

Howard, M., Nicol, A., Campbell, J., Pettinga, J. R., 2005. Holocene paleoearthquakes on the strike-slip Porters Pass Fault, Canterbury, New Zealand, New Zealand Journal of Geology and Geophysics, **48**, 59 - 74.

Kulkarni, R. B., Youngs, R. R., Coppersmith, K. J., 1984. Assessment of confidence intervals for results of seismic hazard analysis, in 8th World Conference on Earthquake Engineering,: San Francisco, CA. p. 263–270.

Langridge, R. M., Berryman, K. R., 2005. Morphology and slip rate of the Hurunui section of the Hope Fault, South Island, New Zealand, New Zealand Journal of Geology and Geophysics, **48**, 43 - 57.

Litchfield, N., Van Dissen, R., Heron, D., Rhoades, D., 2006. Constraints on the timing of the three most recent surface rupture events and recurrence interval for the Ohariu Fault: Trenching results from MacKays Crossing, Wellington, New Zealand, New Zealand Journal of Geology and Geophysics, **49**, 57 - 61.

McGuire, R. K., 2008. Probabilistic seismic hazard analysis: early history, Earthquake Engineering and Structural Dynamics, **37**, 329-338.

McGuire, R. K., Cornell, C. A., Toro, G. R., 2005. The case for mean seismic hazard, Earthquake Spectra, **21**, 879-886.

McVerry, G. H., Zhao, J. X., Abrahamson, N. A., Somerville, P. G., 2006. New Zealand acceleration response spectrum attenuation relations for crustal and subduction zone earthquakes, Bulletin of the New Zealand Society for Earthquake Engineering, **39**, 1-58.

Musson, R. M. W., 2005. Against Fractiles, Earthquake Spectra, **21**, 887-891.

NZS 1170.5, 2004. Structural design actions, Part 5: Earthquake actions - New Zealand. Standards New Zealand: Wellington, New Zealand. p. 82.

Pace, B., Stirling, M. W., Litchfield, N. J., Rieser, U., 2005. New active fault data and seismic hazard estimates for west Otago, New Zealand, New Zealand Journal of Geology and Geophysics, **48**, 75 - 83.

Petersen, M. D., Frankel, A. D., Harmsen, S. C., Mueller, C. S., Haller, K. M., Wheeler, R. L., Wesson, R. L., Zeng, Y., Boyd, O. S., Perkins, D. M., Luco, N., Field, E. H., Wills, C. J., Rukstales, K. S., 2008. Documentation for the 2008 Update of the United States National Seismic Hazard Maps, United States Geological Survey (USGS), United States Geological Survey (USGS), 127pp.

Ruppert, D., Sheather, S. J., Wand, M. P., 1995. An effective bandwidth selector for local least squares regression, Journal of the American Statistical Association, **90**, 1257-1270.

Sadigh, K., Chang, C.-Y., Egan, J. A., Makdisi, F., Youngs, R. R., 1997. Attenuation Relationships for Shallow Crustal Earthquakes Based on California Strong Motion Data, Seismological Research Letters, **68**, 180-189.

Scherbaum, F., Cotton, F., Smit, P., 2004. On the Use of Response Spectral-Reference Data for the Selection and Ranking of Ground-Motion Models for Seismic-Hazard Analysis in Regions of Moderate Seismicity: The Case of Rock Motion, Bulletin of the Seismological Society of America, **94**, 2164-2185.

Stafford, P. J., Strasser, F. O., Bommer, J. J., 2008. An evaluation of the applicability of the NGA models to ground-motion prediction in the Euro-Mediterranean region, Bulletin of Earthquake Engineering, **6**, 149-177.

Stirling, M. W., McVerry, G., Gerstenberger, M., Litchfield, N., Van Dissen, R., Berryman, K., Barnes, P., Beavan, J., Bradley, B. A., Clark, K., Jacobs, K., Lamarche, G., Langridge, R., Nicol, A., Nodder, S., Pettinga, J., Reyners, M., Rhoades, D., Smith, W., Villamor, P., Wallace, L., 2011. National Seismic Hazard Model for New Zealand: 2010 Update, Bulletin of the Seismological Society of America.

Stirling, M. W., McVerry, G. H., Berryman, K. R., 2002. A new seismic hazard model for New Zealand, Bulletin of the Seismological Society of America, **92**, 1878–1903.

Strasser, F. O., Arango, M. C., Bommer, J. J., 2010. Scaling of the Source Dimensions of Interface and Intraslab Subduction-zone Earthquakes with Moment Magnitude, Seismological Research Letters, **81**, 941-950.

Van Dissen, R., et al, 2010. Its Our Fault: Better defining earthquake risk in Wellington, in 11th IAEG Congress Auckland, New Zealand. p. 8.

Van Dissen, R. J., Berryman, K. R., 1996. Surface rupture earthquakes over the last ~1000 years in the Wellington region, New Zealand, and implications for ground shaking hazard, Journal of Geophysical Research, **101**, 5999-6019.

Villamor, P., Berryman, K. R., 2006. Late Quaternary geometry and kinematics of faults at the southern termination of the Taupo Volcanic Zone, New Zealand, New Zealand Journal of Geology and Geophysics, **49**, 1 - 21.

Villamor, P., Berryman, K. R., Webb, T., Stirling, M. W., McGinty, P., Downes, G., Harris, J., Litchfield, N., 2001. Waikato seismic loads - Task 2.1. Revision of seismic source characterisation, GNS Client Report 2001/59, pp.

Wallace, L. M., Martin Reyners1, U. C., Stephen Bannister1, Philip, Barnes2, K. B., Gaye Downes1, Donna Eberhart-Phillips1, Ake, Fagereng3, S. E., Andrew Nicol1, Robert McCaffrey1,4, R. John Beavan1,, Stuart Henrys1, R. S., Daniel H.N. Barker1, Nicola Litchfield1, John, Townend5, R. R., Rebecca Bell1, Kate Wilson1, William Power1, 2010. Characterizing the seismogenic zone of a major plate boundary subduction thrust: the Hikurangi Margin, New Zealand, G gubed, (submitted).

Wasserman, L., 2006. All of non-parametric statistics. Springer: New York.

WGCEP, 2003. Earthquake probabilities in the San Francisco bay region: 2002–2031, USGS Open-File Report 03-214, USGS Open-File Report 03-214, pp.

Youngs, R. R., Chiou, S. J., Silva, W. J., Humphrey, J. R., 1997. Strong ground motion attenuation relationships for subduction zone earthquakes, Seismological Research Letters, **68**, 94-127.

Zachariasen, J., Berryman, K., Langridge, R., Prentice, C., Rymer, M., Stirling, M., Villamor, P., 2006. Timing of late Holocene surface rupture of the Wairau Fault, Marlborough, New Zealand, New Zealand Journal of Geology and Geophysics, **49**, 159 - 174.

Zhao, J. X., 2010. Geometric Spreading Functions and Modeling of Volcanic Zones for Strong-Motion Attenuation Models Derived from Records in Japan, Bulletin of the Seismological Society of America, **100**, 712-732.

Zhao, J. X., Dowrick, D. J., McVerry, G. H., 1997. Attenuation of peak ground accelerations in New Zealand earthquakes, Bulletin of the New Zealand Society for Earthquake Engineering, **30**, 133-158.

Zhao, J. X., Gerstenberger, M., 2010. Attenuation models for rapid post earthquake assessment in NZ, EQC report, pp.

Zhao, J. X., Zhang, J., Asano, A., Ohno, Y., Oouchi, T., Takahashi, T., Ogawa, H., Irikura, K., Thio, H. K., Somerville, P. G., Fukushima, Y., Y., F., 2006. Attenuation relations of strong ground motion in Japan using site classification based on predominant period, Bulletin of the Seismological Society of America, **96**, 898-913.

www.gns.cri.nz

Principal Location

1 Fairway Drive
Avalon
PO Box 30368
Lower Hutt
New Zealand
T +64-4-570 1444
F +64-4-570 4600

Other Locations

Dunedin Research Centre
764 Cumberland Street
Private Bag 1930
Dunedin
New Zealand
T +64-3-477 4050
F +64-3-477 5232

Wairakei Research Centre
114 Karetoto Road
Wairakei
Private Bag 2000, Taupo
New Zealand
T +64-7-374 8211
F +64-7-374 8199

National Isotope Centre
30 Gracefield Road
PO Box 31312
Lower Hutt
New Zealand
T +64-4-570 1444
F +64-4-570 4657